

American University in Cairo

## AUC Knowledge Fountain

---

Theses and Dissertations

Student Research

---

6-1-2015

### Integration of linear alternators in thermoacoustic heat Engines

Moamen Bellah Abdelmwgoud

Follow this and additional works at: <https://fount.aucegypt.edu/etds>

---

#### Recommended Citation

##### APA Citation

Abdelmwgoud, M. (2015). *Integration of linear alternators in thermoacoustic heat Engines* [Master's Thesis, the American University in Cairo]. AUC Knowledge Fountain.

<https://fount.aucegypt.edu/etds/152>

##### MLA Citation

Abdelmwgoud, Moamen Bellah. *Integration of linear alternators in thermoacoustic heat Engines*. 2015. American University in Cairo, Master's Thesis. *AUC Knowledge Fountain*.

<https://fount.aucegypt.edu/etds/152>

This Master's Thesis is brought to you for free and open access by the Student Research at AUC Knowledge Fountain. It has been accepted for inclusion in Theses and Dissertations by an authorized administrator of AUC Knowledge Fountain. For more information, please contact [thesisadmin@aucegypt.edu](mailto:thesisadmin@aucegypt.edu).



THE AMERICAN UNIVERSITY IN CAIRO  
SCHOOL OF SCIENCES AND ENGINEERING

**INTEGRATION OF LINEAR ALTERNATORS IN THERMOACOUSTIC  
HEAT ENGINES**

BY

**MOAMEN BELLAH ABDYOU ABDALLAH ABDELMWGOUD**

**B.Sc. Mechanical Power Engineering, 2010**

**Faculty of Engineering, Cairo University**

A thesis submitted in partial fulfillment of the requirements for the degree of  
**Master of Science in Mechanical Engineering**

Under the supervision of:

**Prof. Ehab Abdel-Rahman**

**Professor, Department of Physics**

**Vice Provost for Research**

**The American university in Cairo**

**Prof. Amr Serag Eldin**

**Professor, Department of Mechanical Engineering**

**Chair of the Petroleum and Energy Engineering Department**

**The American University in Cairo**

**Dr. Abdelmaged Hafez Ibrahim Essawey**

**Research Assistant Professor, School of Sciences and Engineering**

**The American University in Cairo**

May, 2015

## Acknowledgement

Foremost, I would like to thank my advisors Prof. Ehab Abdel-Rahman and Prof. Amr Serag for all the patience, care and continuous support throughout this work. No words could express my deep gratitude for everything I have learnt from them.

I can never deny that without the help, advice and support of my advisor Dr. Abdelmaged this work would not have been completed and presented in this way. I would like to specially thank him for all the time, care, expertise and support that he gave to me without any hesitation.

I wish to express my sincere thanks to the thermoacoustic research-team members. Eng. Amr Taha for assisting in the design and implementation of the stroke control circuit, Eng. Islam Ramadan for assisting in all issues related to the development, de-bugging and optimization of the DeltaEC code used in this work, Eng. Khaled ElBeltagy for assisting in all issues related to the mechanical design and production of the test rig, Eng. Ahmed Yassin for assisting in the experimental work and data acquisition, Eng. Abdel-Rahman Nassief for assisting in developing Matlab codes for data analysis. I also wish to thank all of them for their friendship, support and for creating an enjoyable working atmosphere throughout this working period.

None of this would have been possible without the love and patience of my family. My family to whom this work is dedicated to, has been a constant source of love, concern, support and strength all these years. Therefore, I would like to express my heart-felt gratitude to every member in my family.

I would like to acknowledge the European Union for funding this project. Also, I am thankful for the Egyptian Academy of Scientific Research and Technology for my M.Sc. fellowship.

# Table of Contents

Acknowledgement .....	ii
Table of Contents .....	iii
List of Figures .....	v
List of Tables .....	vii
List of Symbols .....	viii
Abstract .....	x
Chapter 1 - Introduction .....	1
1.1 Thermoacoustic Devices .....	1
1.2 History of Thermoacoustics .....	2
1.3 Modes of Operation .....	3
1.3.1 Standing Wave Engines .....	3
1.3.2 Travelling Wave Engines .....	6
1.4 History of Thermoacoustic Heat Engines .....	9
1.5 Advantages and Challenges of Thermoacoustic Heat Engines .....	10
1.6 Principle of Operation of Linear Alternators .....	11
1.6.1 Types of Linear Alternators .....	11
1.6.2 Linear Alternators Matching .....	12
1.7 Scope of This Work .....	14
Chapter 2 - Experimental Setup and Procedure .....	15
2.1 DeltaEC .....	15
2.2 Experimental Setup .....	16
2.3 Setup Components: .....	18
2.3.1 Resonator .....	18
2.3.2 Enclosure Volume .....	19
2.3.3 Hydrostatic test .....	20
2.3.4 Acoustic Driver and Linear Alternator .....	20
2.3.5 Stroke-Control Circuit .....	22
2.3.6 Load Circuit .....	24
2.4 Instrumentation .....	26
2.4.1 Mean Pressure .....	26
2.4.2 Working Gases .....	26
2.4.3 Mean Gas Temperature .....	27

2.4.4 Coil Temperature .....	27
2.4.5 Dynamic Pressure .....	27
2.4.6 Linear Variable Differential Transducers (LVDT's).....	28
2.4.7 Current and Voltage Measurements.....	30
2.4.8 System Protection .....	30
2.4.9 Digital Oscilloscope.....	30
2.4.10 Data Acquisition Board: .....	31
2.5 Experimental Procedure.....	31
Chapter 3 - Results and Discussion .....	34
3.1 Calculation of Performance Parameters: .....	34
3.2 Basic Case.....	35
3.2.1 Time and Frequency Domain Analysis.....	37
3.2.2 Effects of Operating Parameters on the Basic Case.....	40
3.3 Performance Analysis .....	52
3.3.1 Effects of Gas Composition and Mean Pressure.....	52
3.3.2 Effects of Input Voltage.....	56
3.3.3 Effects of Electric Load Resistance .....	58
3.4 Retest Reliability.....	60
Chapter 4 - Conclusions, Summary and Future Work.....	62
4.1 Conclusions and Summary .....	62
4.2 Suggestions for Recommended Future Work.....	64
References.....	65
Appendix A - DeltaEC Code .....	67
Appendix B - Guesses, Targets and Main Parameters in DeltaEC.....	72
Appendix C - Mechanical Drawings.....	73
Appendix D - Assembly of the Experimental Setup.....	75
Appendix E - Matlab Codes.....	77
Appendix F - Stroke Control Circuit .....	93

## List of Figures

<b>Figure 1.1:</b> One of the very first TAPC [3].....	2
<b>Figure 1.2:</b> Los Alamos National Lab traveling-wave thermoacoustic electric generator [7] .....	3
<b>Figure 1.3:</b> Schematic for standing-wave thermoacoustic engine [8]. The arrow shows the direction of the acoustic power .....	4
<b>Figure 1.4:</b> Relationships between pressure, parcel volume , temperature and axial location of the parcel in standing-wave engine [9] .....	4
<b>Figure 1.5:</b> Dynamic pressure and gas parcel velocity waveforms in standing-wave engines [2].	5
<b>Figure 1.6:</b> Various traveling wave engine designs [9] .....	7
<b>Figure 1.7:</b> Schematic for travelling-wave thermoacoustic engine [6].....	7
<b>Figure 1.8:</b> Relationships between pressure, parcel volume, temperature and axial location in travelling-wave engine. [9] .....	8
<b>Figure 1.9:</b> Dynamic pressure and gas parcel velocity waveforms in travelling-wave engines [2]. .....	9
<b>Figure 2.1:</b> System schematic from DeltaEC.....	16
<b>Figure 2.2:</b> Schematic showing the linear alternator under test and the accessories and instrumentation used. ....	16
<b>Figure 2.3:</b> Digital image for the experimental setup .....	17
<b>Figure 2.4:</b> Left: Three used resonators. Right: flange of one of the resonators .....	18
<b>Figure 2.5:</b> Top: The alternator volumes used to house the acoustic driver and the linear alternator. Bottom: Flange of one of the alternators .....	19
<b>Figure 2.6:</b> Left: outer side of enclosure flange. Right: Inner side of the flange.....	20
<b>Figure 2.7:</b> Three views for the used acoustic driver / Linear alternator .....	21
<b>Figure 2.8:</b> Top: Function generator. Bottom: Power amplifier .....	22
<b>Figure 2.9:</b> Control logic used to protect against over-stroking in the linear .....	23
<b>Figure 2.10:</b> PCB of the stroke control circuit.....	24
<b>Figure 2.11:</b> Left: Set of zeners available in the lab. Right: back-to-back connection of the zeners .....	25
<b>Figure 2.12:</b> connection of the zeners in series with the rheostat .....	25
<b>Figure 2.13:</b> Gauges and control valves used in the experiment .....	26
<b>Figure 2.14:</b> Left: Dynamic pressure microphone. Right: DC amplifier.....	28
<b>Figure 2.15:</b> Left: LVDT probe. Right: LVDT signal conditioner .....	29
<b>Figure 2.16:</b> Left: LVDT rod plug and screw. Right: LVDT fixation to the piston back .....	30

<b>Figure 2.17:</b> Digital storage oscilloscope .....	31
<b>Figure 2.18:</b> Data acquisition board.....	31
<b>Figure 3.1:</b> Time domains of all measured variables Operating conditions: 54 Hz, 12 bar, 40% He 60% Ar, 20 V <sub>RMS</sub> , 22Ω, 6V zener .....	37
<b>Figure 3.2:</b> Frequency domains of all measured variables Operating conditions: 54 Hz, 12 bar, 40% He 60% Ar, 20 V <sub>RMS</sub> , 22Ω, 6V zener.....	38
<b>Figure 3.3:</b> Effect of frequency on the system variables .....	41
<b>Figure 3.4:</b> Effect of Mean pressure on the system variables .....	42
<b>Figure 3.5:</b> Gas mixture properties .....	43
<b>Figure 3.6:</b> Effect of gas mixture on the system variables.....	44
<b>Figure 3.7:</b> Effect of input volt on the system variables.....	46
<b>Figure 3.8:</b> Effect of Electrical resistance on the system variables .....	47
<b>Figure 3.9:</b> Time domains of all measured variables.....	48
<b>Figure 3.10:</b> Frequency domains of all measured variables Operating conditions: 54 Hz, 12 bar, 40% He 60% Ar, 20 V <sub>RMS</sub> , 22Ω, No zener.....	49
Figure 3.11: Effect of zener breakdown voltage on the system variables .....	50
<b>Figure 3.12:</b> Frequency response at 21bar mean gas pressure.....	53
<b>Figure 3.13:</b> Frequency response at 12 bar mean gas pressure.....	54
<b>Figure 3.14:</b> Frequency response at 4 bar mean gas pressure.....	55
<b>Figure 3.15:</b> Electrical resistance response at 12 bar mean gas pressure and 6V zener .....	57
<b>Figure 3.16:</b> Electrical resistance response at 12 bar mean gas pressure and 20 V <sub>RMS</sub> .....	59
<b>Figure 3.17:</b> Frequency response for basic case to check system repeatability.....	61

## List of Tables

Table 2.1: System main dimensions .....	15
Table 2.2: Experimental setup instrumentation list .....	17
Table 2.3: Acoustic driver and liner alternator specifications [20] .....	21
Table 2.4: Specifications of the AC zeners diodes used in the experiments .....	26
Table 3.1: Performance parameters of the case presented. All phases are measured simultaneously with respect to the dynamic pressure in acoustic driver enclosure.....	36



## List of Symbols

### English letters

a	Speed of sound, m/s
A	Piston's area, m <sup>2</sup>
B	Magnetic flux density, Tesla
BL	Transduction coefficient, N/m <sup>2</sup>
d	Piston's stroke, m
E <sub>AD</sub>	Acoustic driver acoustic power, W
E <sub>LA</sub>	Linear alternator acoustic power, W
F	Lorentz force, N
h	Heat transfer coefficient, W/m <sup>2</sup> .k
I <sub>in</sub>	Input current, A
I <sub>out</sub>	Output current, A
k	Thermal conductivity, W/m.k
L	Total length of the coil, m
P <sub>1</sub>	Dynamic pressure inside the resonator, kPa
P <sub>AD</sub>	Acoustic driver dynamic pressure amplitude, kPa
P <sub>in</sub>	Input electric power, W
P <sub>LA</sub>	Linear alternator dynamic pressure amplitude, kPa
P <sub>m</sub>	Mean gas pressure, kPa
P <sub>out</sub>	Output electric power, W
R <sub>m</sub>	Mechanical resistance, N.s/m
U <sub>1</sub>	Volumetric velocity inside the resonator, m <sup>3</sup> /s
U <sub>AD</sub>	Acoustic driver piston's volumetric velocity, m <sup>3</sup> /s
U <sub>LA</sub>	Linear alternator piston's volumetric velocity, m <sup>3</sup> /s
V <sub>AD</sub>	Acoustic driver piston's velocity, m/s

V<sub>in</sub> Input voltage, V

VOC	Open circuit voltage
$V_{out}$	Output voltage, V
Z	Acoustic impedance. Pa.s/m <sup>3</sup>

#### Greek letters

$\omega$	Angular velocity, rad/s
$\eta_{AD}$	Acoustic driver conversion efficiency
$\eta_{LA}$	Linear alternator conversion efficiency
$\eta_{overall}$	Overall conversion efficiency
$\delta_k$	Thermal penetration depth, m
$\delta_v$	Viscous penetration depth, m

#### Acronyms

AC	Alternating Current
AD	Acoustic Driver
AISI	American Iron and Steel Institute
Ar	Argon
ASME	American Society of Mechanical Engineers
DC	Direct Current
DELATEC	Design Environment for Low-Amplitude Thermoacoustic Energy Conversion
FFT	Fast Fourier Transform
He	Helium
LA	Linear Alternator
LVDT	Linear Variable Differential Transducer
pk-pk	peak to peak
RMS	Root Mean Square
TAPC	Thermoacoustic Power Converter
TAE	Thermoacoustic Engine
TAR	Thermoacoustic Refrigerator

## Abstract

A thermoacoustic power converter consists of a thermoacoustic heat engine driving a linear alternator connected to a matched electric load. Accordingly, linear alternators are essential parts of thermoacoustic power converters. However, integration of a linear alternator in a thermoacoustic power converter is complicated since it requires acoustic matching with the thermoacoustic engine as well as electrical matching with the electric load connected to it and fast protection against piston over-stroking. In order to simplify the integration process, an experimental setup designed and built, in which the acoustic power generated by a thermoacoustic engine simulated by an acoustic driver. This setup provides a platform to test and evaluate the performance of a linear alternator in a controlled environment before integrated into thermoacoustic heat engines that allows identification and resolution of potential problems only related to linear alternators. A control circuit designed and built to protect the alternator's piston against over-stroking. A non-linear electric load connected to the alternator to provide a stable operating point of the complete system. In this setup, instrumentation is used to monitor the main variables (input and output current, input and output volt, dynamic gas pressure at exit of acoustic driver and inlet of linear alternator, dynamic gas pressure in the enclosure volume of the acoustic driver and linear alternator, acoustic driver stroke, linear alternator stroke, air and coil temperatures). The setup allows use of different resonators to simulate the effects of different front volumes on the performance of linear alternators and allows alterations in the enclosure volumes housing the acoustic driver and/or alternator to control their resonance frequencies. Results show the performance of a given linear alternator under different operating frequencies, mean gas pressure, gas mixtures, input voltage, electrical resistance and zener break-down voltage.

# Chapter 1 - Introduction

Thermoacoustics deals with the rich interactions between thermodynamics and acoustics. It uses the combinations between thermal gradients and acoustic vibrations either to convert heat supplied at a certain temperature gradient into acoustic energy (which is one form of mechanical work) or to generate a refrigeration effect using input acoustic power.

In any sound wave, there exist coupled pressure, displacement, density, and temperature oscillations. The pressure oscillations induce temperature oscillations which in turn cause heat transfer to (or from) nearby solid surfaces. The combination of these oscillations and the placement of enough solid walls at the proper position in the acoustic wave, close enough to the heated or cooled areas in the gas, produce a rich variety of thermoacoustic effects.

The presence of a solid surface will cause a thermal boundary layer to form in the acoustic field. In this boundary layer, heat transfer takes place between the oscillating gas parcels and the solid surface, resulting in a positive transfer of heat from one end of the solid surface to the other, whose direction depends on whether the device is a heat engine or a refrigerator. The phenomenon of non-zero net heat transport that occurs in an acoustic field is designated the “thermoacoustic effect”.

## 1.1 Thermoacoustic Devices

There are two main types of thermoacoustics devices: thermoacoustic engines (TAE) and thermoacoustic refrigerators (TAR)

In thermoacoustic engines (TAE), thermal energy converted into acoustic energy. The heat must be supplied at a temperature gradient, larger than a certain critical limit known as the critical temperature gradient. The temperature gradient is imposed on the thermoacoustic core (known as a stack in standing-wave engines or a regenerator in travelling-wave engines), which is a porous material sandwiched between two heat exchangers (hot and ambient). The heat applied to the hot heat exchanger and the heat rejection occurs at the cold heat exchanger, the heat transfer rates must be matched to sustain the imposed temperature gradient along the stack/regenerator to be larger than the critical temperature gradient.

In thermoacoustic refrigerators (TAR), acoustic energy introduced into the system by acoustic drivers and used to move heat against a temperature gradient. This takes place via the interaction between the supplied acoustic wave and a solid surface placed at the proper position in the wave.

## 1.2 History of Thermoacoustics

The first observation of thermoacoustics was in the mid of nineteenth century. Glassblowers noticed that when a high temperature glass bulb connected to a relatively cooler bulb a tone would be emitted [1]. This was known as a Soundhauss tube after a German who quantitatively studied the sounds. By the end of the 1800's, Lord Rayleigh found that these tones (pressure oscillations) take place when heat is added to gases at high density and taken from it at low density [2].

**Figure 1.1** shows one of the very first power converters that presented by a patent [3] to Bell Telephone Laboratories around 1950. A heat from an open flame converted to acoustic power with a thermoacoustic engine based on the idea of a Soundhauss tube. This generated acoustic power converted into electricity by cycling an acoustical-to-electrical transducer with an efficiency less than 10%. This engine considered as a breakthrough in the thermoacoustic field as no moving parts were required to convert heat energy into electrical energy; hence, it was not expensive to build besides being reliable.

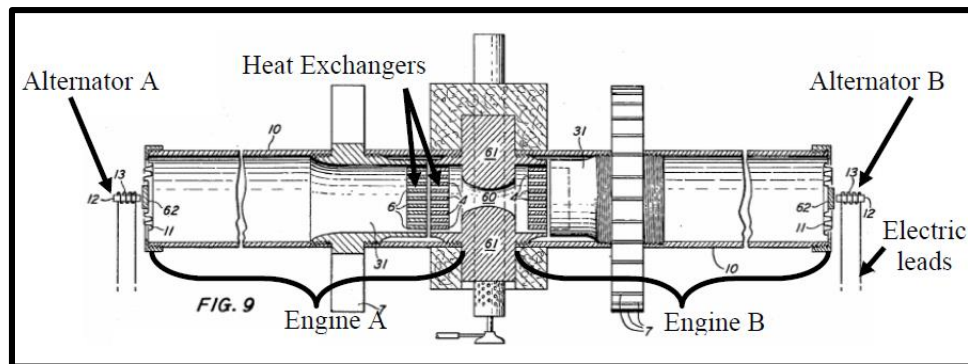


**Figure 1.1:** One of the very first TAPC [3]

In 1979, it was found that enhancement for the thermoacoustic engines efficiencies could be achieved if the acoustic wave produced was forced to undergo phasing similar to the inherently reversible and thus highly thermally efficient Stirling thermodynamic cycle [3].

In 1998, a hybrid thermoacoustic-Stirling engine was demonstrated but it suffered from some inefficiencies due to heat and viscous losses [4]. These problems mainly solved a year later to result in the first hybrid thermoacoustic-Stirling engine converting 30 % [5] of the input heat to acoustic power with no moving parts, which was 50 % better than the most efficient of the non-hybrid thermoacoustic engines. This engine subjected to some updates and modifications to reach an efficiency of 38 % [6].

In 2003, a hybrid thermoacoustic-Stirling engine was built but this time it was connected to two linear alternators to convert acoustic energy to electric energy [7]. **Figure 1.2** shows the engine that successfully generated 57 Watts with 30 % heat o acoustic efficiency and 17.8 % thermal to electric efficiency.

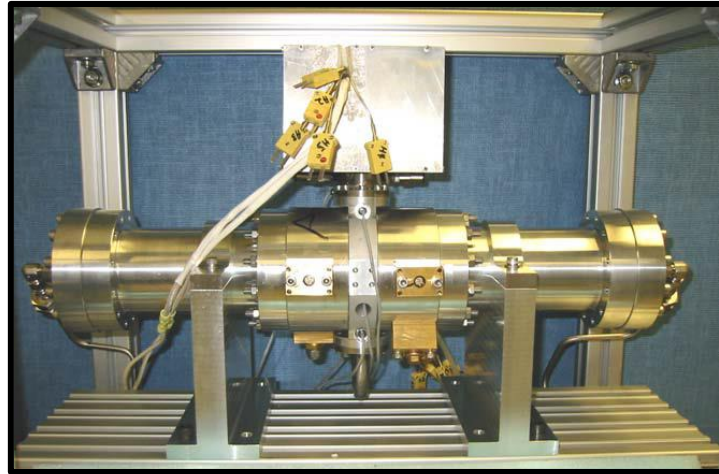


**Figure 1.2:** Los Alamos National Lab traveling-wave thermoacoustic electric generator [7]

### 1.3 Modes of Operation

There are two categories of thermoacoustic engines classified by the oscillating wave type: Standing-wave thermoacoustic engines operate on a cycle similar to that of Brayton cycle. Travelling-wave thermoacoustic engine operate on a thermodynamic cycle similar to that of the Stirling cycle.

#### 1.3.1 Standing Wave Engines

Standing-wave thermoacoustic engines operate on a cycle similar to that of Brayton cycle.

##### 1.3.1.1 Standing Wave Engines Components

As shown in **Figure 1.3**, the standing-wave engine consists of a long tube (resonator) closed from one end and a linear alternator fitted to the other end. A thermoacoustic element (stack) inserted inside the resonator and two heat exchangers fitted on the both sides of the stack. One of the main advantages of these engines is the simple structure.

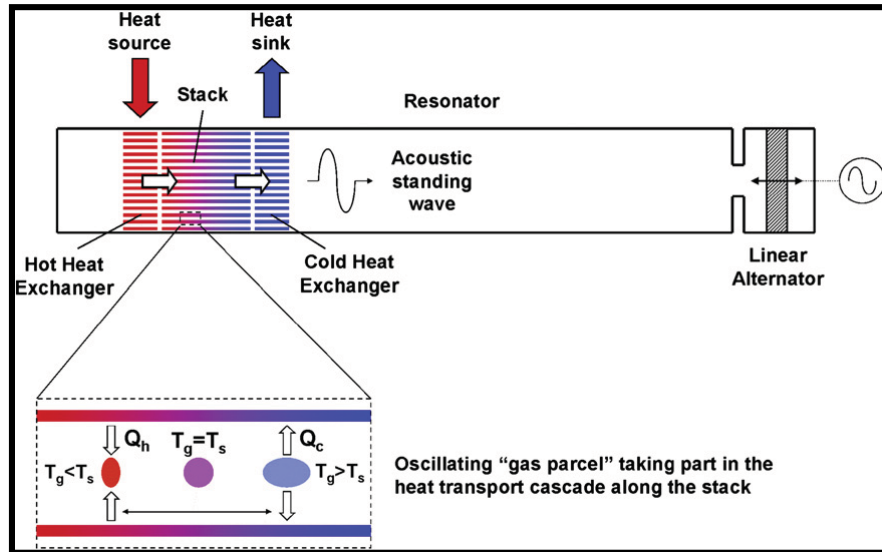


**Figure 1.3:** Schematic for standing-wave thermoacoustic engine [8]. The arrow shows the direction of the acoustic power

### 1.3.1.2 Standing Wave Engines Operation

The thermodynamic processes are adiabatic compression, constant volume heat addition, adiabatic expansion and constant volume heat rejection, as shown in the different diagrams in

**Figure 1.4.**

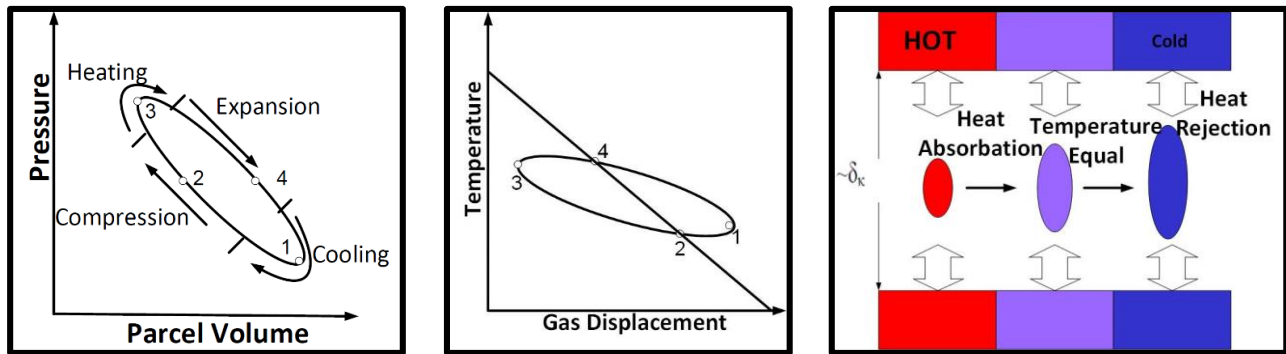


**Figure 1.4:** Relationships between pressure, parcel volume, temperature and axial location of the parcel in standing-wave engine [9]

In standing-wave thermoacoustic engines, the temperature of the gas parcel is always different from the temperature of solid plates. A stack used to satisfy this condition. The spacing between the stack cells should be 3-5 times the thermal penetration depth [10]. A higher value would cause large amounts of the gas to experience adiabatic compression and expansion with no thermoacoustic interactions with the solid walls and thus would decrease the output power and the conversion efficiency. A lower value would cause excessive pressure drop across the stack and large viscous dissipation losses.

Due to the pressure oscillation in the flow there is a temperature oscillation as well. This temperature oscillation creates an adiabatic temperature gradient. Once the temperature gradient across the stack becomes greater than the adiabatic temperature gradient, a sound wave generated. This implies that the acoustic wave is not generated unless the applied temperature gradient exceeds a certain critical temperature gradient.

The generated sound wave has a phase shift close to 90 degrees between the pressure and the velocity waves as shown in **Figure 1.5**. A standing-wave engine with a perfect stack will not deliver acoustic power because pressure and velocity are exactly 90 degrees out of phase. Thus, standing-wave engine operates only when there is less than 90 degrees between dynamic pressure and velocity. This condition achieved with imperfect heat exchange between the solid stack wall and the working gas, hence the term stack rather than regenerator.

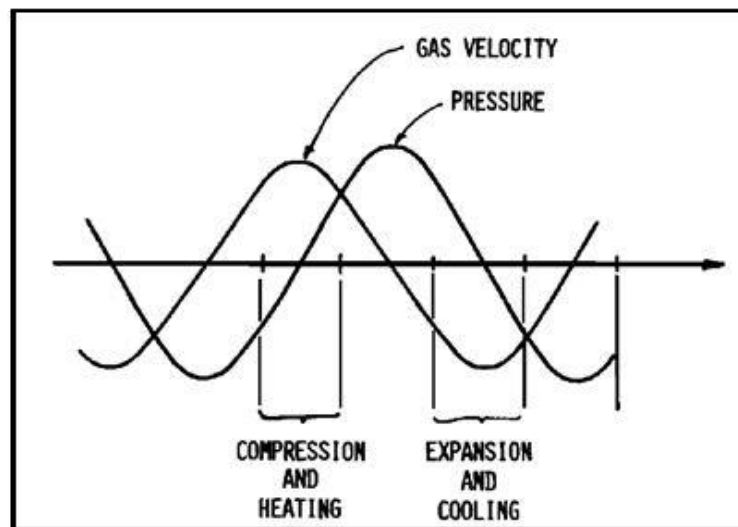


**Figure 1.5:** Dynamic pressure and gas parcel velocity waveforms in standing-wave engines [2].

The dynamic pressure and velocity are in nearly 90 degrees out of phase through the stack

Inside the stack, the gas pressure oscillations are intermediate between perfectly isothermal at the solid–gas interface and nearly adiabatic at distances larger than the thermal penetration depth. This imperfect thermal contact between the gas and the solid introduces a phase shift between the pressure and temperature of the gas over a distance within a few times of the thermal penetration depth. The developed phase shift provides a simple and natural mechanism to produce the required phasing in standing-wave engines. Heat exchange occurs only at the peaks of the gas parcels displacement that causes an inherent irreversibility and thus lower efficiency in standing wave thermoacoustic engines.



This imperfect heat transfer introduces a slight phase shift and hence the required less than 90 degree condition needed for the operation is achieved. Standing-wave engines operate typically at over 85 degrees of phase shift between dynamic pressure and velocity, which makes a high reactive (out of phase) pressure component. This reactive component is resolved either by a long resonant pipe that is expensive, or by a high mass linear alternator (LA) [11].

However, to obtain a resonant high-mass linear alternator requires a large spring. A high-power linear alternator requires a large coil excursion and the combination of a large spring and large excursion is difficult to achieve [12]. These factors limit the use of standing-wave thermoacoustic engines to low power.

### 1.3.1.3 Standing Wave Engines Performance Estimation

For Standing-wave engines, a good estimate of the order of magnitude of the acoustic power flowing through the regenerator is given by [10]:

$$\sim \left(\frac{1}{8}\right) * |p_1| * |U_1| \sim \left(\frac{|p_1|}{P_m}\right) * \left(\frac{|u_1|}{a}\right) * \left(\frac{P_m * a * A}{8}\right) \quad (1)$$

## 1.3.2 Travelling Wave Engines

Travelling-wave thermoacoustic engine operate on a thermodynamic cycle similar to that of the Stirling cycle.

### 1.3.2.1 Travelling Wave Engines Types and Components

The travelling-wave engine consists of a torus attached with the resonator, as shown in **Figure 1.6** and **Figure 1.7**. A thermoacoustic element (regenerator) inserted inside the resonator and two heat exchangers fitted on the both sides of the regenerator. One extra heat exchanger used to remove the additional heat from the working fluid. The regenerator acts as a velocity amplifier and adds power to the wave. The wave passes to the linear alternator that then extracts power.

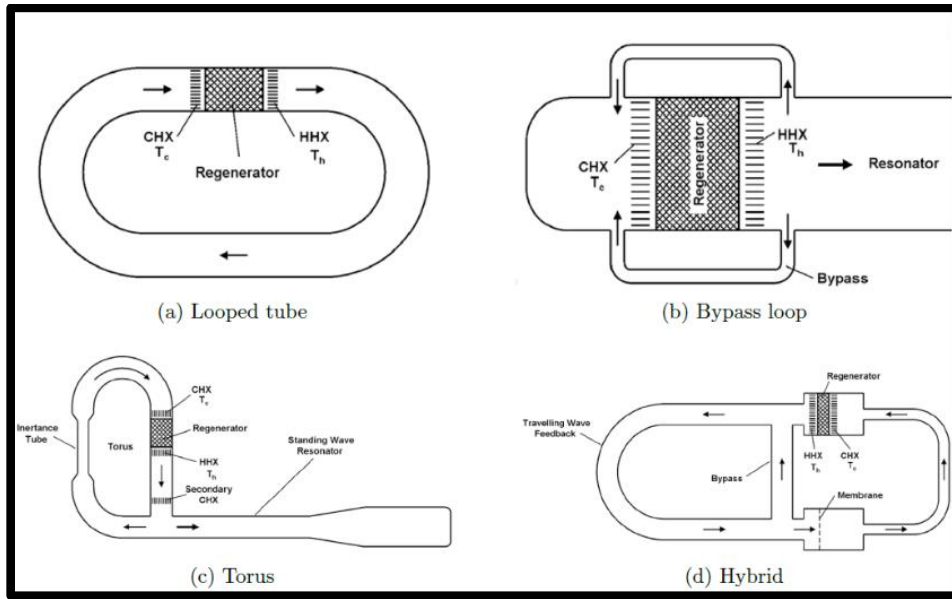


Figure 1.6: Various traveling wave engine designs [9]

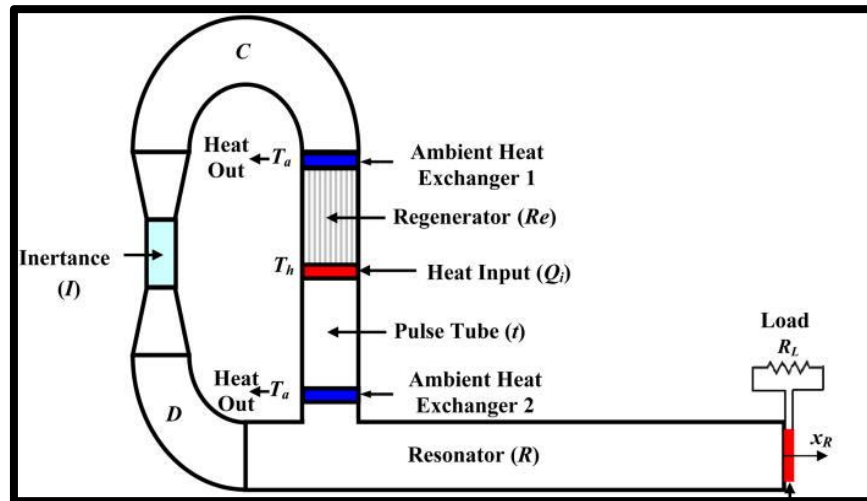
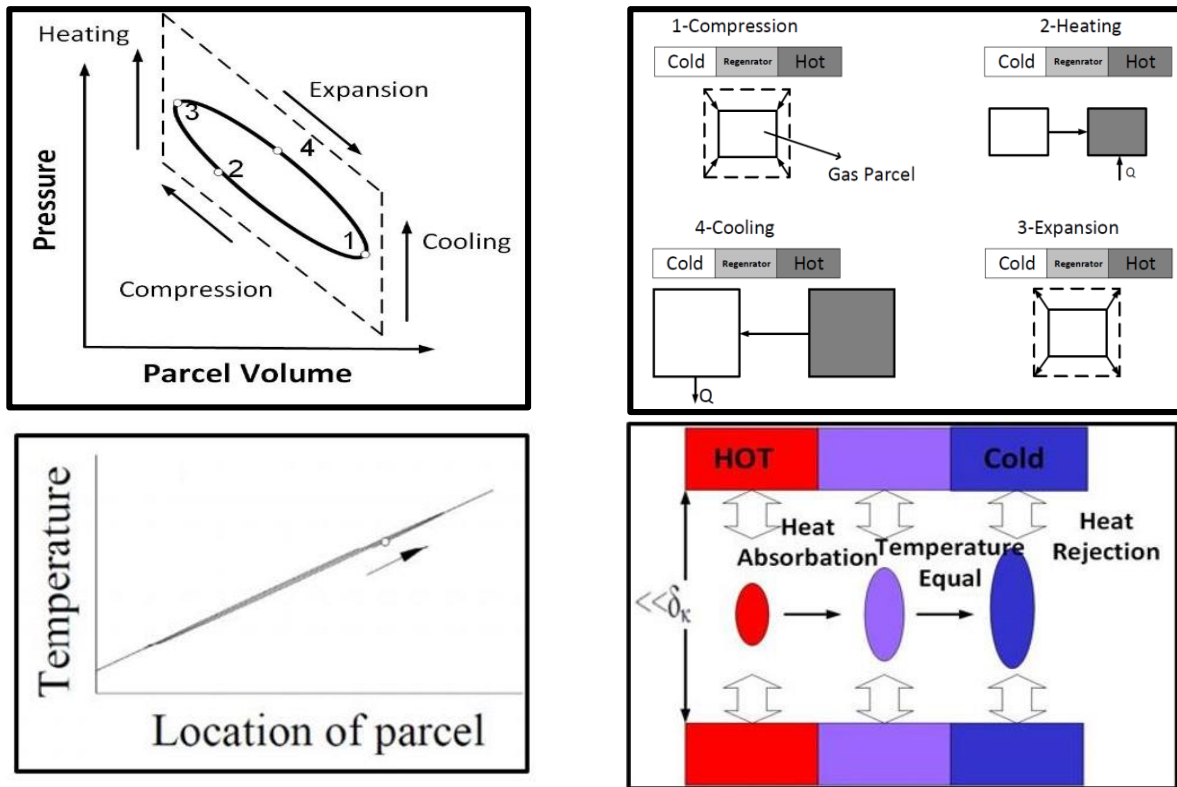


Figure 1.7: Schematic for travelling-wave thermoacoustic engine [6]

### 1.3.2.2 Travelling Wave Engines Operation

The thermodynamic processes are isothermal compression, constant volume heat addition, isothermal expansion and constant volume heat rejection, as shown in the diagrams of Figure 1.8.



**Figure 1.8:** Relationships between pressure, parcel volume, temperature and axial location in travelling-wave engine. [9]

To simulate the Stirling cycle, the temperature of the gas parcel has to be the same as the temperature of solid plates. In order to satisfy this condition a regenerator is utilized. The spacing between the plates of regenerator must be less than the thermal penetration depth. In these engines, the dynamic pressure and velocity are in phase through the regenerator as shown in **Figure 1.9**.

The small pores in the regenerator necessitates a small gas parcel velocity inside the regenerator to avoid large viscous dissipation. Hence, for a travelling-wave engine to perform efficiently and to produce large power density, it is critical to increase the magnitude of the pressure oscillations and reduce the magnitude of the velocity oscillations (i.e., increase the acoustic impedance). This should be done while maintaining the magnitude of their product (i.e., the acoustic power).

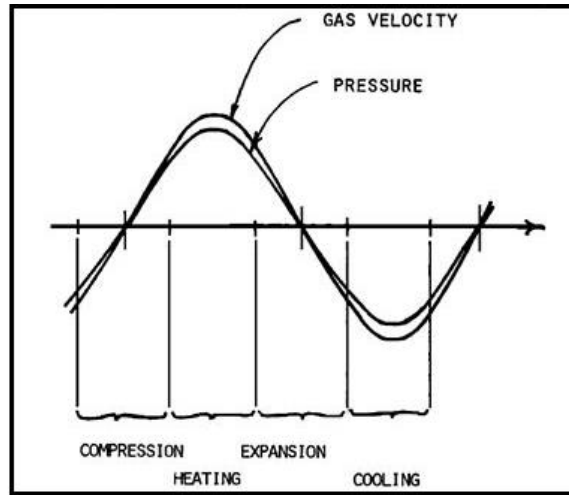


**Figure 1.9:** Dynamic pressure and gas parcel velocity waveforms in travelling-wave engines [2].  
The dynamic pressure and velocity are nearly in phase through the regenerator

### 1.3.2.3 Traveling Wave Engines Performance Estimation

For travelling-wave engines, a good estimate of the order of magnitude of the acoustic power flowing through the regenerator is given by [10]:

$$\sim \left(\frac{1}{2}\right) * |p_1| * |U_1| \sim \left(\frac{|p_1|}{P_m}\right) * \left(\frac{|u_1|}{a}\right) * \left(\frac{P_m * a * A}{2}\right) \quad (2)$$

## 1.4 History of Thermoacoustic Heat Engines

Linear alternators are the parts in TAPC that are responsible for converting the acoustic power generated by the thermoacoustic engine into electric power. Similar to them are the acoustic drivers, which convert electric energy into acoustic energy.

The last decade had witnessed significant development in the generation of electric power from different sources of heat energy through acoustic power. In 2004, thermoacoustic heat engine was constructed that generated 57 Watts of electricity at 17.8 % efficiency. The engine operated using helium at 52 bar with the hot heat exchanger at 900 K and the cold heat exchanger at 353 K [7].

Later in 2006, a thermoacoustic engine was built and operated that could generate 70 Watts of AC electricity but with overall conversion efficiency 11.4 % due to the losses in the hot heat exchangers. this engine operated using helium 30 bar with hot and cold heat exchangers 950 K and 320 K respectively [9].

After that in 2011, a thermoacoustic engine was designed and tested that have relatively low conversion efficiency of 7 % due to excessive streaming in the engine. On the other hand, the

engine was able to generate 100 Watts of electrical power. It used helium at 33.5 bar mean pressure and operated between 873 K hot side temperature and 373 K cold side temperature [13].

In 2012, another thermoacoustic heat engine was operated using helium at 35 bar and over all conversion efficiency of 15 % was able to produce 200 Watts of AC electric power [14]. Finally, in 2014, Qnergy announced that it was able to manufacture a thermoacoustic Stirling heat engine that could generate 1 kW of electrical power during a field test completed at its test facility in Ogden, Utah [15].

## 1.5 Advantages and Challenges of Thermoacoustic Heat Engines

In addition to their design simplicity, Thermoacoustic heat engines manufactured from standard materials that are available in commercial quantities. This essentially reduces the initial cost of such systems and makes them attractive for use in rural areas remote from electricity grids. Another significant advantage is that these systems operate with almost no mechanical moving parts, significantly reducing the cost of maintenance and increasing their operational life. The only moving parts are the acoustic drivers/linear alternators that used to supply the acoustic power in thermoacoustic refrigerators or to extract it in the case of thermoacoustic engines. These explained in more details later in this chapter.

Additionally, these devices utilize environmentally friendly working gases, with no ozone depletion or greenhouse effects. Moreover, a thermoacoustic engine is an external heat engine, in which heat supplied outside the main core of the engine, which facilitates the engine's integration with solar or waste heat sources, making this technology very attractive for solar/waste heat energy applications.

In addition, a thermoacoustic engine converts heat into mechanical power without involving combustion processes or emissions to the environment.

On the other side, thermoacoustic engines still face some challenges, including:

- The device has low power density.
- The linear alternators that are commercially available to convert acoustic energy into electricity currently have low efficiencies compared to rotary electric generators, and only expensive specially-made alternators can give acceptable performance.
- Efficient heat exchanging processes are critical to maintain the power conversion process in TAE. The hot heat exchanger is required to transfer heat to the stack/regenerator and the cold heat exchanger, located on the other side of the stack, has to remove heat at a rate high enough in order to sustain the temperature gradient across the stack/regenerator. However, the heat exchangers cause large blockage to the wave and the oscillating nature of the flow

limits the use of already-developed correlations that are applicable under steady-state conditions.

- The acoustic wave that is self-generated inside the engine at large pressure ratio suffer many kinds of non-linearity like turbulence (causes energy dissipation due to viscous effects), harmonic generation of different frequencies (carries acoustic power in frequencies other than the fundamental frequency and those are not useful to the load).

## 1.6 Principle of Operation of Linear Alternators

The principle of operation is based on the Lorentz force which is induced when relative motion occurs between an electrical conductor, through which a current flows and a magnetic field. Lorentz force on the coil given by:

$$F = B L I \quad (3)$$

### 1.6.1 Types of Linear Alternators

Linear alternators can be of two main types, i.e. moving coil and moving magnet. The moving magnet type is most common now in thermoacoustic power converters. Moving coil technology commonly used only for very small power sizes or for loudspeaker construction, where linearity is preferred over efficiency because they suffer from reliability problems caused by flexible conductor carrying current from the moving coil, large air gaps, reduced efficiency and increased mass of the moving coil.

The following points list the advantages and limitations of the moving-magnet linear alternators, with respect to moving-coil type:

- The magnetic flux generated without external power, thus reducing energy costs, and easing the heat dissipation. Additionally, the flux density can be high and accurately controlled.
- The windings are bonded directly to the yoke giving rise to high reliability and compact structure.
- The oscillating frequency and amplitude of the moving magnet linear actuator can easily controlled.
- Small size and weight, reasonable power handling capacity, reasonable stroke limits (peak-to-peak values in the range of 10 – 20 mm).
- Demonstrated high acoustic-to-electric transduction efficiency.

- Long maintenance-free lifetimes. Some systems have been in continuous operation for over 8 years. Calculated theoretical mean time between failures (per military standard method MIL-STD217F) is 129,760 hours [16].
- There are no wearing parts in the alternator, no traditional bearings, and no sliding seals. Operation without lubrication is possible thanks to a set of flexure bearing. A flexure bearing is composed of a stack of several spiral-cut circular metallic plates with a piston attached to its center. The stack of plates forms a “bearing” that is extremely stiff with respect to radial, twisting, or rocking motion of the piston and is relatively soft in the axial direction. This allows the piston to move in its cylinder with a radial clearance as small as 10  $\mu\text{m}$ . The stiff flexure bearing keeps the piston from touching the cylinder and the small clearance effectively forms a non-wearing seal that requires no lubrication. The flexures designed to operate at very low stress, and each type of flexure subjected to a test to confirm its long-life potential (through accelerated testing at increasing levels of stress).
- One of the main complications in linear alternators is the need for tight control of the length of the stroke of the piston assembly, to avoid having the piston contact the cylinder head at its furthestmost outer position.

## **1.6.2 Linear Alternators Matching**

Two types of matching must be achieved simultaneously in order to allow the linear alternator to work at or near its maximum efficiency and be able to reach its rated electric power output. These types of matching are acoustic matching and load matching.

### **1.6.2.1 Acoustic Matching**

The matching conditions between an acoustic driver and an acoustic load in an acoustic resonator was summarized. These conditions must be satisfied simultaneously at full rated power and they are:

- The acoustic driver must be operated at the design frequency of the acoustic load.
- The acoustic driver must operate at its resonant frequency.
- The acoustic driver must deliver the proper acoustic power to the acoustic load.
- The values of the pressure and volume velocities (i.e., volumetric flow rate) amplitudes and phases must be matched to a design point of the acoustic load.
- The acoustic driver must operate at the full design stroke when operated at full rated power.

The last condition implies that if full acoustic power delivered at less than the rated stroke, excessive driver current will be required. On the other hand, if full rated power delivered at more than the rated stroke, the machine will be stroke-limited and never achieve its rated capacity.

Similarly, operating with full stroke at less than the rated power means carrying the full overhead of motion losses incurred at rated power, while operating at only a fraction of that power. This requires complete understanding of how to control the stroke. Further explanation is that depending on which parameters considered first in the design stage, it is possible in an imperfect design that the design frequency for the acoustic load will not match the resonant frequency of the complete system, or alternatively full acoustic power will not be delivered at full rated stroke [17].

### **1.6.2.2 Load Matching**

The electric load controls the stroke of the linear alternator and the acoustic-to-electric conversion efficiency of the linear alternator. Moreover, the combined system made of the thermoacoustic engine, linear alternator and load must have a single intersection point between the power produced by the engine versus stroke and the power absorbed by the load versus stroke. The power produced by the thermoacoustic engine running on a Stirling cycle is a quadratic function with voltage (and hence approximately quadratic with stroke). A load made of simple resistors has its power absorption also quadratic with voltage (and therefore also with stroke) and thus no stable intersection point exists between the alternator and a simple resistive load since both have quadratic dependence with voltage and stroke.

If the combined system is perfectly balanced, then it will run in a stable mode. However, a perfect balance is not possible or sustainable, especially in the start-up and shutdown operation modes of the combined system.

One of the methods that can be used to resolve this issue is to use a non-linear load, in which the absorbed power is not in proportion to the square of the voltage. Systems built with purely resistive loads suffered from instability of operation and inability to properly test the thermoacoustic engine and the linear alternator [9].

It should be noted that non-linear loads are needed only during initial testing in laboratories because once the thermoacoustic engine and the linear alternator are connected to the grid, the output voltage (and hence the stroke) are imposed by the grid and no special loads are needed then.

Non-linear loads can be made using back-to-back zener diodes, as suggested by [7], or by using an electronic load device, that allows constant voltage or constant current operations. The experimental setup allows the operator to adjust the operating conditions -as shown in chapter 2- (gas mixture composition, mean gas pressure, input acoustic power, operating frequency and load



value) in order to satisfy both proper acoustic matching between the linear alternator and the input acoustic power as well as proper matching with the load. Which should translate into stable operation with high conversion efficiency at the desired stroke.

## **1.7 Scope of This Work**

The purpose of this work is to test a linear alternator in a controlled environment to integrate it into a thermoacoustic heat engine. The linear alternator is driven by an acoustic driver rather than a thermoacoustic engine to make sure that the experiment is well controlled and the data can be reproducible. This allows us to avoid the effect of streaming that are associated with the use of a thermoacoustic engine to drive the alternator. The frequency and intensity of the supplied acoustic power can be easily controlled via a function generator and a power amplifier.

DeltaEC used to provide an initial acoustic design of the system to make sure that the acoustic power will be transferred efficiently from the acoustic driver to the linear alternator for the suggested geometry.

The built setup is built to include the necessary controls (e.g., stroke control circuit) needed to protect the alternator during the test and the necessary instrumentation needed to evaluate its performance. Although the current setup can operate in a stable manner using linear loads (e.g., simple resistors), the real application in thermoacoustic power converters requires non-linear loads. Accordingly, the used experimental setup uses non-linear loads.

## Chapter 2 - Experimental Setup and Procedure

The main purpose of the experimental setup is to provide a flexible platform to test linear alternators under different operating conditions in a controlled environment with all potential issues related to thermoacoustic engines decoupled. To do such decoupling, we use an acoustic driver to drive the linear alternator.

### 2.1 DeltaEC

Design Environment for Low-Amplitude Thermoacoustic Energy Conversion (DeltaEC) [18], is a computer program that solves one-dimensional wave equation in gases to determine the spatial dependence of the acoustic pressure and velocity in thermoacoustic devices. It contains different types of segments (purely acoustic, lumped impedances, electro-acoustic transducers, thermoacoustic stacks and thermoacoustic heat exchangers).

In this work, DeltaEC has been used in order to make a preliminary acoustic design for the experimental setup

The DeltaEC code consists of different segments that are connected in series to each other to simulate the system built. Appendix A and Appendix B presents details of each segment and the full DeltaEC code.

The main purposes of the DeltaEC simulation are to make sure that the suggested geometry of the system (resonator length and enclosures dimensions) will allow efficient transfer of acoustic power from the acoustic driver into the linear alternator and to identify a starting value for the operating frequency that will be used in the experimental work as a starting point. Table 2.1 show the main system dimensions used in the DeltaEC simulation and then in the experimental setup. While, **Figure 2.1** shows a schematic of the preliminary design of the experimental setup.

**Table 2.1:** System main dimensions

Parameter	Value
Resonator length, mm	50
Resonator diameter, mm	50
Acoustic driver enclosure diameter, mm	100
Acoustic driver enclosure length, mm	130
Linear alternator enclosure diameter, mm	100
Linear alternator enclosure length, mm	130

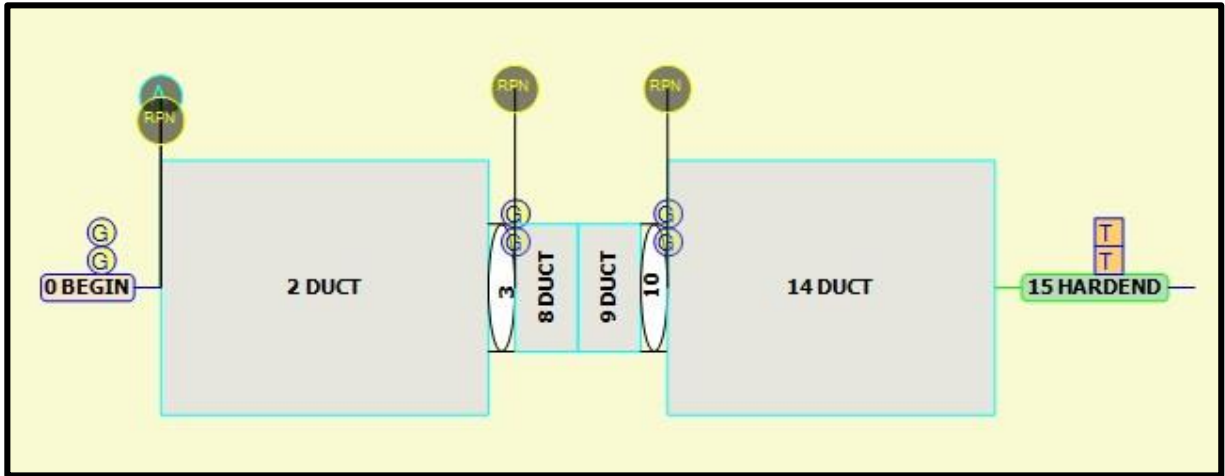


Figure 2.1: System schematic from DeltaEC

## 2.2 Experimental Setup

The setup designed in a modular form to allow ease of change of different components to facilitate studying the effect of different parameters (e.g., front and back volumes) on the behavior of the linear alternator. A schematic of the setup shown in **Figure 2.2** and the instrumentations used are listed in Table 2.2, while **Figure 2.3** shows a digital image of the setup.

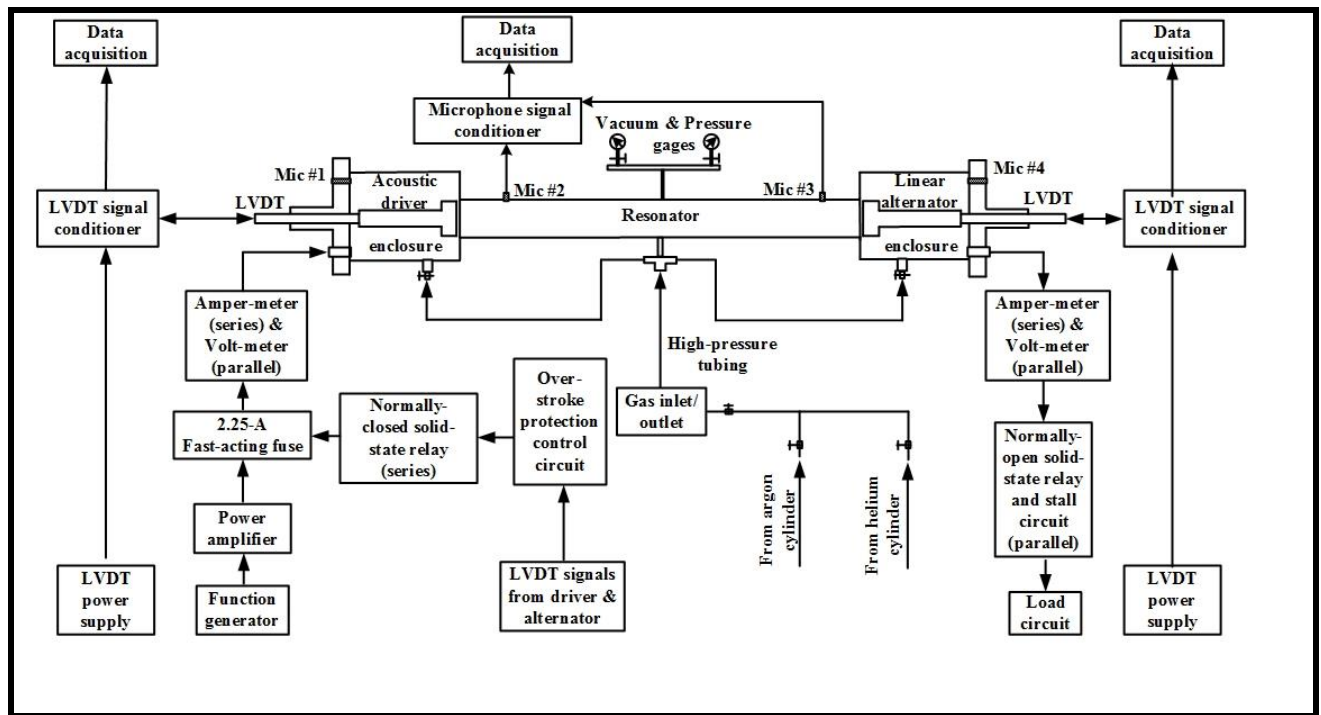
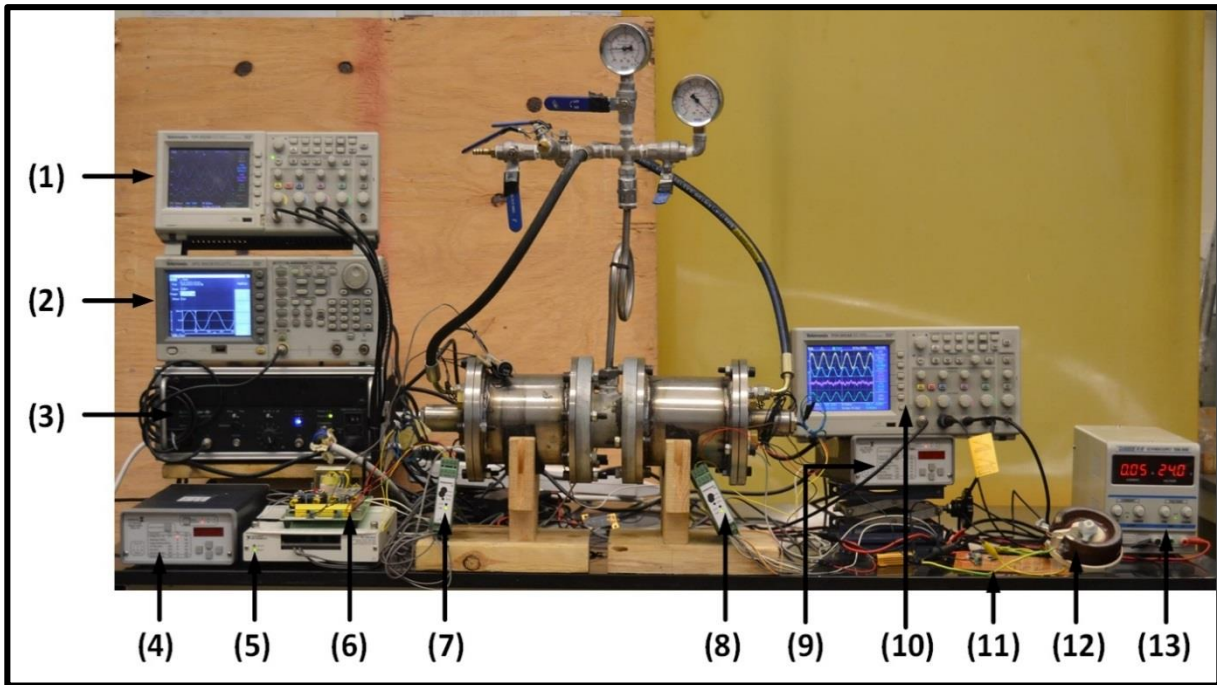


Figure 2.2: Schematic showing the linear alternator under test and the accessories and instrumentation used.



**Figure 2.3:** Digital image for the experimental setup

**Table 2.2:** Experimental setup instrumentation list

Item No.	Item description
1	Input data measuring oscilloscope
2	Function generator
3	Power amplifier
4	DC amplifier
5	Data acquisition card
6	Stroke control circuit
7	LVDT signal conditioner (acoustic driver)
8	LVDT signal conditioner (linear alternator)
9	DC amplifier
10	Output data measuring oscilloscope
11	Zener diode set
12	Rheostat
13	LVDTs power supply

## 2.3 Setup Components:

### 2.3.1 Resonator

The resonator (AKA front volume) is responsible for delivering the acoustic energy from the source of acoustic energy typically a thermoacoustic engine (an acoustic driver in this work) to the linear alternator. The inner surface of the resonator must be of very low surface roughness. This is achieved by using polished stainless steel or polished galvanized steel.

The resonator has two flanges to allow assembly with the enclosure volumes carrying the acoustic driver and the linear alternator. In addition to, it has the following instrumentation ports:

- One gas inlet/outlet port (1/2-inch threaded).
- One thermocouple (1/2-inch) feed through to connect a type-E thermocouple to measure the mean gas temperature inside the resonator.
- Two through openings with M5 thread used to connect dynamic pressure microphones

The round surface of the resonator is flattened using a vertical milling machine at the interface of these ports in order to enhance the sealing of the system and to avoid any gas leakage.

Three resonators of different lengths (5 cm, 15 cm and 25 cm) are manufactured to allow studying the effects of different front volumes on the performance of the linear alternators. These lengths are measured from the face of the piston of the acoustic driver to that of the piston of the linear alternator.

A digital image of the resonator is shown in **Figure 2.4**, while Appendix C shows the mechanical drawings of all three resonators.

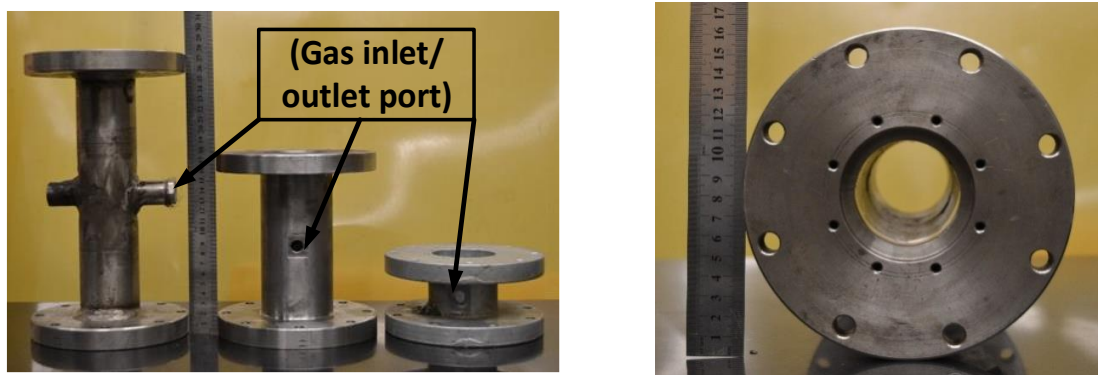


**Figure 2.4:** Left: Three used resonators. Right: flange of one of the resonators

### 2.3.2 Enclosure Volume

The acoustic driver and alternator are housed inside enclosures (AKA back volumes). Enlarging the enclosure volume reduces the pressure wave in the backspace, which in turn reduces the thermal relaxation loss and the seal loss causing an improvement in the conversion efficiency. On the other hand, the increase in volume decreases the TAPC's power density. So, the volume of the enclosure should be optimized to achieve both high conversion efficiency and high power density. **Figure 2.5** shows a digital image of the enclosure volumes. Appendix C presents the mechanical drawings.

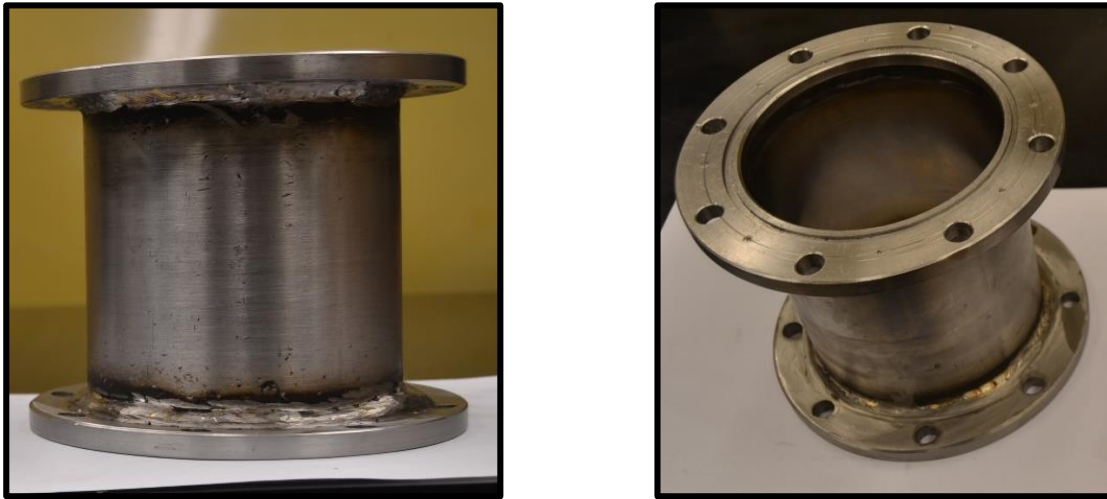


**Figure 2.5:** Top: The alternator volumes used to house the acoustic driver and the linear alternator.  
Bottom: Flange of one of the alternators

The enclosure volume has two flanges. The first one to connect it with the resonator. The other one contain the feed in/out ports as following:

- Electric power input/output feed through (1/2 inch).
- Thermocouple (type E, diameter 810 um) used to measure the mean gas temperature inside the enclosure volume.
- LVDT port to mount the LVDT probe. The LVDT measures the piston displacement.
- Dynamic pressure microphone (Meggitt, Model 8530C-500M5) used to measure the gas dynamic pressure wave at the back of the piston. This is used, in conjunction with the LVDT signal measuring the piston displacement, to estimate the alternator-space thermal (hysteresis) losses.
- Mean pressure equalization port used to equalize the mean pressure between the enclosure volume and the resonator during system charging and discharging.

Figure 2.6 shows a digital image of one of the enclosure volume flanges, while the mechanical drawings presented in Appendix C.

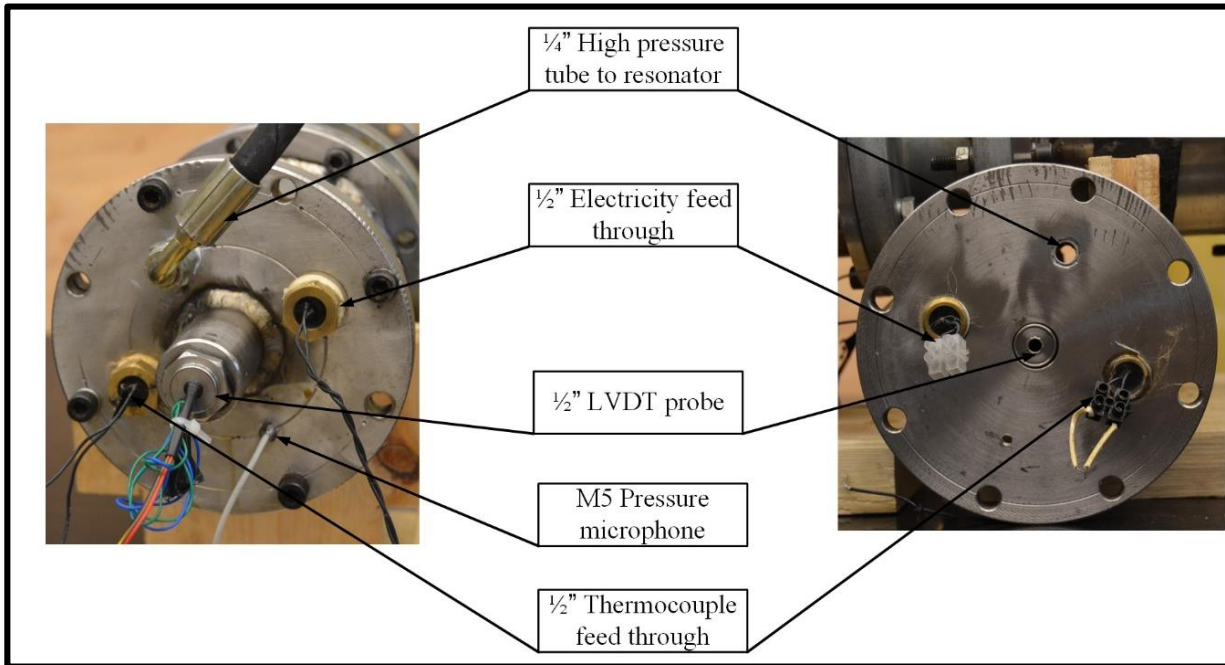


Figure 2.6: Left: outer side of enclosure flange. Right: Inner side of the flange

### 2.3.3 Hydrostatic test

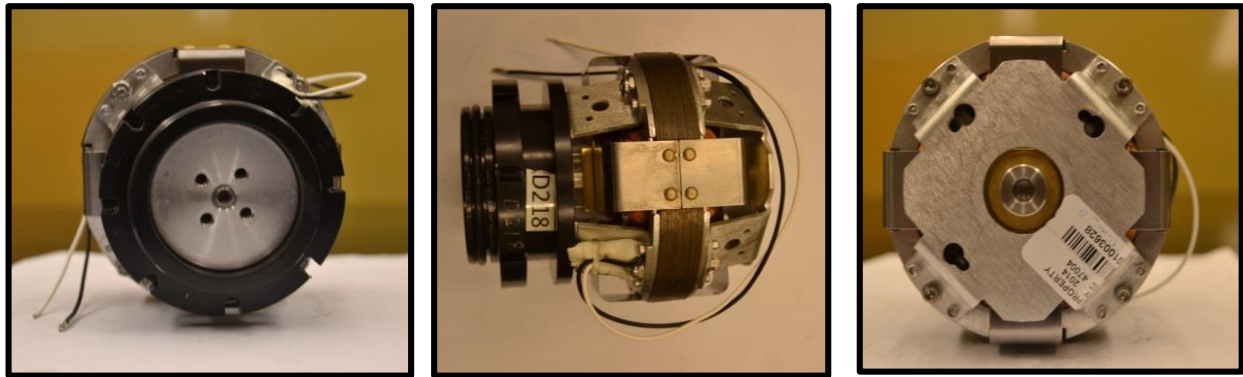
The mechanical design of the resonator and enclosures followed the ASME standards [19]. The resonator and the enclosures are made of steel and they are designed to withstand operation at 40 bar and are tested hydro-statically (by the manufacturer) at 60 bar.

### 2.3.4 Acoustic Driver and Linear Alternator

The experimental setup contains an acoustic driver (model 1S102D, supplied by Q-drive). The acoustic driver in this setup is responsible for generating the acoustic power at the required frequency to simulate the acoustic power resulting from a thermoacoustic engine. This acoustic power drives a linear alternator (model 1S102D, supplied by Q-drive) to generate electricity. Table 2.3 presents the specifications for both of them. A digital image shown in Figure 2.7.

**Table 2.3:** Acoustic driver and liner alternator specifications [20]

Parameter	Acoustic Driver	Linear Alternator
Electric resistance, $\Omega$	6.70	6.72
Inductance, mH	86.4	84.1
Transduction coefficient BL product, N/m <sup>2</sup>	47.69	48.01
Moving mass, kg	0.4922	0.478
Intrinsic stiffness, kN/m	30.49	30.94
Damping, Rm, N.S/m	4.69	4.55
Free decay frequency, Hz	40.51	40.48
Maximum displacement, mm	6.23	6.14
Piston diameter, mm	50.8	50.8
Piston area, m <sup>2</sup>	2.03E-3	2.03E-3
Total weight, kg	1.6	1.6
Ambient operating temperature, °C	0-32	0-32
Nominal stroke, mm	10	10
Nominal power, W	125	100
Voltage at nominal power, V	100 (single phase)	100 (single phase)
Max. operating current, A	2	2
Fuse, A (fast-acting)	2.25	--

**Figure 2.7:** Three views for the used acoustic driver / Linear alternator

In order to operate the experimental setup at different frequencies and different values of input electric power a function generator (Tektronix Model AFG 3021B, single channel, generates signals at a rate of 250 MS/s) is used to energize the acoustic driver with a sinusoidal input wave. The generated wave amplified by a power amplifier (Bruel and Kjaer, Model 2734, 650 W) to the required value of power to be fed to the acoustic driver. This value controlled by the required intensity of the acoustic power.

A fast-acting fuse of 2.25 A (Model: BK/AGC-2.25-R, Supplied by DIGI-KEY) used to protect the acoustic driver against excessive current withdrawal. This value is within the limit recommended by the supplier of the acoustic driver (a maximum of 2.5 A). **Figure 2.8** presents a digital image of the function generator and power amplifier used in this work.



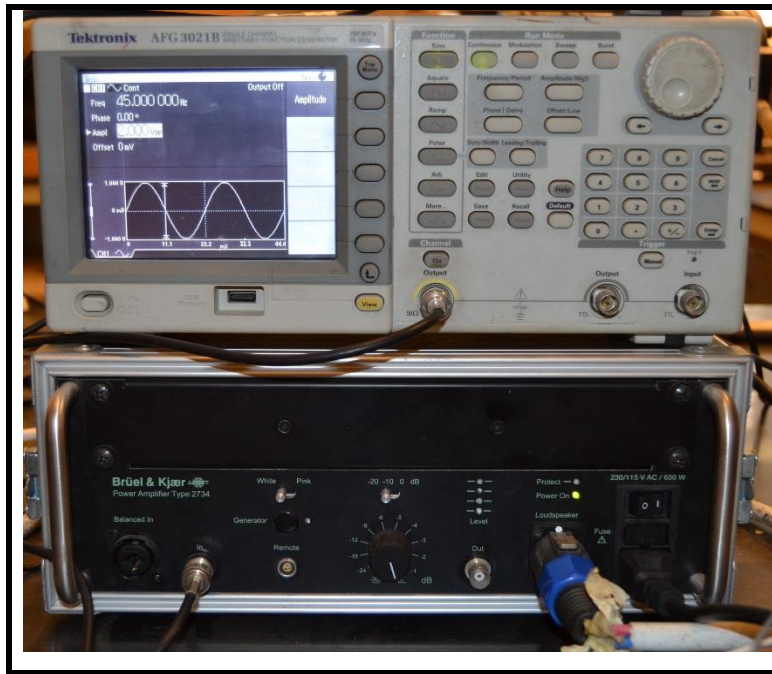


**Figure 2.8:** Top: Function generator. Bottom: Power amplifier

The temperature of the surface enclosing the motor should not exceed 45 C. A thermocouple is used to monitor this temperature. Forced convection or water-cooling in tubes wrapped around the housing can be used to avoid overheating if the input current results in higher surface temperature. Special care must be taken that the input current must not exceed 2A (RMS) in all cases. The ambient temperature should not exceed 35C, and the relative humidity should not exceed 95% [20].

### 2.3.5 Stroke-Control Circuit

The control logic used to protect against piston's over-stroking on the acoustic driver and/or linear alternator is shown in **Figure 2.9**. The stroke of each of the acoustic driver and the alternator is measured using LVDT's. Each LVDT signal is fed into a precision rectifier in order to get the absolute value of the LVDT signal, to provide over-stroking protection in either positive or negative directions. The output signal is fed into an analog comparator (LM324 Op-Amp). Such a signal it is compared against a preset voltage that corresponds to the maximum stroke limit where the result of the analog comparison takes a control action to prevent over-stroking.

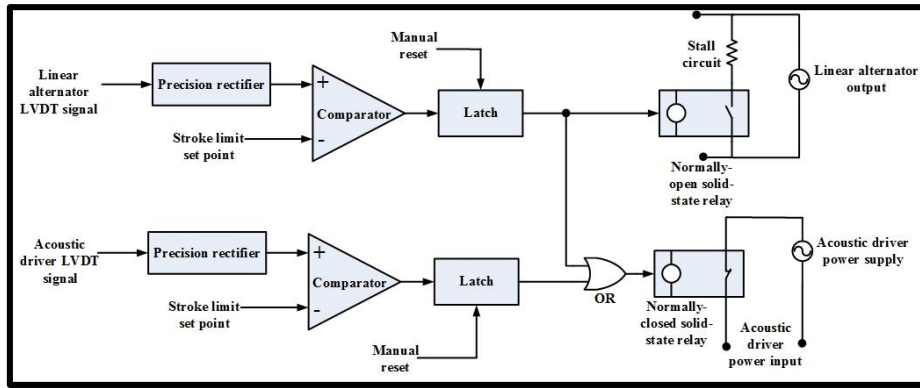


**Figure 2.9:** Control logic used to protect against over-stroking in the linear

If the alternator stroke exceeds the set point, two control actions occur: the input electric power supply to the acoustic driver is turned-off via a normally closed solid-state relay and a stall circuit is introduced parallel to the electric load via a normally open solid-state relay. The later provides a fast enough protection in TAPC's since the linear alternator will continue to operate for a significant time after the source of heat is turned-off. The stall circuit designed in such a way that it has a resistance lower than that of the load and a power rating capable of dissipating the full-generated electric power. The introduction of the stall circuit in parallel to the load reduces the overall resistance seen by the load causing the current generated by the linear alternator to increase and the voltage generated by the alternator to decrease, which forces the alternator stroke to decrease. In this work, the stall circuit is simply a two  $\Omega$  100 W resistance.

Additionally, if the driver stroke exceeds the set point, the input electric power is turned-off via the same normally closed solid-state relay. This operation is made using an analog OR gate. Once any of these control actions is initiated, it remains in effect until a manual reset is made by a human action, to avoid further operation until the cause of over-stroking is identified and resolved.

**Figure 2.10** and Appendix F shows the details of the circuit used for the control process.

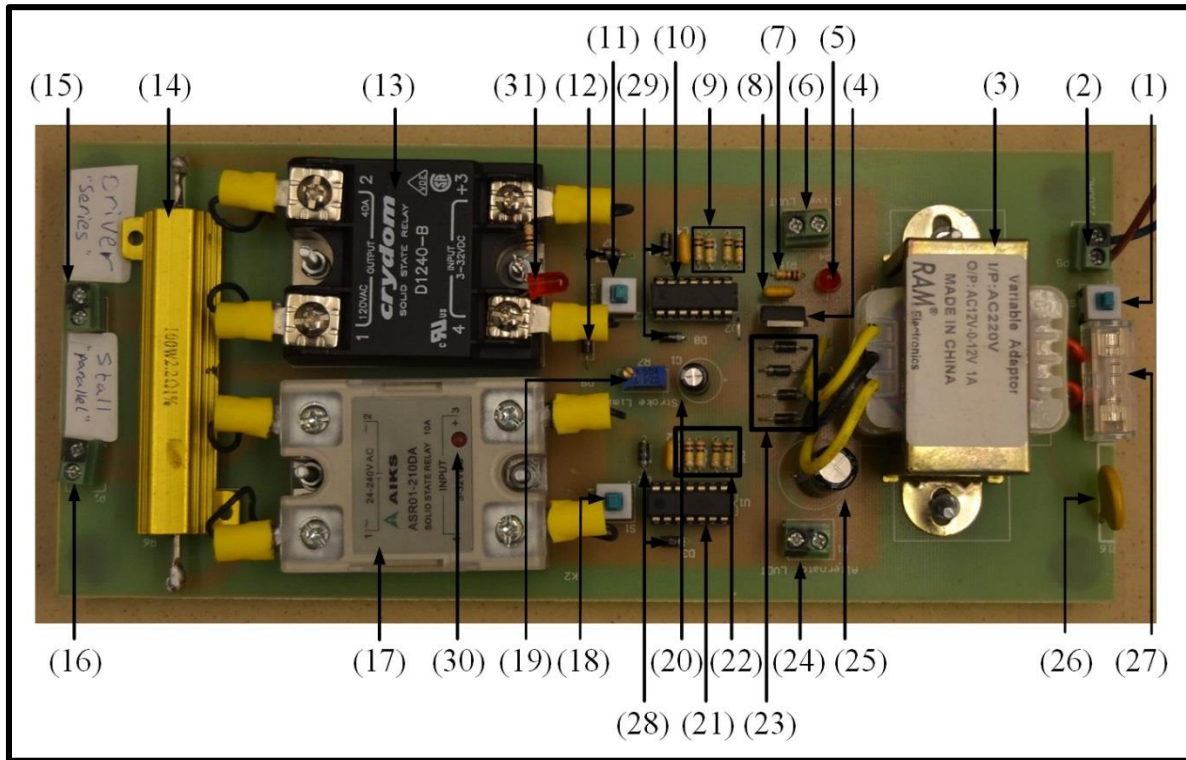


**Figure 2.10:** PCB of the stroke control circuit

### 2.3.6 Load Circuit

The setup allows the use and the control of different electric loads to study the matching between the linear alternator and the electric load. The electric load affects the stroke of the linear alternator and the acoustic-to-electric conversion efficiency of the linear alternator.

The combined system made of the thermoacoustic engine, linear alternator and electric load must have a single intersection point between the curve of the produced power by the engine versus stroke and the curve of power absorbed by the load versus stroke. The power produced by the thermoacoustic engine running on a Stirling cycle is a quadratic function with voltage (and hence approximately quadratic with stroke). A load made of simple resistors has its power absorption also quadratic with voltage (and therefore also with stroke) and thus no stable intersection point exists between the alternator and a simple resistive load curves since both have quadratic dependence with voltage and stroke.

One of the methods that can be used to resolve this issue is to use a non-linear load that is a load that does not draw a sinusoidal current when a sinusoidal voltage is fed to it. For example, non-power factor corrected Switched Mode Power Supplies used in computers, audio video equipment, battery chargers, etc.

Systems built with purely resistive loads, which is a load that draws sinusoidal current when a sinusoidal voltage is fed to it. For example incandescent lamp, heater, etc. Suffered from instability of operation and inability to properly test the thermoacoustic engine and the linear alternator [9].

It should be noted that non-linear loads are needed only during initial testing in laboratories because once the thermoacoustic engine and the linear alternator are connected to the grid, the output voltage (and hence the stroke) are imposed by the grid and no special loads are needed then.

Non-linear loads can be made using back-to-back zener diodes [7], or by using an electronic load device, that allows constant voltage or constant current operations.

The non-linear electric load used in this work consists of a set of back-to-back zener diodes of different breakdown voltages (6, 12, 15 and 20 V) connected in series to a high-power rheostat (Ohmite Wirewound Power Rheostats, Model L 150 Watt). **Figure 2.11** and **Figure 2.12** below show the rheostat and the zeners that have been used to test the effect of the breakdown voltage of the zener on the behavior of the linear alternator. Table 2.4 shows the specifications of the zeners used.

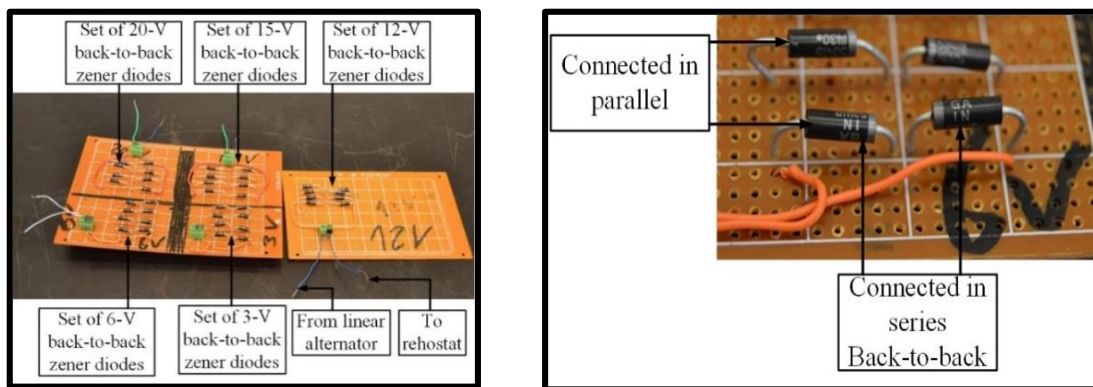


**Figure 2.11:** Left: Set of zeners available in the lab. Right: back-to-back connection of the zeners

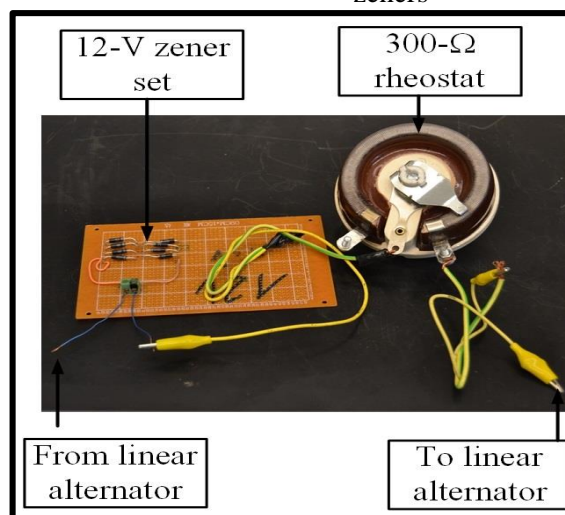


**Figure 2.12:**connection of the zeners in series with the rheostat

**Table 2.4:** Specifications of the AC zeners diodes used in the experiments

Item No.	Break-down voltage	Rated power	Supplier	Serial No.
1	3 V	5 W	RS	1N5334B
2	6 V	5 W	RS	1N5341B
3	12 V	5 W	RS	1N5349B
4	15 V	5 W	RS	1N5352B
5	20 V	5 W	RS	1N5357B

## 2.4 Instrumentation

### 2.4.1 Mean Pressure

The mean gas pressure measured using a Bourdon-tube gauge. During gas filling and discharge, vacuuming used to remove the old gas mixture before introducing the new mixture. Thus, a vacuum pressure gage is also used.

All gauges are isolated from the resonator via stain-less steel valves in order to protect them from exposure to acoustic oscillations and to prevent acoustic power from flowing out of the system in the direction of the gauges and corrupting the data. **Figure 2.13** shows a digital image of the pressure and vacuum gauges and their control valves.

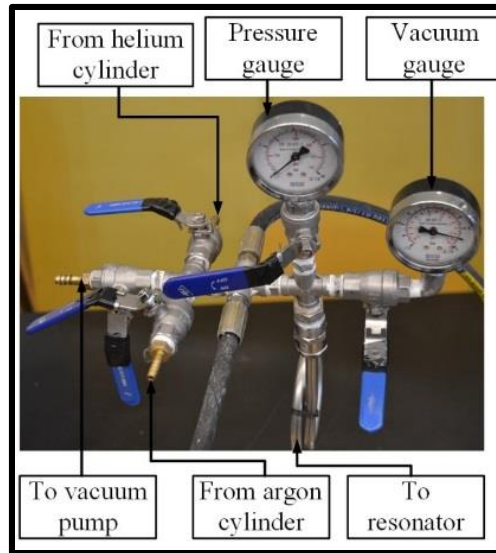


**Figure 2.13:** Gauges and control valves used in the experiment

### 2.4.2 Working Gases

In order to prepare the required gas mixture for each experiment, two high-pressure gas cylinders used for this purpose: a helium high-pressure gas cylinder (purity of 99.9%, DOT 3AA2265) and an argon high-pressure gas cylinder (99% purity, DOT 3AA2265). Each cylinder connected to the setup with its own regulator to control the supply pressure to the system.

### 2.4.3 Mean Gas Temperature

In order to capture any effect of the input acoustic power and/or frequency on the mean temperature of the gas mixture. One thermocouple (type E, 810- $\mu\text{m}$  in diameter and supplied by Omega Engineering) is introduced in the middle of the resonator using a  $\frac{1}{2}$ " feed-through that is connected to the data acquisition card in order to monitor any temperature changes.

### 2.4.4 Coil Temperature

In order to protect the coil of the acoustic driver and the linear alternator from overheating, two thermocouples (type E, 810- $\mu\text{m}$  in diameter and supplied by Omega Engineering) are used to monitor the temperature of the working gas very close to each coil. All thermo-couples are connected to the setup using feed-through and are then connected to data acquisition.

### 2.4.5 Dynamic Pressure

Measurement of dynamic pressure waves in two different points in the system with reasonable accuracy provides information about the acoustic power flux in this region. Hence, it can provide the value of the acoustic power at the acoustic driver exit and at the linear alternator input. In addition, there is a pressure microphone in the back of each enclosure volume in order to measure the value of the dynamic pressure behind the acoustic driver and the linear alternator in order to calculate the alternator-space thermal losses (hysteresis) in the volume of gas behind the pistons.

Four piezo-resistive pressure microphones (Meggitt, Model 8530C-500M5, range 0-500 psi absolute and individually calibrated by the supplier) used to measure the dynamic pressure in the mentioned locations. They operate by sensing the change in electric resistance caused by the change in dynamic pressure. Hence, they need a Wheat-Stone bridge arrangement. The four legs of the bridges are on the sensor already but a signal conditioner that provides excitation to the bridge and provides gain to the signal is needed. In this work, Meggitt amplifier model 136 (three-channels, 200 kHz bandwidth, and programmable-gain) is used for this purpose. When placing the order of the model 136 amplifier, it comes with a built-in low-pass filter with a default cut-off frequency at 10 kHz (plus/minus 12 %). **Figure 2.14** presents a digital image the dynamic pressure microphone and the amplifier used.



**Figure 2.14:** Left: Dynamic pressure microphone. Right: DC amplifier

Some of the main factors that should be considered during the selection of the dynamic pressure microphones are:

1. **Range:** Different models have different ranges. For instance, item 8530B-500 operates up to 500 Psi (34 bar absolute) while item 8530C-50 works up to 50 Psi (3.4 bar absolute). The proper range depends also on the mode of operation (absolute/gage operation).
2. **Absolute/gage pressure:** Some products have absolute pressure outputs (e.g., 8530B-500) and others have gage pressure outputs (e.g., Model 8510B-2). The absolute sensors are better when using gases other than air, because they will not be damaged when subjected to vacuum during the gas refill and the associated vacuuming.

Some of the main factors that should be considered during the installation of the dynamic pressure microphones are:

1. Before the pressure microphone is installed, the round surface is flattened using a vertical milling machine and an O-ring is used to prevent leakage.
2. The proper thread, as instructed by the supplier manual, is made into the resonator wall (through hole).
3. The microphones are installed at certain angles facing the floor and/or away from the operator, to avoid eye injuries in case they are impulsively disconnected from the setup at high operating pressures.

#### 2.4.6 Linear Variable Differential Transducers (LVDT's)

One of the main variables that should be measured and controlled in this experimental setup is the piston stroke of both the acoustic driver and the linear alternator. For this purpose two LVDTs (Measurement Specialties model XS-C 499 and LDM-1000 signal conditioning module) are used. These signals are fed to the control circuit in order to prevent over-stroking. Additionally,

the signal of the acoustic driver/linear alternator LVDT used in conjunction with the dynamic pressure inside the enclosure volume to measure the thermal losses (hysteresis) in the acoustic driver/linear alternator enclosure volume.

Moreover, the same acoustic driver/linear alternator LVDT signals are used in conjunction with the corresponding dynamic pressure microphones located near the acoustic driver/linear alternator to calculate the acoustic power at the exit of the acoustic driver and the inlet of the linear alternator. **Figure 2.15** presents a digital image of the LVDT and its signal conditioner used in this work.



**Figure 2.15:** Left: LVDT probe. Right: LVDT signal conditioner

The LVDT rod must be well fixed and aligned with the piston. For this purpose, a connecting rod between the piston and the LVDT rod is used. Connecting rods are made of magnetized, ferromagnetic, or high conductivity metals (Aluminum, Brass, Copper, etc.) must not be used as they interfere with the LVDT operation. Connecting rods made of plastic or other non-conductive materials are acceptable (AISI 300 Series austenitic (non-ferromagnetic) stainless steel).

In this case, a special homemade Teflon plug and a stainless steel M3 screw are used. **Figure 2.16** shows a digital image of the plug besides how it is connecting the LVDT rod to the piston. When ordering the LVDT probe, care must be taken to order the part with metric thread, and not the default British thread.



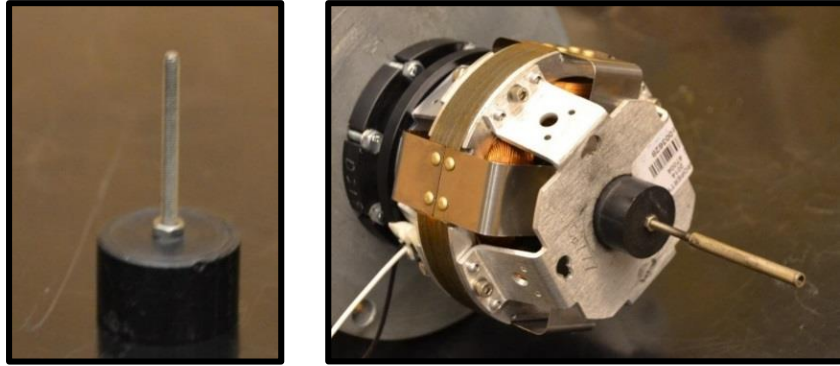


**Figure 2.16:** Left: LVDT rod plug and screw. Right: LVDT fixation to the piston back

The LVDT installed such that it reads zero when the pistons are at their equilibrium positions and this zero reading is checked before and after operation to make sure that the pistons retain their original positions.

#### 2.4.7 Current and Voltage Measurements

The input voltage ( $V_{in}$ ) to the acoustic driver, the output voltage ( $V_{out}$ ) on the electric load, and the open-circuit voltage (VOC) on the linear alternator are measured using a digital storage oscilloscope via a voltage probe (10-X attenuation).

The input and output current ( $I_{in}$  and  $I_{out}$ , respectively) are measured by monitoring the voltage drop on a one  $\Omega$  100 W series resistance.

#### 2.4.8 System Protection

The presented setup is protected against over-stroking (as discussed in subsection 2.3.6), against excessive current withdrawn at the acoustic driver (using a fast-acting fuse of 2.25 A) and against over-heating by monitoring the gas temperature close to the copper coils of the acoustic driver and linear alternator.

#### 2.4.9 Digital Oscilloscope

Data acquisition of the dynamic pressure, LVDT signals, input and output voltages and currents are made using two digital storage oscilloscopes (Tektronix, Model TDS2024B, 4 channels, 200 MHz bandwidths and 2 GS/s) running simultaneously and synchronized using LabVIEW with a sampling rate 5E4 Samples/s for 50ms (corresponding to about two acoustic cycles). This setting used to analyze the data in time domain with a time resolution of 20E-6 s.

**Figure 2.17** presents a digital image of the oscilloscopes.

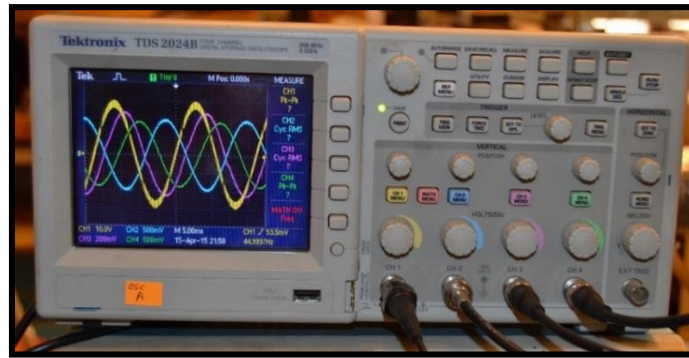


**Figure 2.17:** Digital storage oscilloscope

#### 2.4.10 Data Acquisition Board:

A data acquisition board (NI, Model USB-6225, 16-bit, 250 kS/s) is used to measure the temperature values of all thermocouples. The board is also used to provide visual monitoring of the strokes of the acoustic driver and the linear alternator, as an added protection to visualize if any of the pistons is approaching over-stroking. **Figure 2.18** shows a digital image of the data acquisition board.

Appendix D shows the steps of assembling the experimental setup.

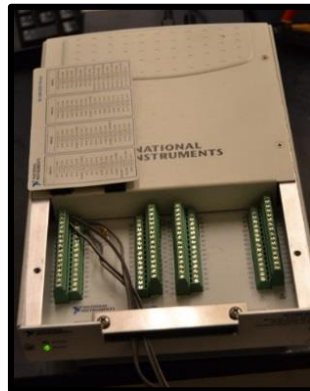


**Figure 2.18:** Data acquisition board

### 2.5 Experimental Procedure

This section summarizes the experimental procedure followed in this work:

- 1- The required gas mixture is introduced to the resonator and the two enclosure volumes as follows:
  - A. The vacuum pump used to evacuate the system from any traces of previous gas mixtures used.
  - B. Argon gas used to fill the resonator and the two enclosure volumes.

- C. The argon gas purged three times to reduce the molar fraction of air traces inside the system. Purging with argon is preferred over purging with helium since the former is less expensive, denser, and easier to vacuum.
  - D. The required gas mixture concentration of argon and helium gases supplied from high-pressure gas cylinders. Dalton's law used to introduce a certain gas mixture composition.
  - E. To check that the gases are well mixed, the system filled to a mean pressure 5% higher than the required value and the operating frequency is monitored. The excess gas is then released and the frequency is observed again. If both values are the same, then the gases are well mixed. This technique utilized in Belcher [21].
- 2- The LVDTs power supply is turned on. It is critical to turn the LVDT power supply on before the stroke control circuit is turned on. This is to eliminate exposure of the stroke control circuit to spikes from the LVDT signal side.
  - 3- The position of the two LVDT's is checked to make sure they retained their original positions by observing a zero reading on the LVDT signal using the oscilloscope display or using the LabView display on the PC screen.
  - 4- The stroke control circuit is turned on. For proper over-stroking protection, the system must not be used when the stroke control circuit is switched off. The circuit is designed in such a way that the system will not operate if the circuit is powered but either LVDT signal is not connected.
  - 5- The function generator is set on the required wave frequency and amplitude and the power amplifier is adjusted to apply the required amplification ratio. This setting will generate acoustic power at the required intensity and frequency.
  - 6- The rheostat is adjusted at the required electrical resistance value and then connected in series to the required set of zeners. The combined system of the rheostat resistance and the zeners form a non-linear electric load. This load is connected in parallel with the linear alternator.
  - 7- The experiment is allowed to operate for five minutes before acquiring any data to ensure that the system has warmed up and reached its steady state.
  - 8- The operator should avoid any sudden changes to the system. Examples of sudden changes are changing the input to the acoustic driver (e.g., changing the signal amplitude on the function generator or through the settings on the power amplifier) or changing the output of the linear alternator (e.g., disconnection of the electric load during system operation).

Sudden disconnection of the electric load will cause the linear alternator stroke to increase significantly. Sudden changes on the input and/or the output will incur severe vibration in the system and should be avoided.

- 9- The digital-storage oscilloscopes are properly synchronized adjusted to the proper settings corresponding to time or frequency domain measurements.
- 10- The required data is acquired using two synchronized oscilloscopes. The operator should ensure that all the required signals appear on the PC screen before starting data acquisition.
- 11- The operating frequency could be changed while the setup is running, but the acoustic driver current is monitored to avoid working at frequencies that make the acoustic driver withdraw excessive current and heat up or vibrate.
- 12- After completion of data acquisition, the system is turned off by switching off the function generator. Then, the power to the stroke control circuit, the power supply of the LVDT, the oscilloscopes and the power amplifiers are turned off.
- 13- The used gas mixture is released to the atmosphere at a very slow rate.

## Chapter 3 - Results and Discussion

This chapter presents and discusses the performance parameters of linear alternators and their calculation methods on a single basic case to demonstrate the abilities of this setup.

In addition to, a parametric study to study the effect of operating frequency, the mean gas pressure and composition, the input volt and the electric load (zener break-down voltage and resistance value) on the basic case.

Finally, the chapter presents and discusses the acoustic matching and the electrical matching via a different set of experiments.

### 3.1 Calculation of Performance Parameters:

The input electric power  $P_{in}$  is calculated using the dot product of the input current and voltage to the acoustic driver, where the bracket denotes averaging made after the dot product operation of the two waves:

$$P_{in} = \langle V_{in}(t). I_{in}(t) \rangle \quad (1)$$

Similarly, the output electric power  $P_{out}$  is calculated as:

$$P_{out} = \langle V_{out}(t). I_{out}(t) \rangle \quad (2)$$

The acoustic power produced by the acoustic driver is calculated using the average of the dot product of the dynamic pressure at the acoustic driver exit and the acoustic driver's piston velocity:

$$E_{AD} = \langle P_{AD}(t). U_{AD}(t) \rangle \quad (3)$$

In the meantime, it should be realized that the time-averaged acoustic power,  $E_{AD}$  supplied by a moving piston of Area  $A$  is given by:

$$E_{AD} = F_{RMS} * V_{AD_{RMS}} = P_{AD_{RMS}} * A * V_{AD_{RMS}} = P_{AD_{RMS}} * U_{AD_{RMS}} = \frac{|P_{AD}| * |U_{AD}|}{2} \quad (4)$$

Since,

$$|U_{AD}| = \omega |d| \quad (5)$$

Where  $d$  is the acoustic driver piston's stroke amplitude.

Thus,

$$E_{AD} = \frac{|P_{AD}| * A * \omega |d|}{2} \quad (6)$$

Indicating that the acoustic power is proportional to the dynamic pressure amplitude, piston area, operating frequency and magnitude of piston stroke.

The acoustic driver dynamic pressure amplitude ( $P_{AD}$ ) can be related to the volumetric velocity of the acoustic driver piston ( $U_{AD}$ ) through the acoustic impedance ( $Z$ ) which is the ratio between the dynamic pressure and the volumetric velocity:

$$Z = \frac{P_{AD}}{U_{AD}} \quad (7)$$

Substituting equation 7 in equation 6 to get:

$$E_{AD} = \frac{Z}{2} * (d * \omega)^2 * A^2 \quad (8)$$

Equation (8) is of great value since for a given acoustic load, it indicates the relationship between the acoustic power, piston stroke, operating frequency and the piston diameter.

The acoustic power received by the linear alternator is calculated as:

$$E_{LA} = \langle P_{LA}(t) \cdot U_{LA}(t) \rangle \quad (9)$$

The electro-acoustic conversion efficiency ( $\eta_{AD}$ ) of the acoustic driver is calculated as:

$$\eta_{AD} = \frac{E_{AD}}{P_{in}} \quad (10)$$

The acoustic-to-electric conversion efficiency ( $\eta_{LA}$ ) of the linear alternator is calculated as:

$$\eta_{LA} = \frac{P_{out}}{E_{LA}} \quad (11)$$

The overall conversion efficiency  $\eta_{overall}$  is calculated as:

$$\eta_{overall} = \frac{P_{out}}{P_{in}} \quad (12)$$

### 3.2 Basic Case

The target of this part was to identify a set of operating conditions that provides reasonable matching, both acoustically and electrically and to thoroughly analyze the results. After many preliminary runs, the domains of the different operating variables were scanned and their effects on the performance evaluated until a set of operating parameters was identified. The criteria of selection of the operating parameters that are used are: large input power, high overall conversion efficiency and large output electric power. Table 3.1 summarizes the performance parameters of this case.

**Table 3.1:** Performance parameters of the case presented. All phases are measured simultaneously with respect to the dynamic pressure in acoustic driver enclosure

<b>Operating conditions</b>		
Gas type	40%He 60%Ar	
Mean gas pressure	12 bar	
Zener break-down voltage	10 forward zeners in parallel and 10 backward zeners in parallel, each of 6 V break-down voltage	
Electric resistance in series with the zener circuit	22 $\Omega$	
Operating frequency	54 Hz	
Input volt to the acoustic driver	Amplitude: 20.69 V <sub>RMS</sub> Phase: 97.2°	
<b>Measured Parameters</b>		
<b>Parameter Name</b>	<b>Value</b>	<b>Phase</b>
Acoustic driver enclosure dynamic pressure amplitude, kPa	5.79	0
Resonator dynamic pressure amplitude inside the resonator, kPa	13.64	103.8
Linear-alternator enclosure dynamic pressure amplitude, kPa	7.48	170
Acoustic driver stroke pk-pk, mm	2.70	56.7
Linear alternator pk-pk, mm	2.80	40
Input current, A <sub>RMS</sub>	0.51	91.7
Input electric power, W	10.40	--
Output volt, V <sub>RMS</sub>	12.89	40.4
Output current, A <sub>RMS</sub>	0.28	36.5
Output electric power, W	3.50	--
Overall conversion efficiency, %	33.64	--
Open-circuit volt, V	35.1	5

### 3.2.1 Time and Frequency Domain Analysis

The following sections present the measured data in time and frequency domains. **Figure 3.1** presents the data in the time domain. This presentation allows observing the wave shape, signal amplitude and phase and relative phasing between all measured variables.

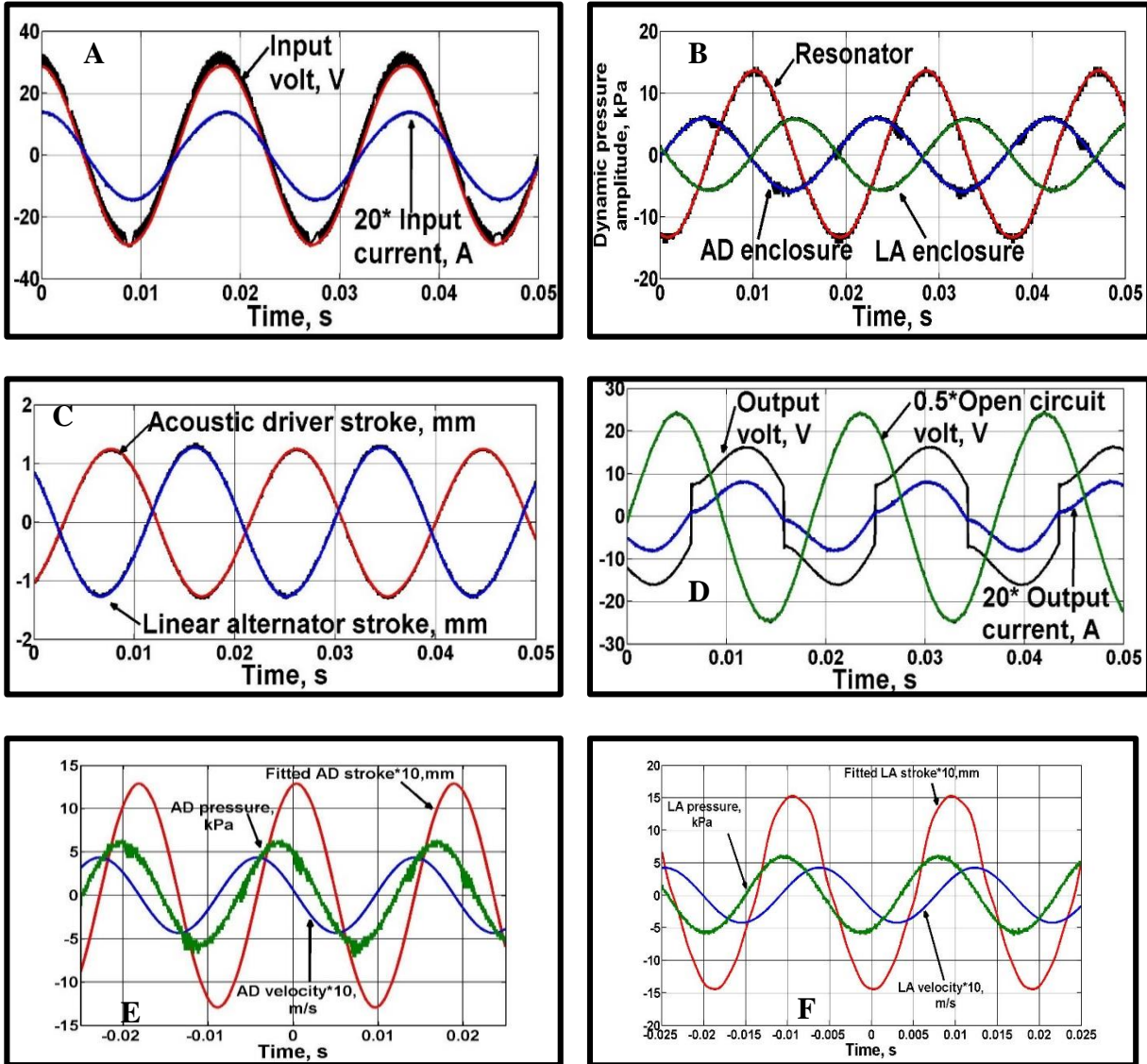


**Figure 3.1:** Time domains of all measured variables  
Operating conditions: 54 Hz, 12 bar, 40% He 60% Ar, 20 V<sub>RMS</sub>, 22Ω, 6V zener

The frequency content of each variable is presented in **Figure 3.2**. The frequency resolution is calculated as the ratio between the sampling rate and the number of data points, to be 2500/2048 = 1.22 Hz.



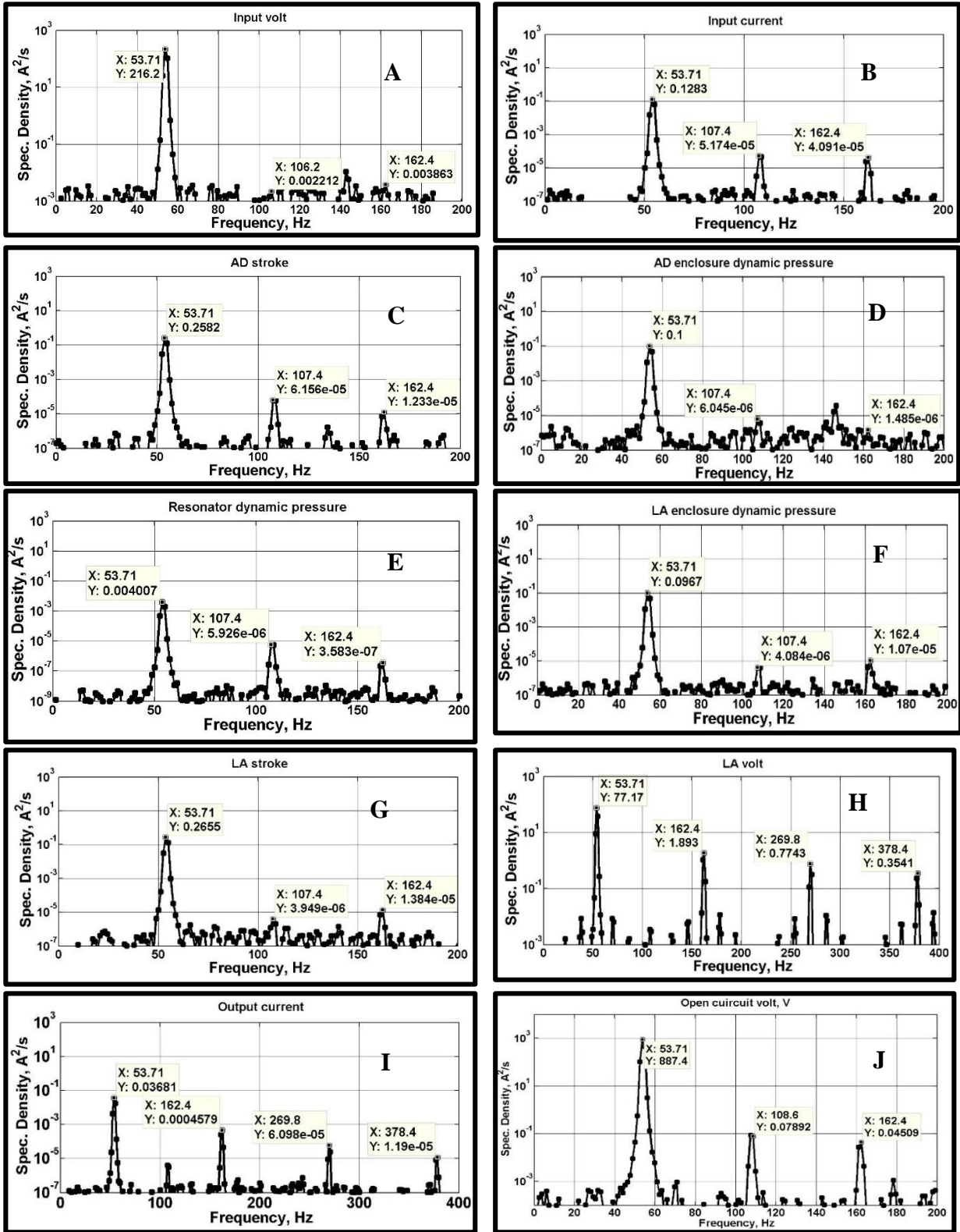


Figure 3.2: Frequency domains of all measured variables  
 Operating conditions: 54 Hz, 12 bar, 40% He 60% Ar, 20 V<sub>RMS</sub>, 22Ω, 6V zener

**This data set shows many important features:**

- The operating conditions (the operating frequency, mean gas pressure and composition and load) allows for loading of the acoustic driver, giving rise to an input electric power of 10.4 Watts.
- The operating conditions yielded a phase difference between the input voltage and current to the acoustic driver of  $5.5^\circ$  (voltage is leading, because of the inductive load in the acoustic driver), indicating a power factor of 0.99.
- The operating conditions (mainly the mean gas pressure and composition) yielded reasonable strokes on both the acoustic driver and the linear alternator. The values of the strokes amplitudes are not too low and not close to the stroke limits.
- The operating conditions yielded reasonable output electric power (3.5 W), with a corresponding overall conversion efficiency of 33.6 %.
- The operating conditions (mainly the operating frequency) yielded large input power, reasonable strokes at low input current. Operating at low input current is critical to avoid overheating and to allow low copper losses and thus large conversion efficiency.
- It was consistently observed that the operating conditions that lead to equal stroke on the acoustic driver and the linear alternator (as shown in **Figure 3.1C**) always lead to maximum conversion efficiency. This is a result of the acoustic matching between the acoustic driver and the linear alternator, which gives rise to having both units operate together as a single unit without slip. The equal-stroke operating point can always be obtained for any given gas mixture, pressure and load by tuning the frequency of operation or by tuning the resistance value of the load at constant operating frequency. However, different equal-stroke points have different conversion efficiencies.
- As a result of the acoustic matching between the acoustic driver and the linear alternator, it is observed that the phase shift between the dynamic pressure in the acoustic driver enclosure and the dynamic pressure in the linear alternator is  $170^\circ$ , which is very close to  $180^\circ$ , as seen in **Figure 3.1B**. This arises from the fact that both the acoustic driver and the linear alternator move “together” in a synchronized manner such that the acoustic driver’s piston is at its top dead center at the same moment in time when the linear alternator’s piston is at the bottom dead center and vice versa.
- The close to  $180^\circ$  phase shift described in point 7 above gives rise to nearly  $180^\circ$  phase shift between the acoustic driver stroke and the linear alternator stroke, as seen in **Figure 3.1C**.

- The use of non-linear load gives rise to non-sinusoidal output current and voltage at the linear alternator output. The harmonic content in both signals show the fundamental component at the operating frequency as well as significant harmonics at the third, fifth and seventh harmonics, as observed in **Figure 3.2**. The rest of the parameters involved (input volt and current, dynamic pressures and strokes) show much less harmonic content.
- **Figure 3.2H** and **Figure 3.2I** show the frequency content of the output volt and output current. Because these AC signals have half-wave symmetry in the time domain (i.e., if shifted one half period and inverted, it is identical to the original function), even harmonics are always absent and only odd harmonics are generated.
- In comparison with the use of linear load (presented in **Figure 3.10**), the use of non-linear load caused some harmonic generation on the input current withdrawn by the acoustic driver (as can be observed by comparing **Figure 3.2B** to **Figure 3.10B**).
- The stroke wave forms of both the acoustic driver and the linear alternator are measured with high temporal resolution (50 kS/s). The captured wave forms then are curve-fitted, using least square method, to a sine wave with a fundamental and seven harmonics, each with its amplitude and phase. The resulting algebraic expression then is differentiated with respect to time yielding an expression for the piston's velocity. The measured stroke, the fitted stroke, the calculated piston's velocity and the dynamic pressure wave forms are compared together in **Figure 3.1E** and **Figure 3.1F**. This comparison allows calculation of the phase shift between the dynamic pressure and the piston's velocity. These phase shifts are  $58^\circ$  (velocity leads) and  $56^\circ$  (pressure leads) for the acoustic driver and the linear alternator enclosures, respectively. These values indicate operation neither at standing-wave mode nor at travelling wave mode.
- In comparison with the use of linear load (presented in **Figure 3.10**), the use of linear load caused the phase shifts between the dynamic pressure and the piston's velocity in the acoustic driver and the linear alternator stated in point 12 above to be  $34^\circ$  (pressure leads) and  $66^\circ$  (velocity leads), respectively. This indicates that the non-linearity of the load propagated upstream to affect the phases between dynamic pressure and velocity in the linear alternator as well as acoustic driver.

### 3.2.2 Effects of Operating Parameters on the Basic Case

This section analyses the effects of the operating parameters on the performance of the basic case presented in section 3.2 above.

### 3.2.2.1 Operating Frequency

Figure 3.3 shows the effects of the operating frequency on the system performance, and the following points can be observed:

- Two important points can be identified on the curve: the point of maximum overall conversion efficiency (54 Hz) and the point of maximum output power (58 Hz). This is a manifestation of the trend generally observed in thermoacoustic devices that conversion efficiency and power density occur at two different points
- The point of minimum current withdrawn by the acoustic driver is also shown (at 47 Hz). This point is of special importance if the system is to be driven at large input voltages
- As the difference between the acoustic driver stroke and the linear alternator stroke increase, the overall efficiency of the system decreases, which is an indication of poor acoustic matching at some frequencies. As indicated in section 3.2.1, the point of maximum efficiency occurs at the point of equal strokes
- In comparison with other operating parameters, as will be seen later, the operating frequency and the use of zener diodes in the load have more pronounced effects on the system performance more than any other operating parameter.

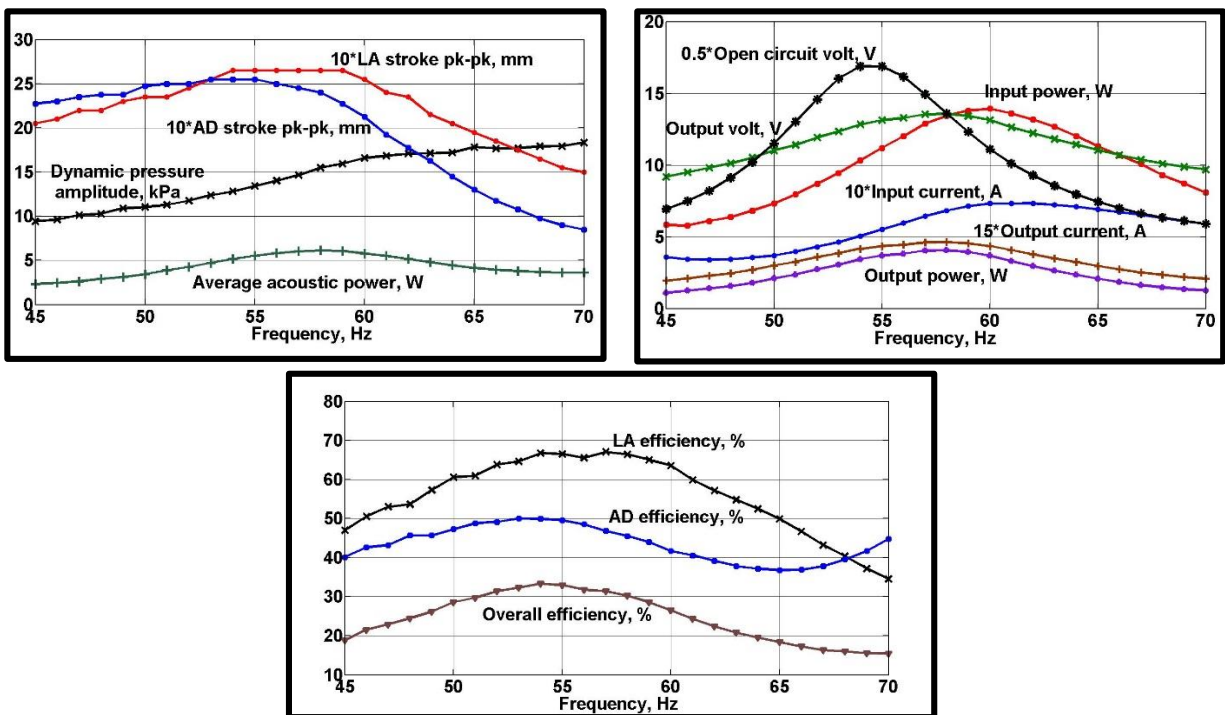
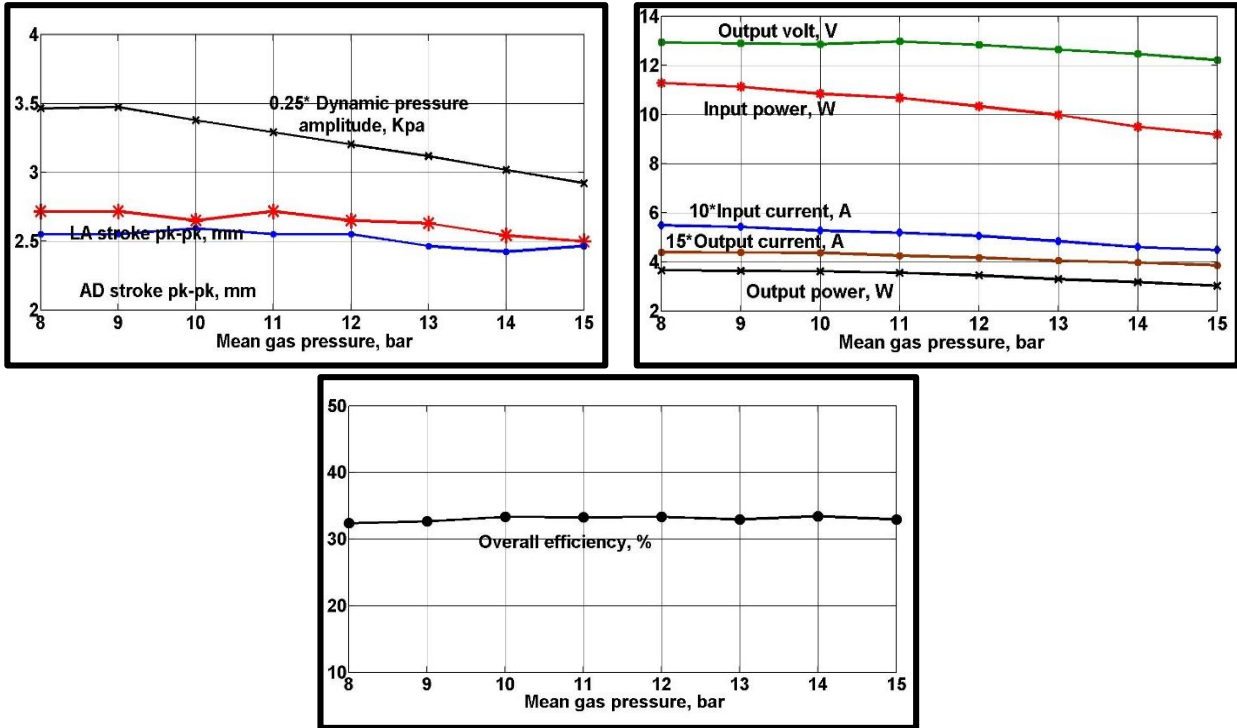


Figure 3.3: Effect of frequency on the system variables  
Operating conditions: 12 bar, 40% He 60% Ar, 20 V<sub>RMS</sub>, 22Ω, 6V zener

### 3.2.2.2 Mean Gas Pressure

This range of selected working pressure in **Figure 3.4** (from 8 bar to 15 bar) does not show a significant effect on the performance of the system. Section 3.3.1 below shows detailed effect of the mean gas pressure on the performance. Nevertheless, the mean gas pressure affects the product of the mean density and the speed of sound, which in turns affects the output acoustic power.



**Figure 3.4:** Effect of Mean pressure on the system variables  
Operating conditions: 54 Hz, 40% He 60% Ar, 20 V<sub>RMS</sub>, 22Ω, 6V zener

### 3.2.2.3 Mixture Composition

When choosing a specific gas mixture to use in a TAPC, the following criterion must be considered:

- The gas mixture used should maximize the power density in the setup. The power density is proportional to the product of the cross sectional area, the gas mixture density and the velocity of sound in the gas mixture. Thus, the product of gas mixture density and gas mixture speed of sound is of interest. The increase of this product decreases the stroke of the acoustic driver (since it increases the acoustic load seen by the driver), increases the stroke of the linear alternator (since it improves the acoustic coupling between the acoustic driver and the linear alternator), and increases the dynamic pressure and increases the output electric power. These effects are further affected by the Prandtl number effects

described below. According to **Figure 3.5D**, this selection factor recommends the use of pure argon gas at large mean pressures.

- The gas mixture used should minimize the Prandtl number in order to decrease the viscous losses. This is because the Prandtl number can be expressed as ( $Pr = \text{kinematic viscosity}/\text{thermal diffusivity}$ ). According to **Figure 3.5A** below, this selection factor recommends the use of a gas mixture of 60% Helium and 40% Argon.
- The gas mixture used should enhance the heat transfer coefficient on the gas side of the hot and cold heat exchangers used in thermoacoustic devices. For this purpose, the gas side heat transfer coefficient can be expressed as [22]:

$$h = 0.7 \frac{k}{\delta_k} \quad (13)$$

Where,  $h$  is the heat transfer coefficient,  $k$  is the thermal conductivity and  $\delta_k$  can be represented as following:

$$\delta_k = \sqrt{\frac{2k}{\rho * C_p * \omega}} \quad (14)$$

and thus large thermal conductivity is preferred. For this purpose, practical thermoacoustic engines that are built already use helium at high pressures. Since the current work does not employ a thermoacoustic engine, and thus will not employ hot/cold heat exchangers, this selection factor will not be considered for this setup. This issue is an important and critical factor in real TAPC, however. Clearly, the above selecting criterion do not lead to a single optimum gas or gas mixture.

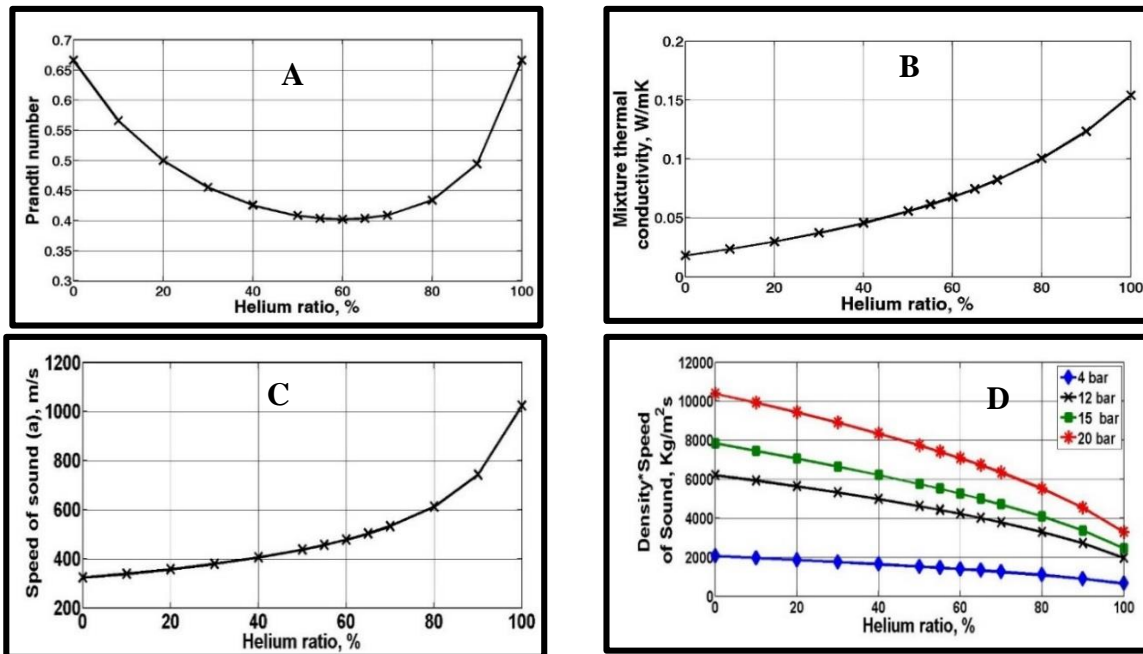


**Figure 3.5:** Gas mixture properties

A: Prandtl number. B: Thermal conductivity. C: Speed of sound. D: Density multiplied by speed of sound

The current work studies different gases/gas mixtures, including 100% argon, 100% helium and different helium molar fractions in between. The effect of the working gas mixture on the system behavior is shown in **Figure 3.6**.

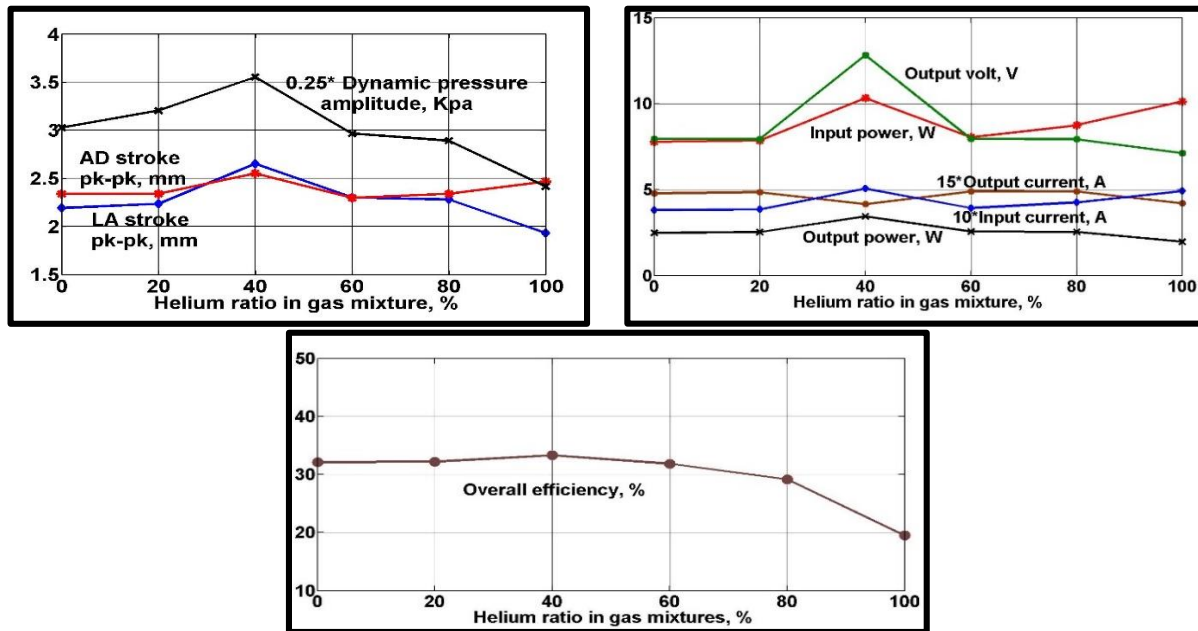


**Figure 3.6:** Effect of gas mixture on the system variables  
Operating conditions: 54 Hz, 12 bar, 20 V<sub>RMS</sub>, 22Ω, 6V zener

The gas mixture has a great effect on the behavior of the system as it affects all the parameters of the system. These effects are as follows:

- At mixture 40% He 60% Ar, the system performance is enhanced (large dynamic pressure at the resonator and large input and output electric powers). In view of the parameters affected by the gas mixture listed above in this section, this peak in the system performance can be explained by the decrease in the viscous losses encountered in the system since this gas mixture results in the minimum Prandtl number amongst the different mixtures used. This in turn indicates the importance of proper surface finish (minimum surface roughness) on the inner surfaces of the system parts and the importance of the lengths of the different parts involved.
- Beside the low value of Prandtl number of this gas mixture, the used gas mixture has a mean pressure of 12 bar (abs) in order to achieve a large product of the mean density times the speed of sound.
- Once this mixture is identified, based on the minimum Prandtl number point, the operating frequency is set in order to observe equal strokes of the acoustic driver and linear alternator, in order to achieve proper acoustic matching.

- At helium molar fraction larger than 60%, two negative effects take place: The first is that the product of the mean density times the speed of sound decreases, and the second is that the Prandtl number (and hence viscous losses) increases. The net effect of these two combinations give rises to a deteriorated system performance (for example, an increase in helium molar fraction from 60% to 100% decreases the overall conversion efficiency from 31% to 19%).
- In contrast, at helium molar fractions less than 40%, only one negative effect takes place, which is the increase in Prandtl number and associated increase in viscous losses. The effect on the system performance is not as pronounced as in item 4 above, giving rise to a gradual decrease in system performance. For example, a decrease in helium molar fraction from 40% to 0% decreases the overall conversion from 33% to 32%.
- In reference to **Figure 3.5C** above showing the speed of sound in He/Ar mixtures, it can be seen that the speed of sound in the mixture decreases significantly as the argon molar fraction increases from zero upwards. For example, the speed of sound in helium is 1029 m/s and is 747 m/s at 90%He/10% Ar. This significant sudden change in the speed of sound at high helium molar fractions gives rise to the need to use larger operating frequencies in order to maintain the acoustic matching.

#### 3.2.2.4 Input Electric Power

All the input and output parameters are expected to increase with the increase of the input volt, which is realized in the results presented in **Figure 3.7**. Few points can be observed:

- There are main losses in the system: Viscous fluid losses in the resonator/enclosures (decrease as the Prandtl number decrease), Ohmic heating losses ( $I^2R$ ), motion losses ( $R_m U_{AD}^2$  and  $R_m U_{LA}^2$ ), seal losses (proportional to  $P^2$  across the piston seal, which is 19.1 um [20] in the models used in this work) and motor/alternator space thermal hysteresis losses. It is a design objective to always keep these losses balanced. In this work, the increase in the input voltage causes the current withdrawn/generated at the acoustic driver/linear alternator to increase (thus increasing the  $I^2R$  losses), the dynamic pressure to increase (thus increasing the seal and thermal hysteresis losses), the strokes of the acoustic driver/linear alternator to increase (thus increasing the motion losses  $R_m U_{AD}^2$  and  $R_m U_{LA}^2$ ). The results presented in **Figure 3.7** indicate that as the input voltage increases, a slight decrease in the overall conversion efficiency beyond an input volt of 31  $V_{RMS}$  occurs. This indicates that in the considered range, the different losses remain almost balanced.



- Without consideration of the losses, the input voltage in itself does not affect the acoustic matching (which controlled mainly by the operating frequency). Consequently, the system continue to experience equal stroke operation until an input voltage of 52 V<sub>RMS</sub> Beyond this point, the motion and viscous losses cause the linear alternator's stroke to be slightly less than the acoustic driver's stroke.

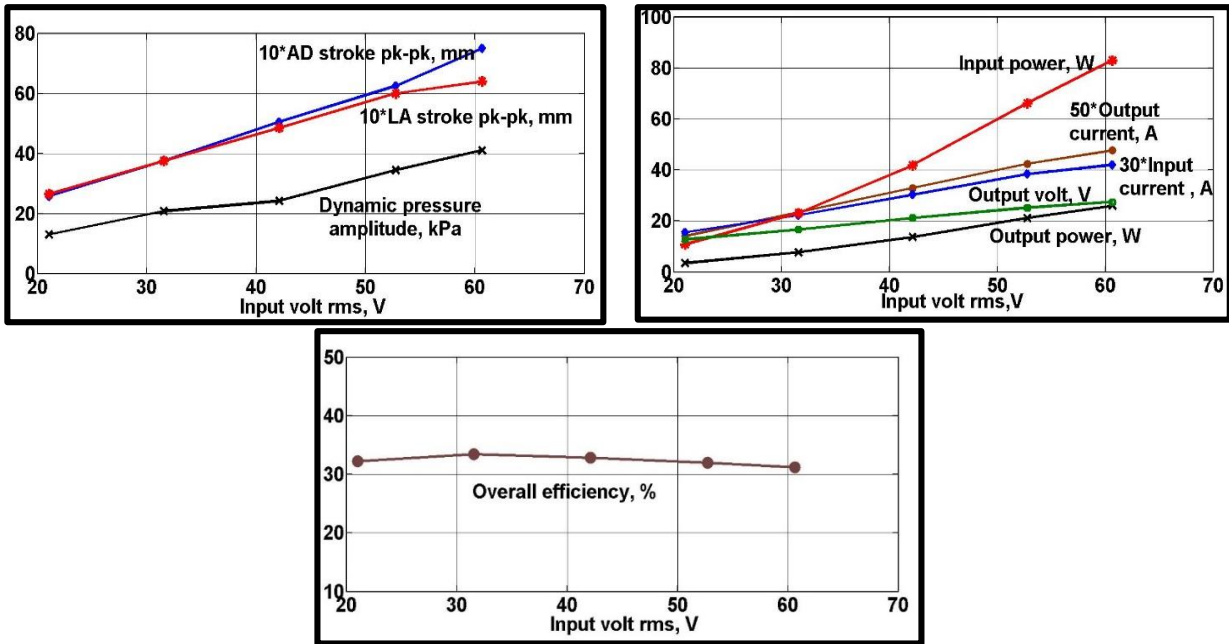


**Figure 3.7:** Effect of input volt on the system variables  
 Operating conditions: 54 Hz, 12 bar, 40% He 60% Ar, 22Ω, 6V zener

### 3.2.2.5 Electrical Resistance

The value of the electrical resistance directly affects the load matching. The presented results in **Figure 3.8** indicate the following:

- Again, the point of equal stroke (corresponding to a resistance value of 20Ω) is the point of maximum overall conversion efficiency.
- In this work where the frequency at which the generated acoustic power is supplied and the value of the load resistance can be both controlled, finding a point of maximum conversion efficiency is relatively easy. However, in real TAPC's, the operating frequency cannot be controlled, making the need for simultaneous acoustic and electric matching much more complicated.
- Beyond the point of maximum conversion efficiency, as the value of the electric load increases, the acoustic driver stroke's increases with respect to the linear alternator's causing the input power (~ acoustic driver's stroke) to increase at a faster rate than the

output power ( $\sim$  linear alternator's stroke). Consequently, the conversion efficiency decreases.

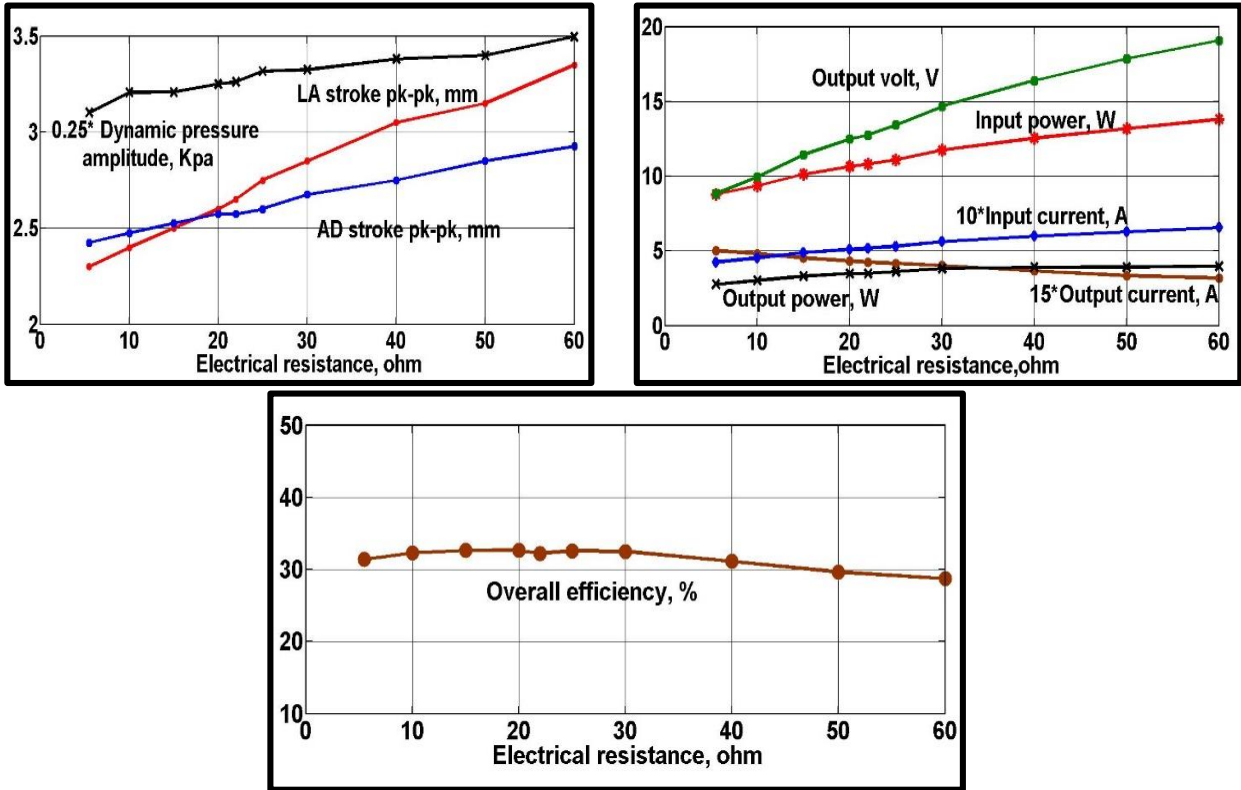


**Figure 3.8:** Effect of Electrical resistance on the system variables  
Operating conditions: 54 Hz, 12 bar, 40% He 60% Ar, 20 V<sub>RMS</sub>, 6V zener

### 3.2.2.6 Zener Diode Breakdown Voltage

Real TAPC's will be connected to the grid, which is a non-linear load. However, in the development phase they must be connected to a load in the laboratory. Section 2.3.6 discussed the need that this load must be of non-linear nature. However, the effects of the use of these non-linear loads on the performance of the system must be investigated. For this purpose, the data presented in section 3.2.1 above are repeated but without the nonlinear element represented in the zener parts. Their results are shown in **Figure 3.9** and **Figure 3.10** below.

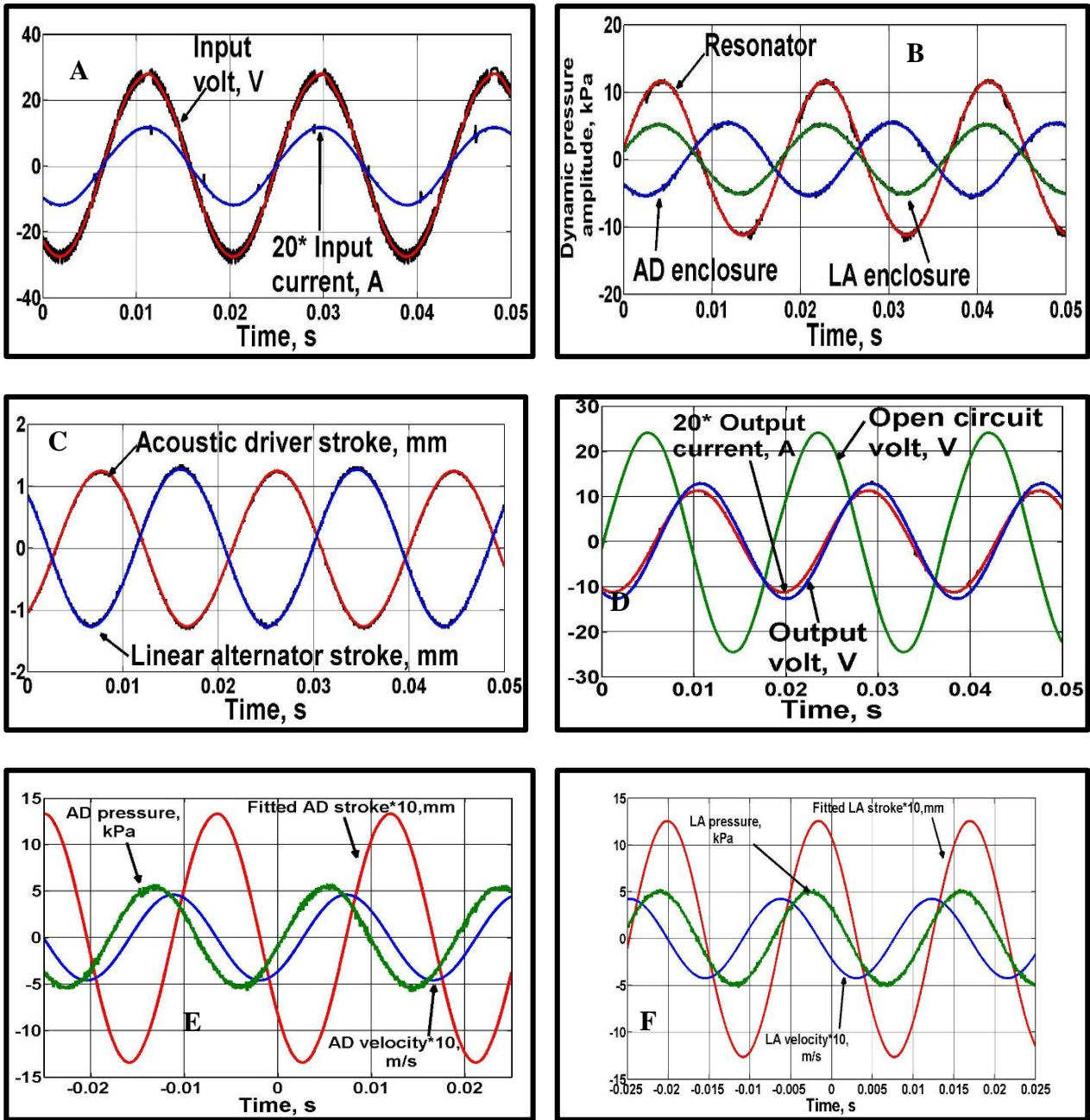


**Figure 3.9:** Time domains of all measured variables

Operating conditions: 54 Hz, 12 bar, 40% He 60% Ar, 20 V<sub>RMS</sub>, 22Ω, No zener

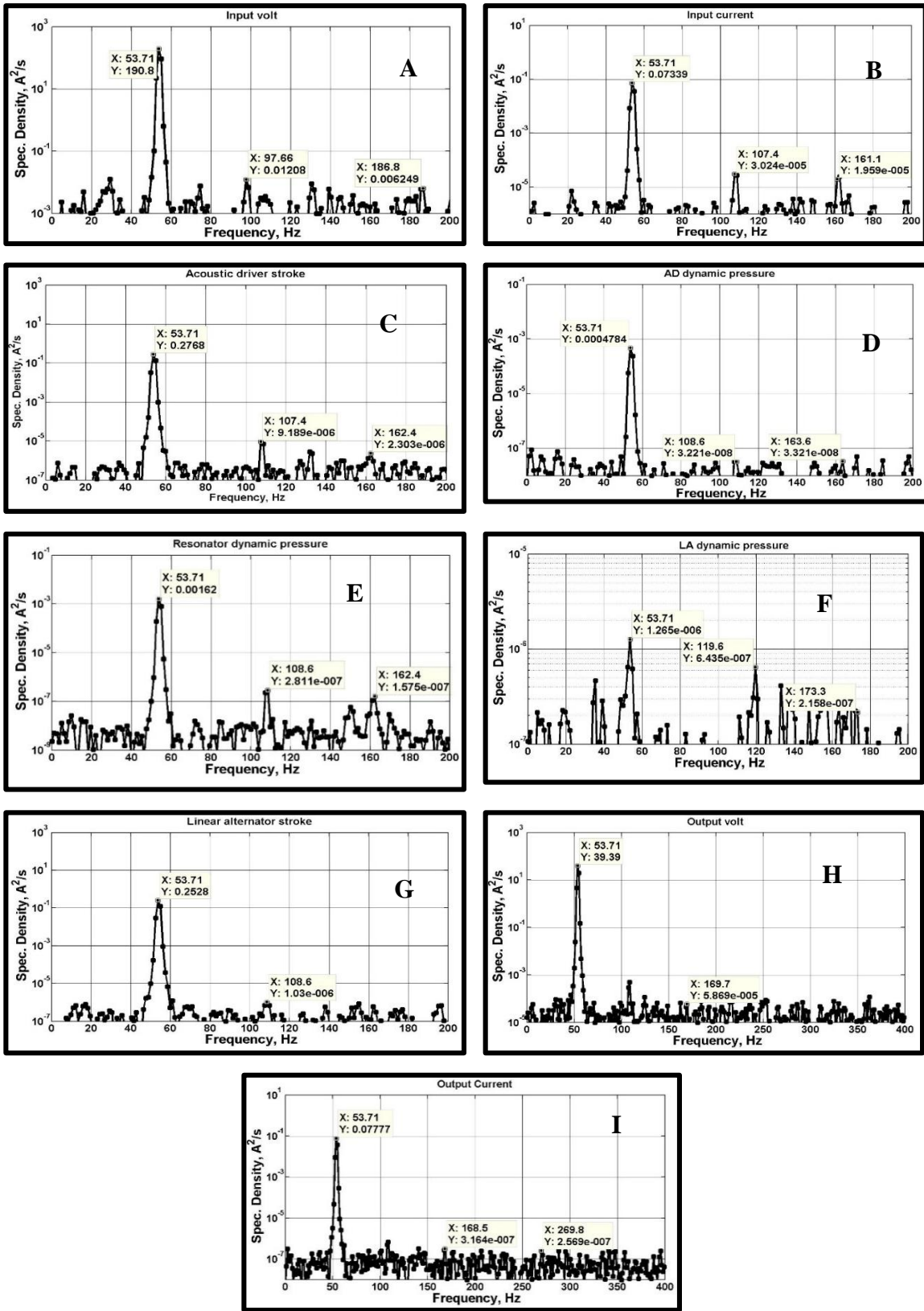


**Figure 3.10:** Frequency domains of all measured variables  
 Operating conditions: 54 Hz, 12 bar, 40% He 60% Ar, 20 V<sub>RMS</sub>, 22Ω, No zener

The following points can be observed:

- In comparison with the use of linear load (presented in **Figure 3.10**), the use of non-linear load caused some harmonic generation on the input current withdrawn by the acoustic driver (as can be observed by comparing **Figure 3.2B** to **Figure 3.10B**).
- In comparison with the use of linear load (presented in **Figure 3.10**), the use of linear load caused the phase shifts between the dynamic pressure and the piston's velocity in the acoustic driver and the linear alternator stated in point 12 above to be  $34^\circ$  (pressure leads) and  $66^\circ$  (velocity leads), respectively as opposed to  $58^\circ$  (velocity leads) and  $56^\circ$  (pressure leads) for the non-linear load case. This indicates that the non-linearity of the load propagated upstream to affect the phases between dynamic pressure and velocity in the linear alternator as well as acoustic driver.

The use of different zeners with different break-down voltages is investigated as well. The larger the break-down voltage of the zener the larger is the non-linearity involved. The results are presented in **Figure 3.11**.

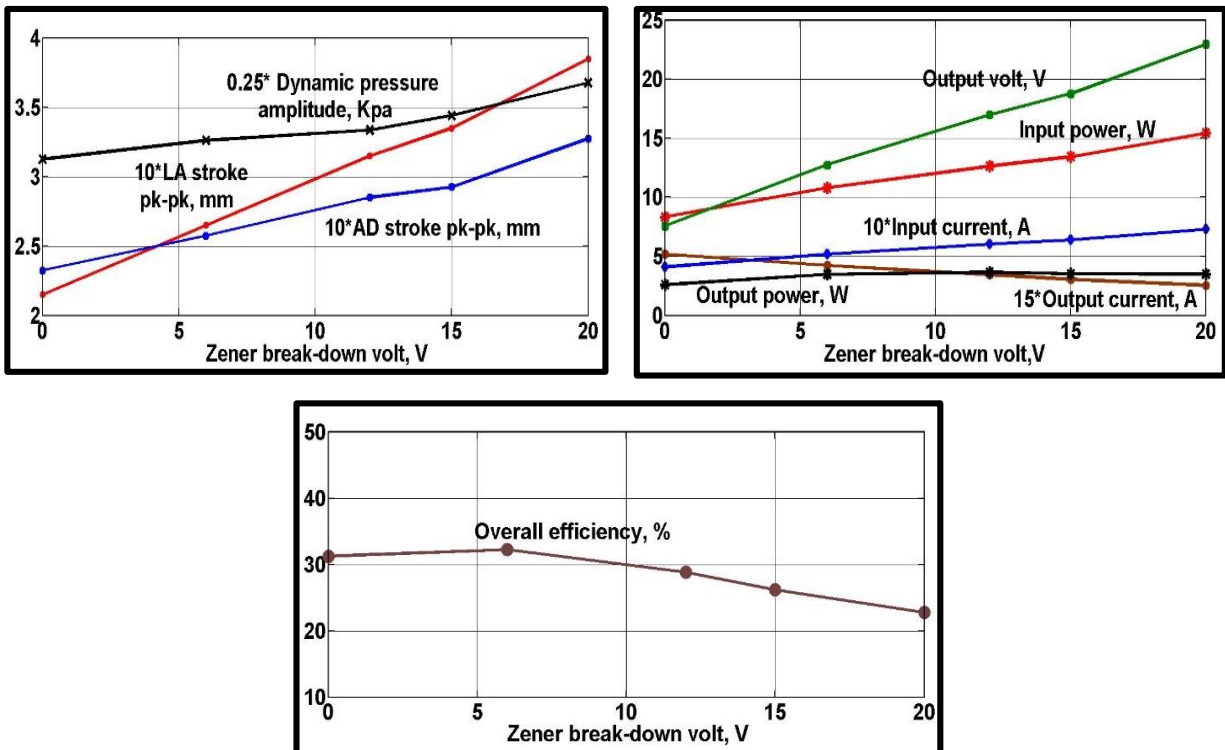


**Figure 3.11:** Effect of zener breakdown voltage on the system variables  
Operating conditions: 54 Hz, 12 bar, 40% He 60% Ar, 20 V<sub>RMS</sub>

Zener diode breakdown voltage has a significant effect on the performance of the system and can be summarized as follows:

- As the zener break down voltage increases, the system is faced with a larger resistance and is forced to generate a larger output voltage and a larger output power. However, the use of larger break-down voltages increases the non-linearity and the corresponding losses and causes the overall conversion efficiency to decrease after a certain limit.
- The selection of the break-down voltage should be made carefully because a value that is too low causes the system to develop low output power, a value that is too high causes significant non-linearity and lower conversion efficiency and a value even higher simulates an open circuit (if the break-down voltage is higher than the open-circuit voltage). Another limit on the break down zener voltage is discussed below.
- The linear alternator stroke is generally proportional to the generated voltage. Thus, as the zener break-down voltage increases, the developed voltage at the linear alternator increases and the linear alternator stroke increases. This increase in the linear alternator stroke may negatively affect the acoustic matching with the acoustic driver.

(The relationship between voltage and piston stroke is not completely straightforward - it depends on how close the system is to resonance, for example. If the charge pressure changes as the engine warms up or cools down, that could change the proportionality between them).

- The typical power rating of zener diodes is usually around 5 W. The developed output power is shared between the zeners and the resistances. If the zener is subjected to an output power larger than its rated value, then more zeners are to be used in parallel such that they have equal power sharing. However, the minimum number of zeners should be used, without overheating of any of them, to reduce the non-linearity involved.

### 3.3 Performance Analysis

This part presents the system performance under different operating conditions, including different frequencies, mean gas pressures, gas mixtures, break-down voltages, input voltages, and resistances.

#### 3.3.1 Effects of Gas Composition and Mean Pressure

The following three figures present the performance indices (input and output powers, acoustic driver and linear alternator strokes, dynamic pressure at the resonator, input and output volts and current and the overall conversion efficiency) for an array of operating conditions. (Frequency range 45-70 Hz, mean gas pressures: 4 bar, 12 bar and 21 bar, gas mixture composition: 100% helium, 60% helium /40% argon, 40% helium /60% argon, and 100% argon, 22 Ohm load resistance with 6V zeners at 20 Vrms input to the acoustic driver). The results are presented at 21 bar (**Figure 3.12**) then at 12 bar (**Figure 3.13**), and finally at 4 bar (**Figure 3.14**).

Mean pressure has a significant effect on the performance of the system and can be summarized as follows:

- As the mean gas pressure increase the overall conversion efficiency increase as the increase in mean gas pressure, increase the power density without an increase in the required input power.
- Increasing the mean pressure decrease the acoustic driver stroke which allows more loading of the acoustic driver without suffering of over-stroking of either in the acoustic driver or in the linear alternator.
- For all different pressures, still the point of maximum efficiency differ from the point of maximum power. Which is considered as a known phenomenon in thermoacoustic devices.

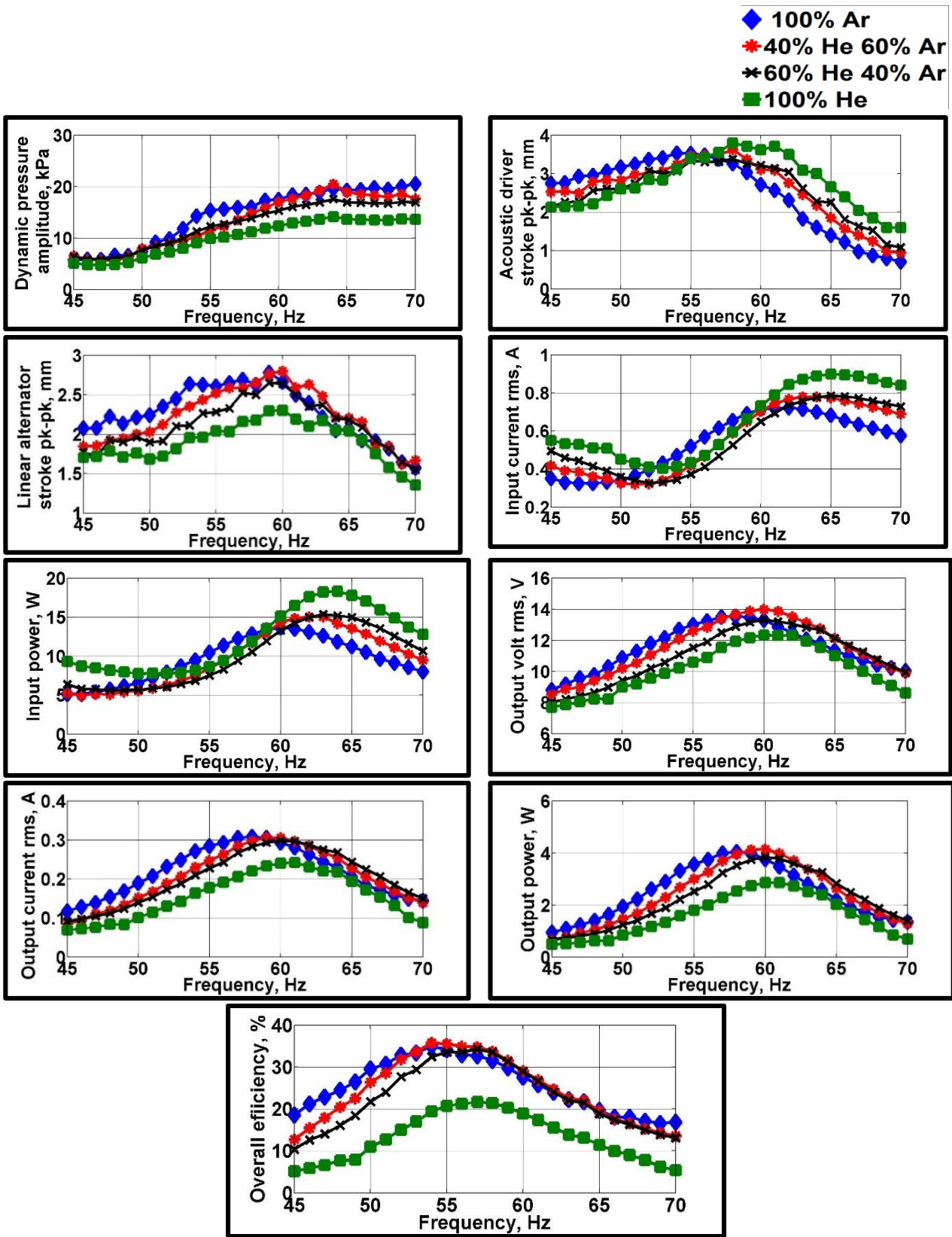


Figure 3.12: Frequency response at 21bar mean gas pressure  
20 V<sub>RMS</sub>, 22 Ω, 6V zener



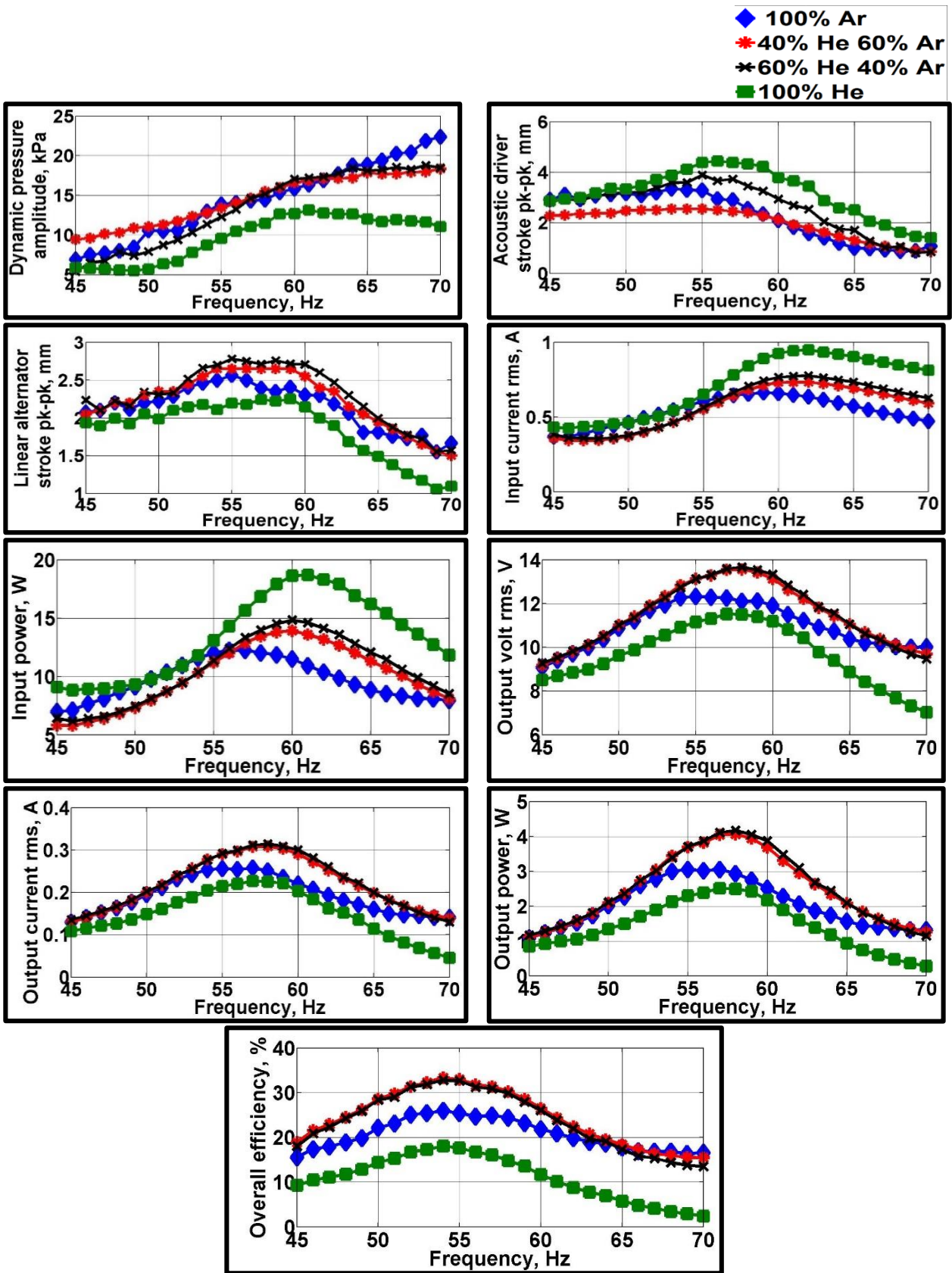


Figure 3.13: Frequency response at 12 bar mean gas pressure  
20 V<sub>RMS</sub>, 22 Ω, 6V zener

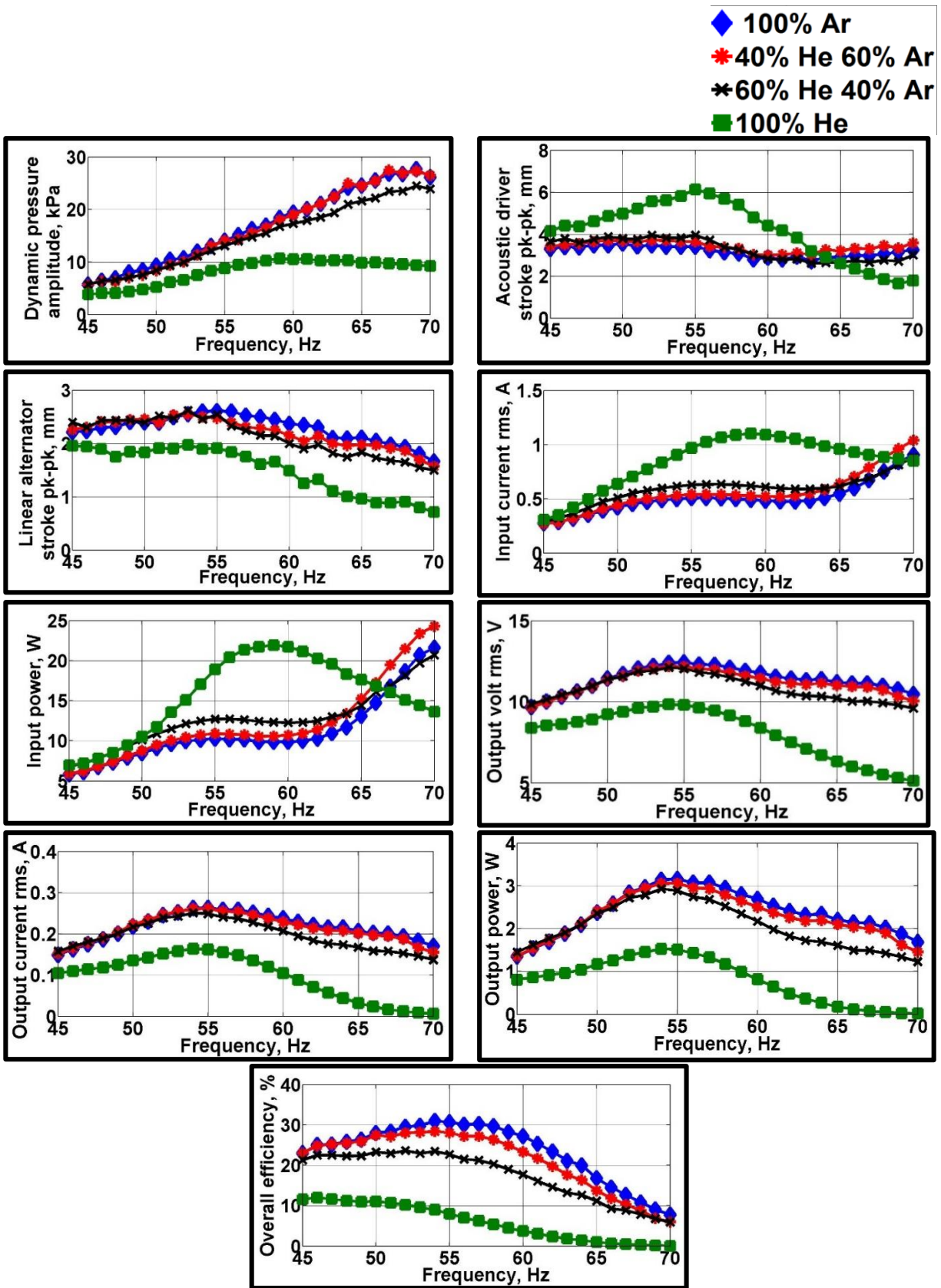


Figure 3.14: Frequency response at 4 bar mean gas pressure  
 20 V<sub>RMS</sub>, 22 Ω, 6V zener

### 3.3.2 Effects of Input Voltage

Figure 3.15 present the performance indices (input and output powers, acoustic driver and linear alternator strokes, dynamic pressure at the resonator, input and output volts and current and the overall conversion efficiency) for an array of operating conditions. (Electric resistance range: 5-60  $\Omega$ , mean gas pressures: 12 bar, gas mixture composition: 40% helium /60% argon with 6V zeners at an input volt range: 20-60  $V_{rms}$  to the acoustic driver).

Input electric volt has a significant effect on the performance of the system and can be summarized as follows:

- Varying the electrical resistance does not have a significant effect on the value of the dynamic pressure amplitude as the input volt.
- The linear alternator stroke is strongly affected by both the increase in the input volt and the increase in the value of the electrical resistance.
- The value of the linear alternator increase with a uniform value as the input volt increase, except for the increase from 50  $V_{RMS}$  to 60 $V_{RMS}$  a slight increase is monitored this could be due to the increase of the non-linearity inside the system with the increase of the input power to the acoustic driver.
- The overall conversion efficiency seems to be decreasing with the increase of the input electric power to the acoustic driver. Which is also considered as an indicator of non-linearity with the increase of input power.

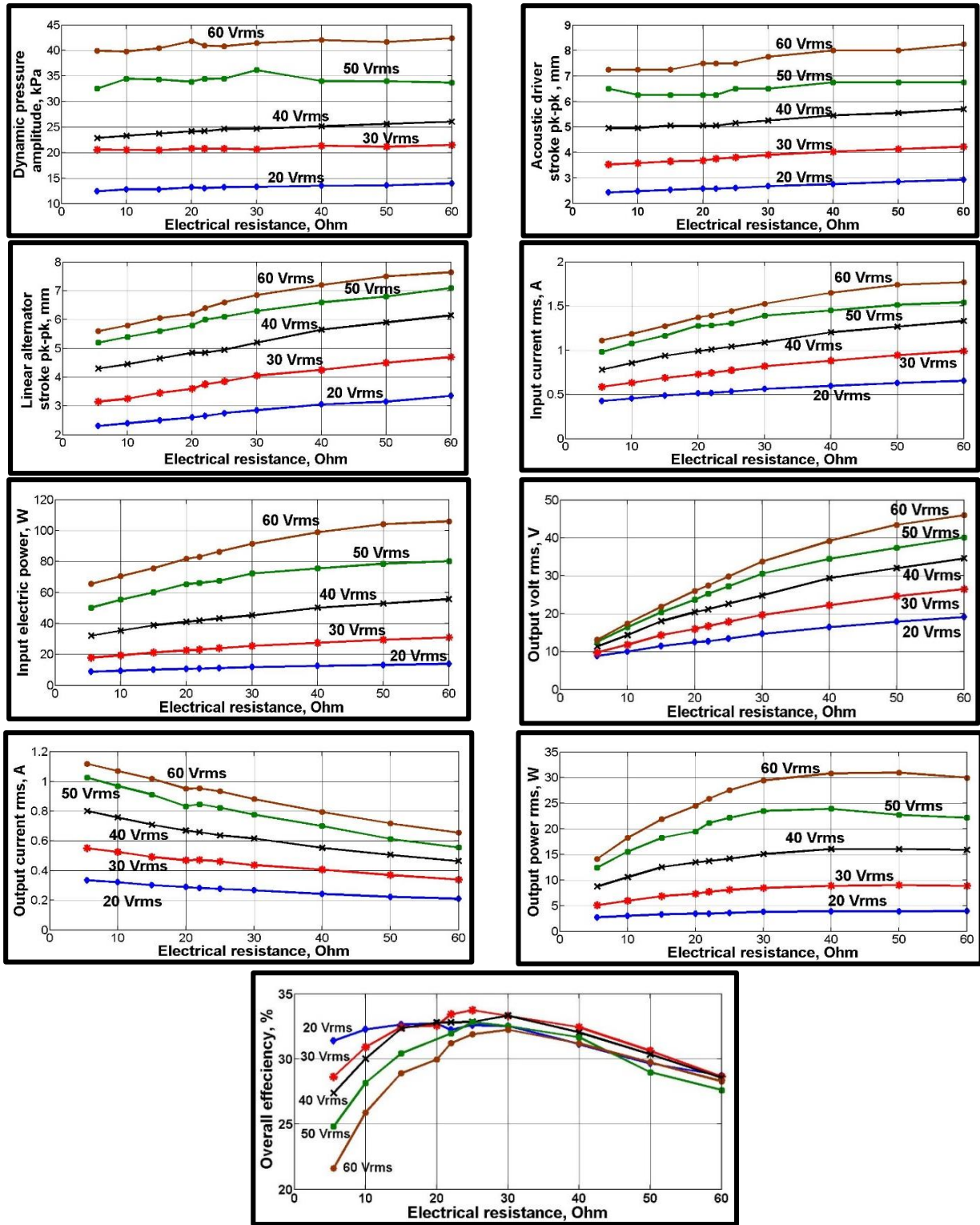


Figure 3.15: Electrical resistance response at 12 bar mean gas pressure and 6V zener

### 3.3.3 Effects of Electric Load Resistance

This set of results show very valuable data on how to control the linear alternator's stroke using the load resistance and/or the zener breakdown voltage, with and without non-linear loads, as well as the effects of the change in the load resistance on the other parameters of the system.

**Figure 3.16** present the performance indices (input and output powers, acoustic driver and linear alternator strokes, dynamic pressure at the resonator, input and output volts and current and the overall conversion efficiency) for an array of operating conditions. (Electric resistance range: 5-60  $\Omega$ , mean gas pressures: 12 bar, gas mixture composition: 40% helium /60% argon with zeners Breakdown voltage range: 6V – 20V at an input volt range: 20 Vrms to the acoustic driver).

Zener breakdown voltage has a significant effect on the performance of the system and can be summarized as follows:

- Working with linear load -no zener- gives high conversion efficiency as the value of electrical resistance increase. In real TAE this could not be used as linear load will cause the engine either to over stroke or to have problems in startup due to the presence of transient region as stated in [9].
- With the increase of the value of the zener breakdown voltage the overall conversion efficiency decrease due to the increase of non-linearity inside the system. So that's why it is recommended to use the least value of zener breakdown voltage.
- Zener breakdown voltage has a significant effect on the value of linear alternator stroke. As the breakdown voltage increase the output volt from linear alternator increase hence the linear alternator stroke increase.

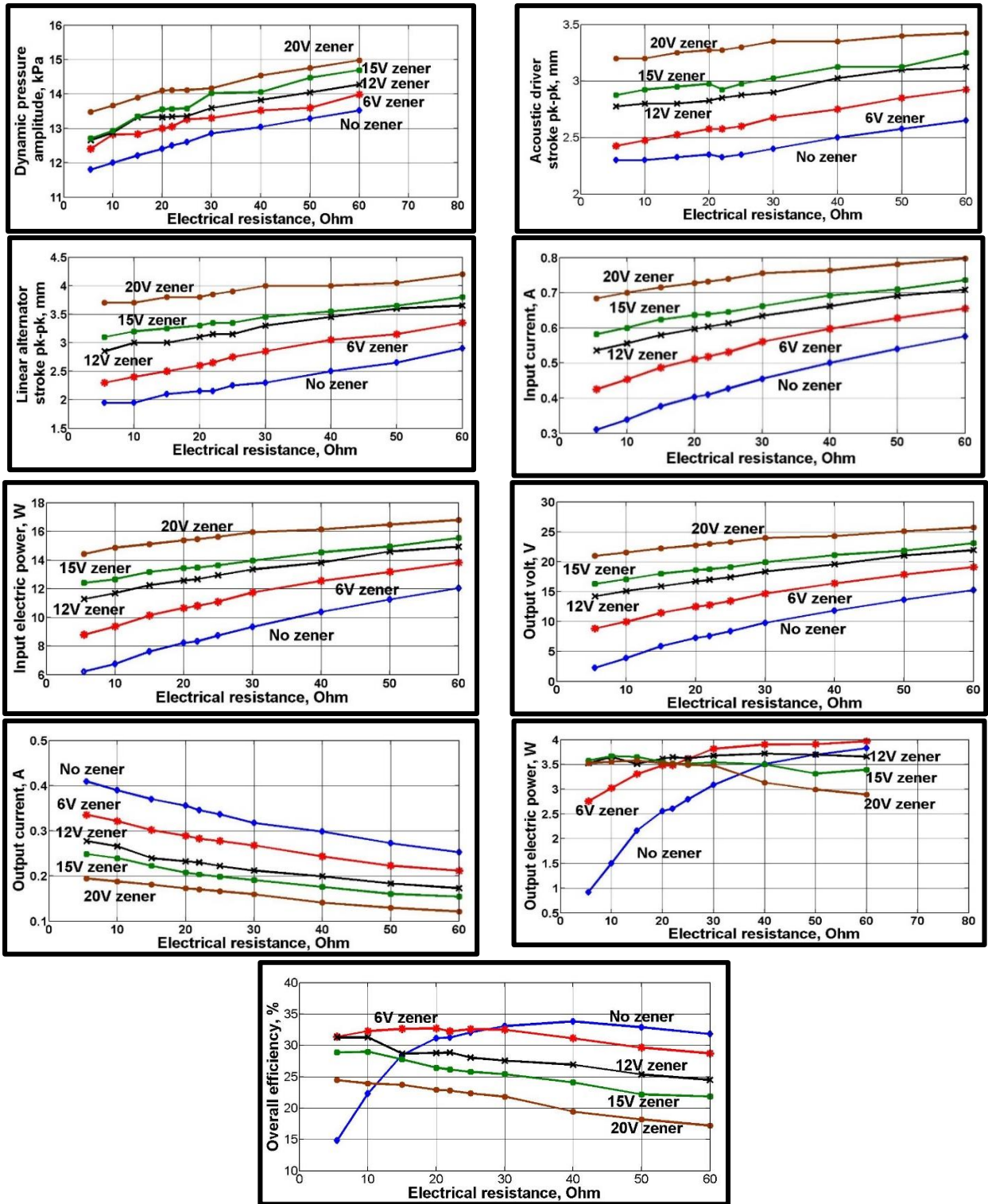
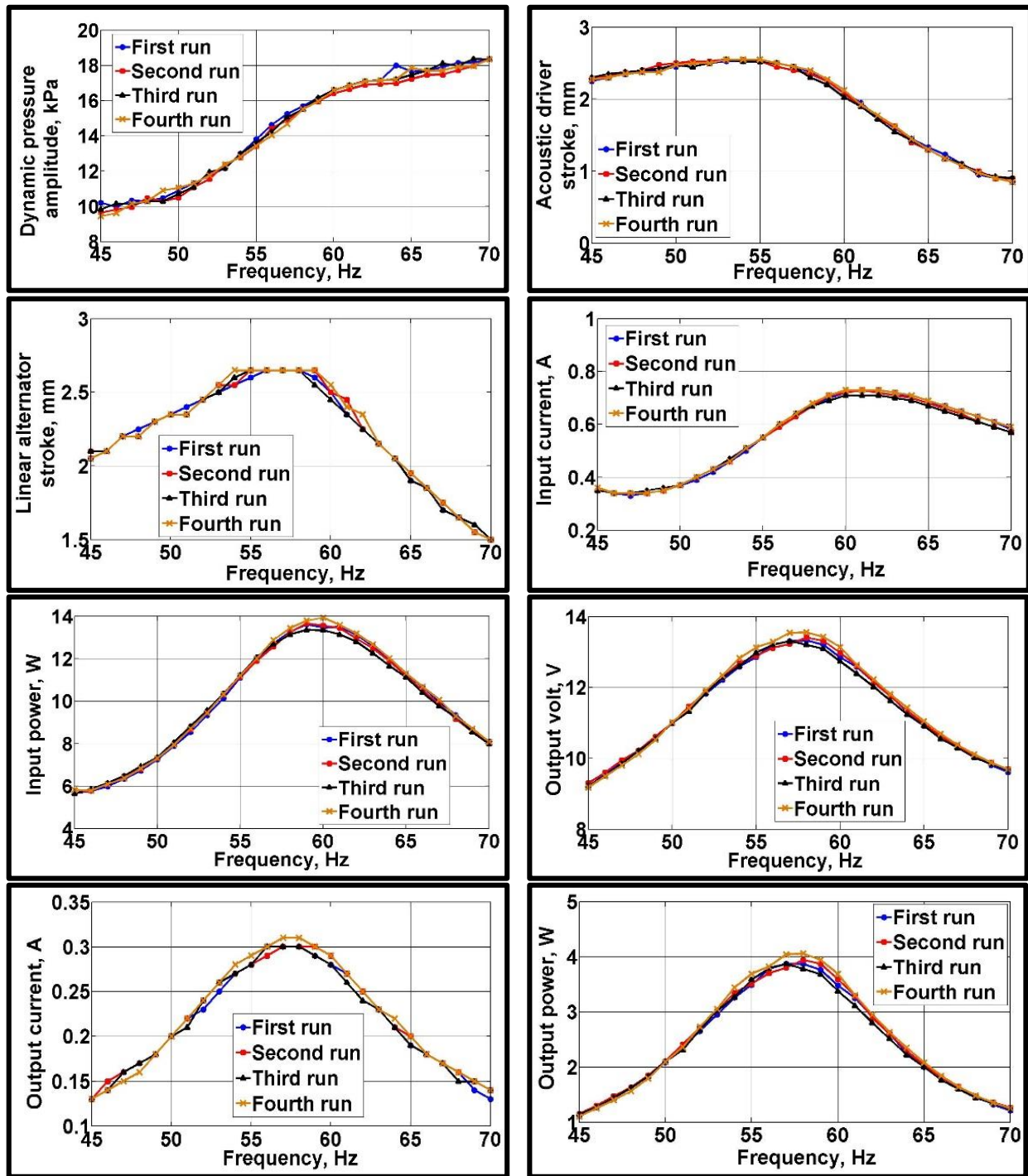
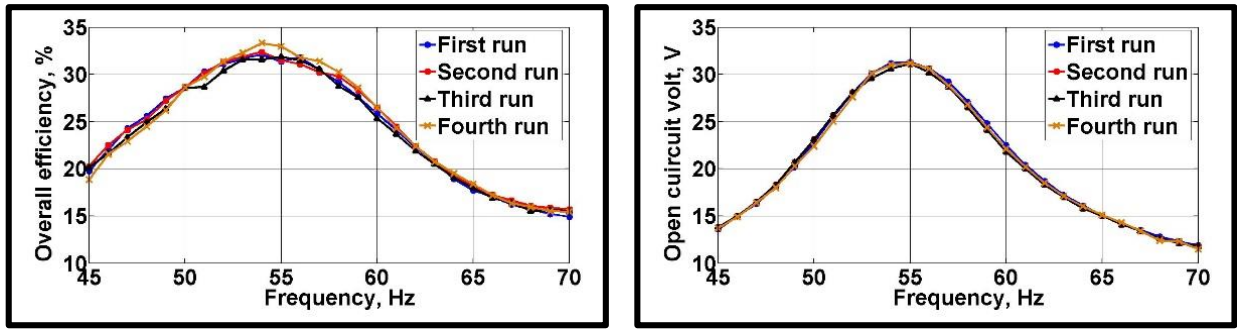


Figure 3.16: Electrical resistance response at 12 bar mean gas pressure and 20 V<sub>RMS</sub>

### 3.4 Retest Reliability

The repeatability of the results presented is studied for a certain set of operating conditions. This set is as follows: a working mixture of 40% He/ 60% Ar, a mean gas pressure of 12 bar, an input voltage to the acoustic driver of 20 V<sub>RMS</sub>, a load resistance of 22Ω, and a ten set of 6V zener. The results for four repeated sets are presented in **Figure 3.17** below.





**Figure 3.17:** Frequency response for basic case to check system repeatability



# Chapter 4 - Conclusions, Summary and Future Work

## 4.1 Conclusions and Summary

Linear alternators are essential parts of TAPC's. They require two simultaneous matching: acoustic matching with the thermoacoustic engine (or source of acoustic power) and electric matching with the load used. In this regard, the current work presents and discusses the following issues:

- 1- The experimental method to test linear alternators in the absence of thermoacoustic engines (and their associated problem) and under controlled conditions.
- 2- The experimental technique to test the acoustic and electric matching of linear alternators under different conditions.
- 3- The work discussed the need of non-linear loads and the use of back-to-back zener diodes as non-linear loads.

The effects of the use of non-linear parts on the system performance via comparison with linear simple resistive loads

Proper operation of TAPC's require simultaneous observation of two conditions: proper frequency and achievement of rated stroke at the rated output power. An additional constraint is protection against over-stroking. Simultaneous satisfaction of these conditions is usually complicated. The present work presents some general guidelines that can be used to help at the design stage. They guidelines are:

- 1- It is critical to be able to know which load corresponds to which stroke. The linear alternator's stroke is proportional to the resistance of the load up to a certain limit. This valuable information can help to adjust the stroke to the required level. Real operation with TAPC's will either feed into the grid (a fixed load that cannot be controlled) or either into a user's load (can be controlled). (If connected to the electrical grid, the voltage is forced by the grid, and thereby the stroke (proportional to voltage) is also fixed. The grid acts as a very non-constant resistor: near zero if generated voltage is lower than grid, and near infinite if the voltage is higher than grid. Similar non-linear loads can be built with solid-state components that switch resistance levels rapidly (much faster than engine cycle frequency) to give a similar effect).

- 2- Based on item 1 above, a stall circuit is introduced that introduces a high-power low resistive-load in parallel to the linear alternator to limit the stroke of the alternator if the measured stroke exceeds a certain critical limit. This is critical in actual TAPC's, particularly during the development and initial testing phase.
- 3- The working gas used has large effects on the satisfaction of these conditions simultaneously. The effects of the product of the mean gas density times the speed of sound are presented and discussed. Actual TAPC's require more conditions like large thermal conductivity (for enhanced heat transfer coefficient on the gas side) as well as low Prandtl number (for low viscous losses).

## 4.2 Suggestions for Recommended Future Work

The following are suggestions for possible work in this field

- 1- Investigate the effects of the front volume (AKA compression volume) on the linear alternator performance. This volume refers to the compressible volume in front of the alternator's piston. Reducing this volume reduces the viscous losses and affects the stroke required to generate a certain power, thus affecting the conversion efficiency. However, there is a limit on the minimum volume required to house the different components and special care should be taken since a smaller volume may incur sudden changes in shape while smooth transitions correspond to large compression volumes. Some of the methods include modifying the piston so that it has a stepped profile or an added-on piece that occupies some of the compression volume, but this increases the moving mass and lowers the mechanical resonance frequency.
- 2- Studying the role of the back volume (the volume enclosing the alternator, AKA the enclosure volume) on the conversion efficiency and the mechanical resonance frequency. Enlarging this volume reduces the pressure wave in the backspace, which in turn reduces the thermal relaxation losses and the seal losses, causing an increase in the conversion efficiency. However, this significantly increases the total volume of the system, causing a decrease in the power density.
- 3- Use of electronic loads that employ pulse width modulations, to simulate matching of different non-linear loads (constant voltage, constant current on constant power) on the linear alternator's performance.
- 4- Replacing the acoustic driver with thermoacoustic engine in order to test the effect of the transient work on the behavior of the linear alternators.

## References

- [1] S. Garret and S. Backhaus, "American Scientist Online - The Power of Sound," [Online]. Available: [www.americanscientist.org](http://www.americanscientist.org). [Accessed 13 January 2015].
- [2] S. Backhaus and G. Swift, "New Varieties of Thermoacoustic Engines," in *9th International Congress on Sound and Vibration*, 2002.
- [3] W. Marrison, "Heat-Controlled Acoustic Wave System". U.S. Patent 2,836,033, 1958.
- [4] T. Yazaki, A. Iwata, T. Maekawa and A. Tominaga, "Traveling Wave Thermoacoustic Engine in a Looped Tube," *Physical Review Letters*, vol. 81, pp. 3128-3131, 1998.
- [5] S. Backhaus and G. Swift, "A thermoacoustic-Stirling heat engine: Detailed Study," *J. Acoust. Soc. Am.*, vol. 107, pp. 3148-3166, 2000.
- [6] S. Backhaus and G. Swift, "A thermoacoustic Stirling heat engine," *Nature*, vol. 399, pp. 335-338, 1999.
- [7] M. Petach, E. Tward and S. Backhaus, "Design Of A High Efficiency Power Source (HEPS) Based On Thermoacoustic Technology," Final report, NASA contract no. NAS3-01103, 2004.
- [8] P. H. Riley, "Designing a low-cost electricity-generating cooking stove for high-volume implementation," Thesis submitted for the degree of Doctor of Philosophy to the University of Nottingham, Nottingham, 2014.
- [9] M. P. Telesz, "Design and testing of a thermoacoustic power converter," Master of science in the School of Mechanical Engineering, Georgia Institute of Technology, 2006.
- [10] G. W. Swift and Steven L. Garrett, "Thermoacoustics: a unifying perspective for some engines and refrigerators.," *J. Acoust. Soc. Am.*, vol. 113, pp. 2379-2381, 2003.
- [11] S. Garret, "Resource letter: TA-1: Thermoacoustic engines and refrigerators," *American Journal of Physics*, vol. 72, no. 1, pp. 11-17, 2004.
- [12] C.M. Johnson, P.H. Riley and C.R. Saha, " Investigation of a thermo-acoustically driven linear alternator," in *U21 Energy Conference*, Birmingham, UK, 2008.
- [13] D.A. Wilcox, "Experimental investigation of a thermoacoustic-stirling engine electric generator with gideon streaming suppression," M.Sc. from The Graduate School, The Pennsylvania State University, 2011.
- [14] Zhanghua Wu, Wei Dai, Man Man and Ercang Luo, "A solar-powered traveling-wave thermoacoustic electricity generator," *Solar Energy*, vol. 86, pp. 2376-2382, 2012.

- [15] Qnergy, [Online]. Available: <http://www.qnergy.com/>. [Accessed April 2015].
- [16] Private communication with P.Spoor and G.Reid at Q-Drive (Chart Industries), 2014.
- [17] J. A. Corey and J. Martin, "Matching an acoustic driver to an acoustic load in an acoustic resonant system". Patent US 6604363 B2, 2001.
- [18] J. Clark, W. Ward and G. Swift, "Design environment for low-amplitude thermoacoustic energy conversion (DeltaEC)," *J. Acoust. Soc. Am.*, vol. 122, no. 5, 2007.
- [19] "ASME standards for pressure vessels (section VIII)," [Online]. Available: [www.asme.org](http://www.asme.org). [Accessed 2015].
- [20] "1S102D-X Acoustic Driver, User manual," CHART, Qdrive.
- [21] James R. Belcher, William V. Slaton, Richard Raspet, Henry E. Bass and Jay Lightfoot, "Working gases in thermoacoustic engines," *J. Acoust. Soc. Am.*, vol. 105, pp. 2677-2684, 1999.
- [22] S. Garrett, D. Perkins and Ashok Gopinath, "Thermoacoustic refrigerator heat exchangers: design, analysis and fabrication," in *10th International Heat Transfer Conference*, Brighton, England, 1994.
- [23] P. Ceperley, "A Pistonless Stirling Engine – The traveling wave heat engine," *J. Acoust. Soc. Am.*, vol. 66, pp. 1508-1513, 1979.

## Appendix A - DeltaEC Code

### **Begin segment**

This segment contains the required mean working gas pressure and mixture, the operating frequency, the dynamic gas pressure amplitude and the volumetric gas velocity and their phases at the starting point of the system, which is end of the acoustic driver enclosure.

### **Anchor segment**

The sole target of this segment is to dissipate any heat energies in the system in order to only study the acoustic behavior of the system. This is used because the system does not contain heat exchangers.

### **Acoustic driver (VESPEAKER segment)**

The segment of the acoustic driver is chosen as (VESPEAKER) because in this segment the amplitude of the input volt to the acoustic driver and its angle relative to the dynamic pressure are input parameters by the user. Thus, this selection facilitates the process of controlling the input power to the acoustic driver.

### **Linear alternator (IESPEAKER segment)**

The linear alternator is chosen as (IESPEAKER) in order to be able to monitor the amplitude and the phase of the generated current from the linear alternator. The recommended maximum current limit by the supplier is 2A (RMS) in order to protect the coil of the linear alternator from overheating.

An important point is the value of the BL product (transduction coefficient): since the linear alternator used in the lab originally is designed and built as an acoustic driver, its BL product is de-rated by 0.8 [16].

### **Resonator (DUCT segment)**

Resonator (AKA front volume) is chosen as (DUCT) segment. Its diameter must be equal to the piston diameter of the linear alternator to avoid any minor losses due to sudden diameter changes. The DeltaEC allows numerical simulation of the effects of the resonator length on the system performance.

### **Enclosure volumes (DUCT segment)**

Enclosure volumes (AKA back volumes) are chosen as (DUCT) segment. The length and diameter must be greater than the outer dimensions of the used acoustic driver and linear alternator. The DeltaEC allows numerical simulation of the effects of the enclosure volume (via a controlled change in the length) on the system performance.

## Other segments (RPN segments)

Different (RPN) segments are used to monitor and control the following parameters:

- 1- Acoustic driver stroke amplitude =  $\frac{\text{amplitude of volumetric velocity of acoustic driver}}{\text{piston area} \cdot \text{angular frequency}}$
- 2- Acoustic driver electric-to-acoustic efficiency =  $\frac{\text{Output acoustic power}}{\text{Input electric power}}$
- 3- Enforcing resonance at the beginning of the resonator:  
Phase (Dynamic pressure) – Phase of (Volumetric velocity)
- 4- Enforcing desired dynamic pressure amplitude inside the resonator
- 5- Linear alternator acoustic-to-electric efficiency =  $\frac{\text{Output electric power}}{\text{Input acoustic power}}$
- 6- Linear alternator stroke amplitude =  $\frac{\text{amplitude of volumetric velocity of linear alternator}}{\text{piston area} \cdot \text{angular frequency}}$
- 7- Enforcing the angle between volt and current in linear alternator  
Phase (LA volt) – Phase of (LA current)
- 8- Over all conversion efficiency for the setup =  $\frac{\text{Output electric power}}{\text{Input electric power}}$

```

!----- 0 -----
BEGIN
1.2000E+06 a Mean P Pa
50.019 b Freq Hz G
300.00 c TBeg K
8908.1 d |p| Pa G
0.0000 e Ph(p) deg
0.0000 f |U| m^3/s
0.0000 g Ph(U) deg
0.6000 jnL
HeAr Gas type
!----- 1 -----
ANCHOR Energy dissipation
!----- 2 -----
DUCT Acoustic driver enclosure
8.0000E-03 a Area m^2 8874.8 A |p| Pa
0.8600 bPerim m 3.0900E-03 B Ph(p) deg
0.1300 c Length m 1.4648E-03 C |U| m^3/s
0.0000 d Srough -90.42 D Ph(U) deg
-4.7992E-02 E Htot W
ideal Solid type -4.7992E-02 F Edot W

```

!----- 3 -----  
 VESPEAKER Qdrive (1s102d-x) - Acoustic Driver (S/N:777)  
 2.0000E-03 a Area m^2 1.2000E+04 A |p| Pa  
 6.7000 b R ohms -90.427 B Ph(p) deg  
 8.6400E-02 c L H 1.4645E-03 C |U| m^3/s  
 47.690 d BLProd T-m -90.427 D Ph(U) deg  
 0.4922 e M kg 8.7873 E Htot W  
 3.0490E+04 f K N/m 8.7873 FEdot W  
 4.6900 g Rm N-s/m 12.099 G WorkIn W  
 31.370 h |V| V G 31.370 H Volts V  
 127.17 iPh(V) deg G 0.77324 I Amps A  
 -4.0236 JPh(V/I) deg  
 1.4979E+04 K |Px| Pa  
 ideal Solid type -126.76 L Ph(Px) deg

!----- 4 -----  
 RPN Acoustic driver efficiency  
 0.0000 a G or T 72.631 A %  
 3F 3G / 100 \*

!----- 5 -----  
 RPN Acoustic driver stroke (amplitude)  
 2.3300E-03 a G or T =5A 2.3300E-03 A ChngeMe  
 3C 3a / w /

!----- 6 -----  
 RPN enforce Resonance  
 0.0000 a G or T =6A 0.0000 A deg  
 3B 3D -

!----- 7 -----  
 RPN enforce desired pressure amplitude  
 1.2000E+04 a G or T =7A 1.2000E+04 A pa  
 p1 mag

!----- 8 -----  
 DUCT Change Me  
 sameas 9a a Area m^2 Mstr 1.1998E+04 A |p| Pa  
 0.15853 b Perim m 8a -90.672 B Ph(p) deg  
 sameas 9c c Length m 1.4669E-03 C |U| m^3/s  
 0.0000 d Srough -94.133 D Ph(U) deg  
 8.7840 E Htot W  
 ideal Solid type 8.7840 F Edot W

!----- 9 -----  
 DUCT Resonator



2.0000E-03 a Area m^2 Mstr 1.1993E+04 A |p| Pa  
 0.39354 b Perim m 9a -90.917 B Ph(p) deg  
 2.5000E-02 c Length m 1.4743E-03 C |U| m^3/s  
 0.0000 d Srough -97.844 D Ph(U) deg

8.7758 EHtot W

ideal Solid type 8.7758 F Edot W

!----- 10 -----

IESPEAKER Qdrive (1s102d-x) - Linear Alternator(S/N:774)

2.0000E-03 a Area m^2 8930.6 A |p| Pa  
 6.7200 b R ohms 172.59 B Ph(p) deg  
 8.4100E-02 c L H 1.4740E-03 C |U| m^3/s  
 38.408 d BLProd T-m -97.838 D Ph(U) deg

0.4780 e M kg 4.8597E-02 E Htot W

3.0940E+04 f K N/m 4.8597E-02 F Edot W

4.5500 g Rm N-s/m -5.8582 G WorkIn W

0.6967 h |I| A G 16.817 H Volts V

221.57 iPh(I) deg G 0.6967 I Amps A

180.00 J Ph(V/I) deg

1.5742E+04 K |Px| Pa

ideal Solid type 123.39 L Ph(Px) deg

!----- 11 -----

RPN Linear alternator efficiency

0.0000 a G or T 66.753 A %

10G 9F / -100 \*

!----- 12 -----

RPN Linear alternator stroke (Pk-Pk)

0.0000 a G or T 2.3451E-03 A m

10C 10a / w /

!----- 13 -----

RPN angle between volt and current in linear alternator

180.00 a G or T =13A 180.00 A deg

10J

!----- 14 -----

DUCT Linear alternator enclosure volume

8.0000E-03 a Area m^2 8964.2 A |p| Pa

0.8600 b Perim m 172.58 B Ph(p) deg

0.1300 c Length m 1.1596E-18 C |U| m^3/s

0.0000 d Srough -135.47 D Ph(U) deg

3.2038E-15 E Htot W

ideal Solid type 3.2038E-15 F Edot W

!----- 15 -----

HARDEND Rigid termination

0.0000 a R(1/z) =15G 8964.2 A |p| Pa

0.0000 b I(1/z) =15H 172.58 B Ph(p) deg  
 1.1596E-18 C |U| m^3/s  
 -135.47 D Ph(U) deg  
 3.2038E-15 E Htot W  
 3.2038E-15 F Edot W  
 4.1918E-17 G R(1/z)  
 5.3546E-17 H I(1/z)

!----- 16 -----

RPN Overall Efficiency  
 0.0000 a G or T 48.421 A %  
 10G 3G / -100 \*

! The restart information below was generated by a previous run  
 ! and will be used by DeltaEC the next time it opens this file.

guessz 0b 0d 3h 3i 10h 10i  
 xprecn 2.3355E-04 3.3854E-02 4.3399E-04 -4.0609E-03 -3.9771E-07 3.2610E-03  
 targs 5a 6a 7a 13a 15a 15b  
 mstr-slave 2 8 -2 9 -2

! Plot start, end, and step values. May be edited if you wish.  
 ! Outer Loop: | Inner Loop .

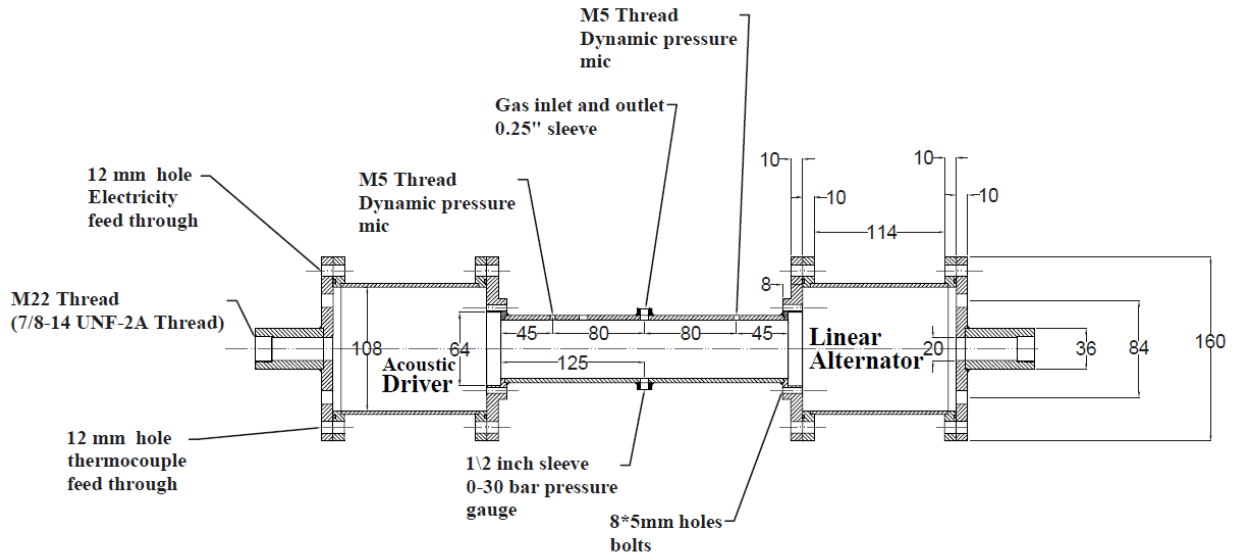
## Appendix B - Guesses, Targets and Main Parameters in DeltaEC

The DeltaEC code is based on some parameters to be guessed, some parameters to be targeted and some parameters to be only monitored by the user. The following table shows all guesses, targets and other monitored parameters that have been used to reach the preliminary design of the built system.

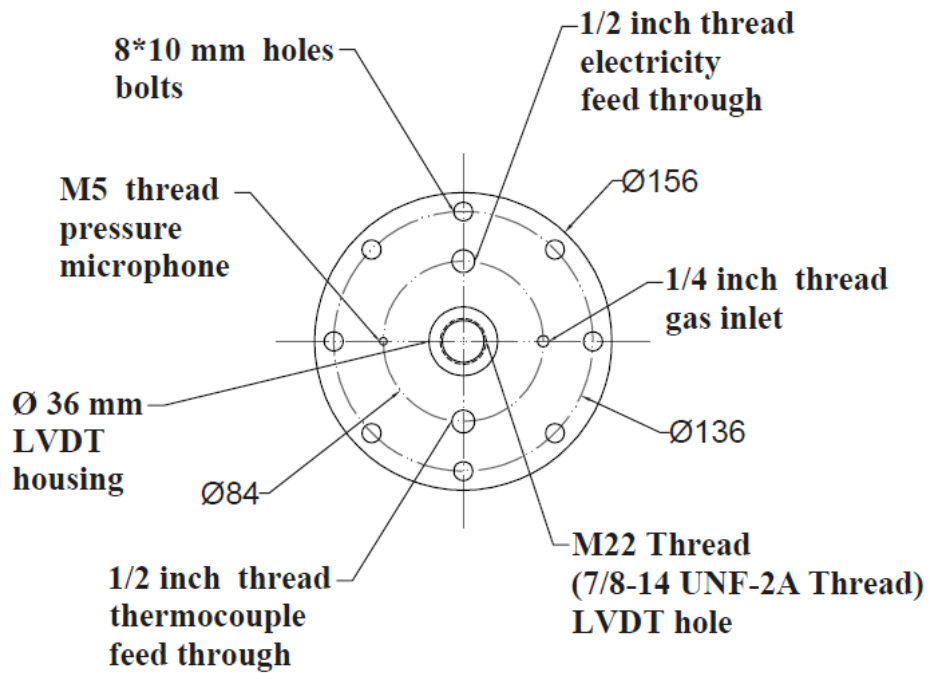
Guesses, targets and main parameters used in DeltaEC simulation

tem No.	Description	Segment	Type	Value
1	Frequency	BEGIN	Guess	50 Hz
2	Dynamic pressure amplitude in AD enclosure	BEGIN	Guess	8.9kPa
3	Acoustic driver volt amplitude	VESPEAKER	Guess	31.37 V
4	AD volt phase relative to AD enclosure dynamic pressure	VESPEAKER	Guess	127.1 °
5	Acoustic driver stroke amplitude	RPN	Target	2.33 mm
6	Enforce resonance inside the resonator	RPN	Target	0°
7	Enforce desired pressure amplitude inside the resonator	RPN	Target	12 kPa
8	Linear alternator current amplitude	IESPEAKER	Guess	0.69 A
9	LA current phase relative to AD enclosure dynamic pressure	IESPEAKER	Guess	221.5°
10	Angle between volt and current in linear alternator	RPN	Target	180°
11	Impedance real part	HARDEND	Target	0
12	Impedance imaginary part	HARDEND	Target	0
13	Input electric power to acoustic driver	VESPEAKER	--	12.1 W
14	Acoustic driver efficiency	RPN	--	72.6 %
15	Resonator dynamic pressure amplitude	RPN	--	11.9 kPa
16	Output electric power from linear alternator	IESPEAKER	--	5.8 W
17	Linear alternator efficiency	RPN	--	66.7 %
18	Linear alternator stroke amplitude	RPN	--	2.34 mm
19	Overall conversion efficiency	RPN	--	48.4%

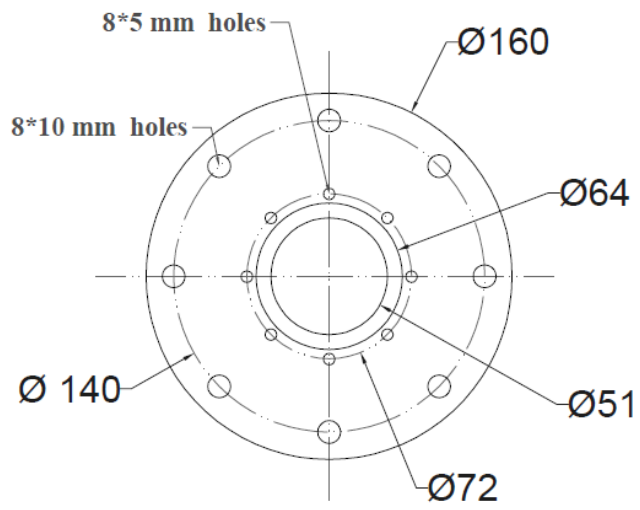
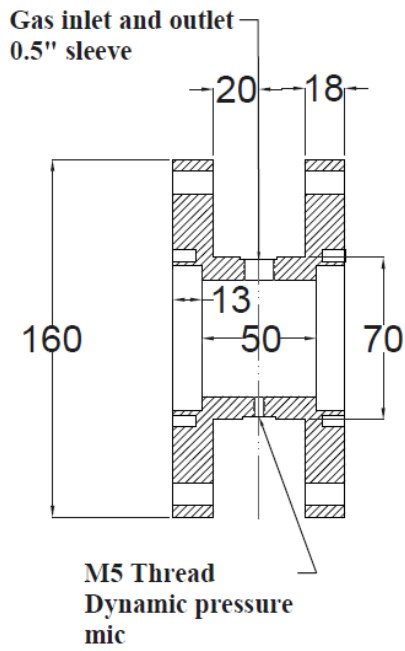
## Appendix C - Mechanical Drawings



SECTIONAL FRONT VIEW



SIDE VIEW



## 5 cm Module

## Appendix D - Assembly of the Experimental Setup

In this section the details of the assembly process of the experimental setup are explained

- 1- The resonator under test, corresponding to the required front volume ahead of the linear alternator is used. Its internal surface is cleaned in house before use to remove dust (in addition to the polishing made during manufacturing). **Figure I** shows a digital image of the 5 cm resonator.



**Figure I:** Left: the gas inlet port. Right: The pressure microphone port and how the resonator surface is flattened to provide proper sealing

- 2- Acoustic driver is fixed on one side using eight M5 bolts in order to be well placed in its place. The same procedure is made for the linear alternator on the other side. **Figure II** shows the fixation of the acoustic driver and linear alternator on the resonator

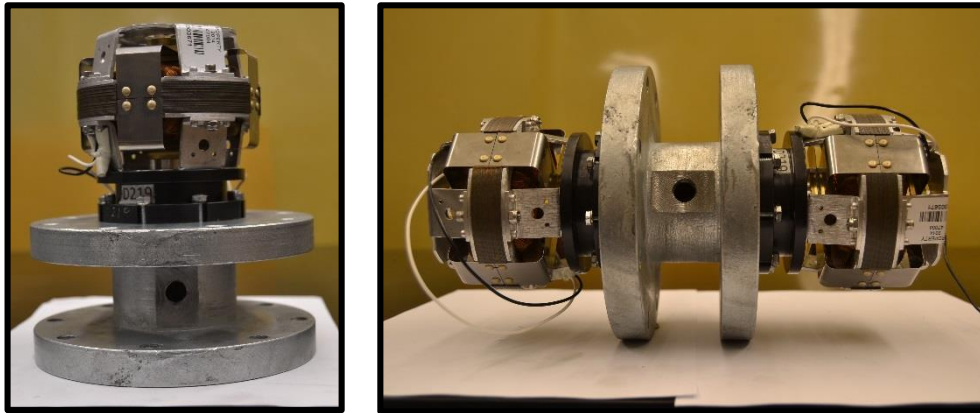


**Figure II:** Left: Acoustic driver fixed on the resonator. Right: Acoustic driver and linear alternator fixed on the resonator

- 3- Then the enclosure volume of the acoustic driver and the linear alternator are assembled to the resonator using eight M10 bolts and nuts for each side (using antilock washers is recommended due to presence of vibration). **Figure** shows the fixation of the two enclosure volumes.

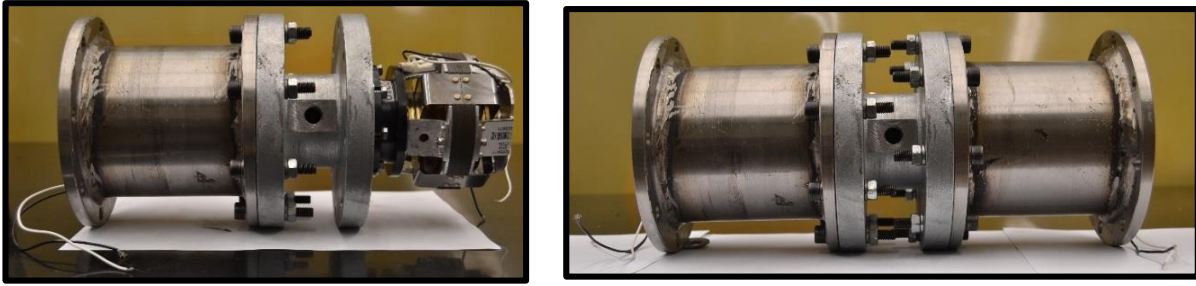


**Figure III:** Right: Acoustic driver enclosure fixation. Right: Both enclosures are fixed

- 4- The LVDT rod is fixed in the back of the piston as shown in **Figure IV**.
- 5- The enclosure volume flange is then fixed at the back of each enclosure volume using eight M10 bolts and nuts with antilock washers. The system should be tested during the fixation of the flange to be sure that the LVDT probe is aligned and that the LVDT is reading zero displacement after fastening the bolts to avoid any zero error in the piston stroke measurement. The signal conditioner has a special screw that can be used to null the reading and is used for this purpose.
- 6- The set of the mean pressure and vacuum gages and their flow control valves is installed at the proper port of the resonator. A digital image of the whole assembly is shown in Figure .

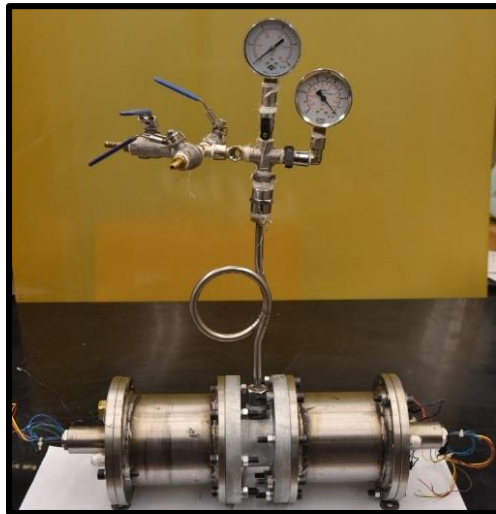


**Figure IV:** System after assembling all its parts

# Appendix E - Matlab Codes

## Main Data reading, manipulation and plotting code

```
%%%plot_external.m and psd_harmonics.m are two user defined functions needed to run this code
```

```
{
This code takes excel sheets files found in folder as a input, it reads each file seperatley inlcuding all its tabs and does some data manipulation and outputs to another excel sheet (result file). The whole process goes on all the excel files found in the folder defined by directory then it plots the data with respect to 1st column in result excel or random range defined by the user
```

```
inputs
```

```
1.directory containing the excel sheets.
2.flag to choose random range of data.
3.Array contains the random values that will be inserted in the result excel sheet.
4.the start value of the 1st column in the result excel sheet and x-axis of the plots.
5.the end value of the 1st column in the result excel sheet and x-axis of the plots.
6.the sensitivity of the LVDT in mm/volt
7.the sensitivity if the pressure microphone in mV/kPa
8.the gain of the signal amplifier
9.flag to get PSD of multiple cycles signals that will override other data manipulation done on two cycles signals.
10.the sampling rate in samples per second used in computing the PSD.
11.ensemble average used in computing the PSD.
```

```
All the raw data in the Excel Sheets are in Voltage
```

```
outputs
```

```
1. result excel file contains all the data manipulation
2. plots of the each columns starting from the second to the last one w.r.t the 1st column
%}
```

```
clear all
close all
clc
```

```
prompt={'Enter the directory (should have all the .xlsx sheet which contains the excel file (ex: E:\Work\AUC\Experimental Data\2):',...
'Enter the name of the files before the variable',...
'Enter the unit of the variable',...
'Enter the LVDT Sensitivity in mm/Volt (ex: 1.25)',...
'Enter the Pressure Microphone Sensitivity in kPa/mV corresponding to the serial number of the microphone used (ex: 0.101)',...

```



```

        'Enter the gain of the signal conditioner amplifier (ex: 100)',...
        'Enter 1 to calculate the acoustic power, PSD of the many cycles
excel sheets and phase calculation (ex: [1,0,0])',...
        'Enter Sampling rate in Samples per second (ex: 50000)',...
        'Enter number of Ensemble Average for FFT (ex: 1 or 2)',...
        'Enter Frequency at which the PSD figures will be calculated (ex:
47Hz)'
                };

name='Inputs';
numlines=1; % leaves one line empty in the blank space in the graphical user
interface
defaultanswer={'E:\Work\AUC\Experimental Data\Load Response @ 2 Vpp 54
Hz',' ',' Hz Voc  two cycles
5ms','1.25','0.103','100','[0,0,0]','2500','1','47'};
answer=inputdlg(prompt,name,numlines,defaultanswer);

i=1;
j=2;

%this creates a matrix with number of rows equal to the length of the
%frequency column and with 11 columns
LVDT_sensitivity = str2num(answer{4});
MICRO_sensitivity = str2num(answer{5});
gain = str2num(answer{6});
flag_array = str2num(answer{7});
acoustic_power_flag = flag_array(1);
FFT_flag = flag_array(2);
phase_flag = flag_array(3);
samprate = str2num(answer{8});
numens = str2num(answer{9});
PSD_freq = str2num(answer{10});

Folder=cd(answer{1});
folder_var1 = answer{2};
folder_var2 = answer{3};
% change the working directory to the directory where the files are placed

d = dir('*.xlsx');
name = {d.name};
str = sprintf('%s#',name{:});
num = sscanf(str, strcat(folder_var1, '%f', folder_var2, '.xlsx#'));
[sorted,index] = sort(num);
d = d(index)

freq_range = sorted';

output_array = zeros(length(freq_range),11);

power_array = zeros(length(freq_range),2);

e = actxserver ('Excel.Application');

```

```

% opens a server to open excel application that is faster than xlsread

for file_index = 1:length(d)
    %% Extracting data from each excel file
    sheet_names = {};
    excelworkbook = e.workbooks.Open(fullfile(Folder,d(file_index).name));

    sheet = excelworkbook.Sheets.Item(1);
    range=sheet.UsedRange;
    sheet_range = excelworkbook.Sheets.count;
    time = cell2mat(range.value([9:end],1));

    for k =1:sheet_range
        sheet_names{k} = excelworkbook.Sheets.Item(k).name;
    end

    for k=1:sheet_range
        sheet = excelworkbook.Sheets.Item(k);
        range=sheet.UsedRange;
        if strcmp(sheet_names{k}, 'Middle pressure') ||
        strcmp(sheet_names{k}, 'pressure')
            pressure = cell2mat(range.value([9:end],2));
        end
        if strcmp(sheet_names{k}, 'AD pressure')
            AD_enc_pressure = cell2mat(range.value([9:end],2));
        end
        if strcmp(sheet_names{k}, 'LA pressure')
            LA_enc_pressure = cell2mat(range.value([9:end],2));
        end
        if strcmp(sheet_names{k}, 'AD stroke')
            AD_stroke = cell2mat(range.value([9:end],2));
        end
        if strcmp(sheet_names{k}, 'AD current')
            AD_current = cell2mat(range.value([9:end],2));
        end
        if strcmp(sheet_names{k}, 'AD volt')
            AD_volt = cell2mat(range.value([9:end],2));
        end

        end
        if strcmp(sheet_names{k}, 'LA stroke')
            LA_stroke = cell2mat(range.value([9:end],2));
        end
        if strcmp(sheet_names{k}, 'LA current')
            LA_current = cell2mat(range.value([9:end],2));
        end
        if strcmp(sheet_names{k}, 'LA volt')
            LA_volt = cell2mat(range.value([9:end],2));
        end
    end

end

excelworkbook.Close;

%

```

```

%% Data Manipulation on each excel file
% compute the rms value of the voltage and current in Volt and Amperes,
% respectively

AD_volt_rms = sqrt(mean((AD_volt).^2));
AD_current_rms = sqrt(mean(AD_current.^2));
LA_volt_rms = sqrt(mean(LA_volt.^2));
LA_current_rms = sqrt(mean(LA_current.^2));

% compute the instanuos power in Watt
power_in = mean(AD_volt.*AD_current);
power_out = mean(LA_volt.*LA_current);

% compute the efficiency
eff = (power_out/power_in)*100;

% compute peak to peak of stroke in mm
if ismember('AD stroke',sheet_names) == 1
pk2pk_stroke_in= (max(AD_stroke)-min(AD_stroke))*LVDT_sensitivity;
end
if ismember('LA stroke',sheet_names) == 1
pk2pk_stroke_out = (max(LA_stroke)-min(LA_stroke))*LVDT_sensitivity;
end
% compute pressure amplitude in kPa
%check units here pleaaaaase
if ismember('Middle pressure',sheet_names) == 1 ||
ismember('pressure',sheet_names) == 1
amp_pressure = ((max(pressure) -
mean(pressure))*1000)/(gain*MICRO_sensitivity);
% where 100 gain of the signal amplifier and 1000 for unit conversion
end

if ismember('AD pressure',sheet_names) == 1
amp_AD_enc_pressure = ((max(AD_enc_pressure) -
mean(AD_enc_pressure))*1000)/(gain*0.101);
end
if ismember('LA pressure',sheet_names) == 1
amp_LA_enc_pressure = ((max(LA_enc_pressure) -
mean(LA_enc_pressure))*1000)/(gain*0.089);
end

%
%

%% Getting Phase difference between pressure and strokes using
% curve fitting (fourier Transform)
if phase_flag == 1
if ismember('AD pressure',sheet_names) == 1
B0 = mean(AD_enc_pressure);
B1 = (max(AD_enc_pressure) - min(AD_enc_pressure))/2;
B2 = 2*pi*freq_range(file_index);
B3 = 0;

% fit_1 = NonLinearModel.fit(time,pressure, 'y ~ b0 +
b1*sin(b2*x1 + b3)', [B0, B1, B2, B3]);
opt =
fitoptions('Method','NonlinearLeastSquares','Startpoint',[B0,B1,B2,B3]);
f = fittype('p1 + p2*sin(p3*x + p4)','options',opt);

```

```

        fit_1 = fit(time,AD_enc_pressure,f);
    end

    Z0 = mean(LA_current);
    Z1 = (max(LA_current) - min(LA_current))/2;
    Z2 = 2*pi*freq_range(file_index);
    Z3 = 0;

    % fit_2 = NonLinearModel.fit(time,LA_stroke, 'y ~ b0 + b1*sin(b2*x1 +
b3)', [Z0, Z1, Z2, Z3]);
    opt =
fitoptions('Method','NonlinearLeastSquares','Startpoint',[Z0,Z1,Z2,Z3]);
    f = fittype('p1 + p2*sin(p3*x + p4)', 'options', opt);
    fit_2 = fit(time,LA_current,f);

    Z0 = mean(LA_volt);
    Z1 = (max(LA_volt) - min(LA_volt))/2;
    Z2 = 2*pi*freq_range(file_index);
    Z3 = 0;

    % fit_2 = NonLinearModel.fit(time,LA_stroke, 'y ~ b0 + b1*sin(b2*x1 +
b3)', [Z0, Z1, Z2, Z3]);
    opt =
fitoptions('Method','NonlinearLeastSquares','Startpoint',[Z0,Z1,Z2,Z3]);
    f = fittype('p1 + p2*sin(p3*x + p4)', 'options', opt);
    fit_3 = fit(time,LA_volt,f);

    K0 = mean(AD_volt);
    K1 = (max(AD_volt) - min(AD_volt))/2;
    K2 = 2*pi*freq_range(file_index);
    K3 = 0;

    % fit_3 = NonLinearModel.fit(time,AD_stroke, 'y ~ b0 + b1*sin(b2*x1 +
b3)', [K0, K1, K2, K3]);

    opt =
fitoptions('Method','NonlinearLeastSquares','Startpoint',[K0,K1,K2,K3]);
    f = fittype('p1 + p2*sin(p3*x + p4)', 'options', opt);
    fit_4 = fit(time,AD_volt,f);

    K0 = mean(AD_current);
    K1 = (max(AD_current) - min(AD_current))/2;
    K2 = 2*pi*freq_range(file_index);
    K3 = 0;

    % fit_3 = NonLinearModel.fit(time,AD_stroke, 'y ~ b0 + b1*sin(b2*x1 +
b3)', [K0, K1, K2, K3]);

    opt =
fitoptions('Method','NonlinearLeastSquares','Startpoint',[K0,K1,K2,K3]);
    f = fittype('p1 + p2*sin(p3*x + p4)', 'options', opt);
    fit_5 = fit(time,AD_current,f);

    if ismember('AD pressure',sheet_names) == 1
        phase_1 = fit_1.p4;
    end
    phase_2 = fit_2.p4;

```

```

phase_3 = fit_3.p4;
phase_4 = fit_4.p4;
phase_5 = fit_5.p4;

if ismember('AD pressure',sheet_names) == 1
    phase_shift_Fitted_AD_volt_P = mod(abs(phase_1-phase_4),pi/2);
    phase_shift_Fitted_LA_current_P = mod(abs(phase_1-phase_2),pi/2);
end
phase_shift_Fitted_LA_current_LA_volt = mod(abs(phase_2-
phase_3),pi/2);
phase_shift_Fitted_AD_current_AD_volt = mod(abs(phase_4-
phase_5),pi/2);
end

    %% Acoustic Power Calculation using direct numerical integration on the
    strokes signals
    if acoustic_power_flag == 1
        LA_stroke_fitted = fit_external(time,((LA_stroke-
mean(LA_stroke))*LVDT_sensitivity)/1000,freq_range(file_index));
        AD_stroke_fitted =
fit_external(time,AD_stroke*LVDT_sensitivity/1000,freq_range(file_index));
        pressure_fitted =
fit_external(time,(pressure*1000*1000)/(gain*MICRO_sensitivity),freq_range(fi
le_index));
        for k = 1:length(LA_stroke_fitted)
            if k == length(LA_stroke_fitted)
                diff_LA_stroke(k) = (LA_stroke_fitted(k)-LA_stroke_fitted(k-
1))/((time(k)-time(k-1)));
                diff_AD_stroke(k) = (AD_stroke_fitted(k)-AD_stroke_fitted(k-
1))/((time(k)-time(k-1)));
            else
                diff_LA_stroke(k) = (LA_stroke_fitted(k+1)-
LA_stroke_fitted(k))/((time(k+1)-time(k)));
                diff_AD_stroke(k) = (AD_stroke_fitted(k+1)-
AD_stroke_fitted(k))/((time(k+1)-time(k)));
            end
        end
        sprintf('Numerical Differentiation on the strokes signals')
        LA_acoustic_power =
mean(pressure_fitted.*diff_LA_stroke'*((pi/4)*(0.0508^2))) % 0.0508 is the
diameter of the linear alternator in m^2
        AD_acoustic_power =
mean(pressure_fitted.*diff_AD_stroke'*((pi/4)*(0.0508^2)))
        % 0.0508 is the diameter of the linear alternator in m^2
    end

    %% Output the manipulated data to result excel file
    output_array(i,:) =
[freq_range(file_index),amp_pressure,pk2pk_stroke_in,pk2pk_stroke_out,AD_volt
_rms,AD_current_rms,power_in,LA_volt_rms,LA_current_rms,...
power_out,eff];
    xlsxwrite('result.xls',output_array(i,:),1,strcat('A',num2str(j)));
    if acoustic_power_flag == 1
        power_array(i,:) =
[freq_range(file_index),AD_acoustic_power,LA_acoustic_power];
    end

    xlsxwrite('power_results.xls',power_array(i,:),1,strcat('A',num2str(j)));
end

```

```

        if phase_flag == 1
            phase_array(i,:) =
[freq_range(file_index), (phase_shift_Fitted_AD_volt_P*180)/pi, (phase_shift_Fi
tted_LA_current_P*180)/pi,...

(phase_shift_Fitted_LA_current_LA_volt*180)/pi, (phase_shift_Fitted_AD_current
_AD_volt*180)/pi];

xlswrite('phase_result.xls',phase_array(i,:),1,strcat('A',num2str(j)));
        end

        if ismember('LA pressure',sheet_names) == 1 && ismember('AD
pressure',sheet_names) == 1
            AUX_array(i,:) =
[freq_range(file_index),amp_AD_enc_pressure,amp_LA_enc_pressure];
            elseif ismember('AD pressure',sheet_names) == 1
                AUX_array(i,:) = [freq_range(file_index),amp_AD_enc_pressure];
            elseif ismember('LA pressure',sheet_names) == 1
                AUX_array(i,:) = [freq_range(file_index),amp_LA_enc_pressure];
            end

        if ismember('LA pressure',sheet_names) == 1 || ismember('AD
pressure',sheet_names) == 1
            xlswrite('AUX_result.xls',AUX_array(i,:),1,strcat('A',num2str(j)));
        end

        i = i+1;
        j = j+1;
        % this output array is a matrix of 26 rows (each row for a frequency
        % value starting from 45 and ending with 70) and 11 columns (each
        % column for a data set, like one column for LA_current_rms, one column
for LA_volt_rms
        disp(strcat('Total files: ',num2str(length(d)), ' Done:
',num2str(file_index), ' Remaining: ',num2str(length(d)-file_index)));
        end

e.Quit;
e.delete;

if FFT_flag == 0
info_array = {'Frequency (Hz)', 'Dynamic Pressure Amplitude (kPa)', 'Stroke AD
pk-pk (mm)', 'Stroke LA pk-pk (mm)', 'AD Voltage rms (V)', 'AD Current rms
(A)', 'Input Power (Watt)',...
            'LA Voltage rms (V)', 'LA Current rms (A)', 'Output Power (Watt)', 'Eff
(%)'};
xlswrite('result.xls',info_array,1,'A1');
if acoustic_power_flag == 1
    info_array = {'Frequency (Hz)', 'Acoustic Power AD (watt)', 'Acoustic Power
LA (watt)'};
    xlswrite('power_results.xls',info_array,1,'A1');
end
if phase_flag == 1
    info_array = {'Frequency (Hz)', 'Phase diff. P_AD_volt (deg)', 'Phase diff.
P_LA_current (deg)',...
                'Phase diff. LA_current_volt (deg)', 'Phase diff. AD_current_volt
(deg)'};
    xlswrite('phase_result.xls',info_array,1,'A1');
end

```

```

if ismember('LA pressure',sheet_names) == 1 || ismember('AD
pressure',sheet_names) == 1
    info_array = {'Frequency (Hz)', 'AD enclosure pressure (kPa)', 'LA
enclosure pressure (kPa)'};
    xlswrite('AUX_result.xls',info_array,1, 'A1');
end

%this writes the info at the top of the result.xls file

%closing the server

%% Time Domain Plots

figure(1)
plot_external(output_array(:,1),output_array(:,2));

for k = 3:11
    figure(k-1)
    plot_external(output_array(:,1),output_array(:,k));
end

% now you have finished plotting all time domain data using the user-defined
function (subroutine) plot_external
else

figure(1)
PSD_HARMONIC(LA_volt(:,PSD_freq),samprate,numens, 'Current');
figure(2)
PSD_HARMONIC(LA_current(:,PSD_freq),samprate,numens, 'Current');
figure(3)
PSD_HARMONIC(LA_stroke(:,PSD_freq),samprate,numens, 'Current');
figure(4)
PSD_HARMONIC(AD_volt(:,PSD_freq),samprate,numens, 'Current');
figure(5)
PSD_HARMONIC(AD_current(:,PSD_freq),samprate,numens, 'Current');
figure(6)
PSD_HARMONIC(AD_stroke(:,PSD_freq),samprate,numens, 'Current');
figure(7)
PSD_HARMONIC(pressure(:,PSD_freq),samprate,numens, 'Current');

% now you have finished plotting all frequency domain data using the user-
defined function (subroutine) psd_harmonic
end

```

---

## PSD Harmonic

```
%{
This function is used to plot the power sepectral denisty of
multiple
cycles signal (PSD)

input
1. 1D array contains the data to be converted into the frequency domain.
2. sampling rate in sample per second.
3. number of ensemble average.
4. string to be compared with 'Current' or otherwise voltage.

output
one figure contains two plots the top contains the PSD and the other
contains the location of harmonics.

%}

function PSD_HARMONIC(data,samprate,numens,title_var)

samples = length(data);
delta = 1/samprate;
nyq_freq = samprate/2;
reclength = samples/samprate;
avg = mean(data);
stddev = std(data);
bndwidth = 1/(reclength);

disp(' ')
disp(strcat('The mean of the data is ',num2str(avg),'.'));
disp(strcat('The standard deviation of the data is ',num2str(stddev),'.'));
disp(strcat('The effective bandwith is ',num2str(bndwidth),'.'));
disp(' ')

%%%% Data Standardization %%%%

x = data - avg;

%%%% Autospectrum Estimate %%%%

% % % % numens = input('Enter the number of ensembles to average. ');

N = 2^floor(log2(samples/numens));

% 'N' is the number of points per ensemble.
% It is coerced to be power of 2

nd = floor(samples/N);
disp('For efficiency (i.e. power of 2 algorithm),')
disp(['the actual number of ensembles is ',num2str(nd),'.'])
```



```

disp(' ')
% 'nd' is the number of ensembles based on
% 'N' and total samples

q = 0.5;

% 'q' is the overlap parameter. Overlapping
% is done to minimize random error induced
% by Hanning tapering

ilng = nd/q;
j = (1:1:ilng);
T = N*delta;
frqres = 1/T;
rnderr = 1/(nd)^(1/2);

autoout1=['The frequency resolution is approximately ',num2str(frqres),'
Hz.'];
autoout2=['The random error is about ',num2str(rnderr),'.'];

disp(' ');
disp(autoout1);
disp(autoout2);

for count = 1:nd/q-1
    specmat(:,count) = x(q*(count-1)*N+1:(q*(count-1)+1)*N);
end
%%
% apply Hanning window

t = (0:delta:T-delta)';
hann = 1 - (cos(t*pi/T)).^2;

clear count

for count = 1:nd/q-1
    specdata(:,count) = specmat(:,count).*hann;
end

specint = abs(delta*(8/3)^(1/2)*fft(specdata));

specest = 2/(N*nd*delta)*sum(specint.^2,2);

k = (0:1:N/2)';

fk = k/(N*delta);

% Strouhal No. scaling using user input
% characteristic length and freestream velocity

disp(' ')
disp(' ')
% % % % % disp('Would you like to scale the frequency axis using')
% % % stquery = input('Strouhal No. ("Y" for yes)? ','s');
stquery= 'N';

```

```

disp(' ')

srtspecf = sortrows([fk(2:N/2+1)';specest(2:N/2+1)'],'',2);

%%

subplot(2,1,1)

semilogy(fk, specest(1:N/2+1), '-ks', 'linewidth', 1, 'MarkerSize', 3);
axis([0 max(fk) 0 max(specest(1:N/2+1))]);
title('\bf Power Spectral Desnisty', 'fontsize', 15, 'color', 'k')
xlabel('\bf Frequency, Hz', 'fontsize', 15, 'color', 'k');
%axis auto

if strcmp (title_var, 'Current')
    ylabel('\bf Spec. Density, A^2/s', 'fontsize', 15, 'color', 'k');
else
    ylabel('\bf Spec. Density, V^2/s', 'fontsize', 15, 'color', 'k');
end
grid on
set(gca, 'gridlinestyle', '-')
set(gca, 'fontsize', 12);
set(gca, 'linewidth', 2);
if strcmp (title_var, 'Current')
    set(gca, 'YTick', [1E-9 1E-7, 1E-5, 1E-3, 1E-1, 1E1, 1E3])%{, 1E3, 1E4, 1E5})
    axis ([0 samprate/2 1E-9 1E3])
else
    set(gca, 'YTick', [1E-9, 1E-7, 1E-5, 1E-3, 1E-1, 1E1, 1E3, 1E5])
    axis ([0 samprate/2 1E-9 1E5])
end

subplot(2,1,2)
axis([0 1 -0.4 1])
text(0.33, 7/8, '\bf Max. Autospectral Density
Location', 'fontsize', 15, 'color', 'k')
text(0.25, 5/8, ['1) ', num2str(srtspecf(N/2, 1)), '
Hz'], 'fontsize', 15, 'color', 'k')
text(0.25, 3/8, ['2) ', num2str(srtspecf(N/2-1, 1)), '
Hz'], 'fontsize', 15, 'color', 'k')
text(0.25, 1/8, ['3) ', num2str(srtspecf(N/2-2, 1)), '
Hz'], 'fontsize', 15, 'color', 'k')
text(0.5, 5/8, ['4) ', num2str(srtspecf(N/2-3, 1)), '
Hz'], 'fontsize', 15, 'color', 'k')
text(0.5, 3/8, ['5) ', num2str(srtspecf(N/2-4, 1)), '
Hz'], 'fontsize', 15, 'color', 'k')
text(0.5, 1/8, ['6) ', num2str(srtspecf(N/2-5, 1)), '
Hz'], 'fontsize', 15, 'color', 'k')
text(0.75, 5/8, ['7) ', num2str(srtspecf(N/2-6, 1)), '
Hz'], 'fontsize', 15, 'color', 'k')
text(0.75, 3/8, ['8) ', num2str(srtspecf(N/2-7, 1)), '
Hz'], 'fontsize', 15, 'color', 'k')
text(0.75, 1/8, ['9) ', num2str(srtspecf(N/2-8, 1)), '
Hz'], 'fontsize', 15, 'color', 'k')
text(0.33, (-0.25/2), ['Frequency Resolution = ', num2str(frqrres), '
Hz'], 'fontsize', 15, 'color', 'k')

```

end

## **Plot External**

```
function plot_external(x_data,y_data)
prompt={'Enter plot type (L for Linear,SX for semilogx,SY for semilogy and LL
for loglog):',...
'Enter plot color and format:',...
'Enter title:',...
'Enter title's fontsize:',...
'Enter xlabel:',...
'Enter xlabel's fontsize:',...
'Enter ylabel:',...
'Enter ylabel's fontsize:',...
'Enter axes's fontsize and linewidth:',...
'Enter 1 to enable grid:',...
'Enter plot's linewidth and markersize:',...
'Enter 1 for multiple plots'
};
```

```
name='Plot Parameters';
numlines=1;
%===== used in subplotting =====%
% defaultanswer={'L','k-','Title example','15','Xlabel
example,s','15','Ylabel example, A_r_m_s','15','[12,2]','1','[1,3]'};
%===== used in normal plotting =====%
defaultanswer={'L','k-','','24','Frequency,
Hz','30','','30','[24,2]','1','[4,10]','0'};
```

```
answer=inputdlg(prompt,name,numlines,defaultanswer);
```

```
size_y_data = size(y_data);
```

```
plot_color = ['b','r','k','c','m','y','g'];
```

```
if strcmp(answer{1},'L')
    if str2num(answer{12}) == 1
        p = plot(x_data,y_data)
    else
        p = plot(x_data,y_data,answer{2});
    end
elseif strcmp(answer{1},'SX')
    if str2num(answer{12}) == 1
        p = semilogx(x_data,y_data)
    else
        p = semilogx(x_data,y_data,answer{2});
    end
elseif strcmp(answer{1},'SY')
    if str2num(answer{12}) == 1
        p = semilogy(x_data,y_data)
    else
        p = semilogy(x_data,y_data,answer{2});
    end
elseif strcmp(answer{1},'LL')
    if str2num(answer{12}) == 1
        p = loglog(x_data,y_data)
```

```

    else
        p = loglog(x_data,y_data,answer{2});
    end
end

title(strcat('\bf',answer{3}),'fontsize',str2num(answer{4}),'color','k');
xlabel(strcat('\bf',answer{5}),'fontsize',str2num(answer{6}),'color','k');
ylabel(strcat('\bf',answer{7}),'fontsize',str2num(answer{8}),'color','k');

axis_temp = str2num(answer{9});
set(gca,'fontsize',axis_temp(1));
set(gca,'linewidth',axis_temp(2));
set(gca,'FontWeight','bold');

if strcmp(answer{10},'1')
    grid on
    set(gca,'gridlinestyle','-')
end

plot_temp = str2num(answer{11});
if str2num(answer{12}) == 1
    set(p,'linewidth',plot_temp(1));
    set(p,'markersize',plot_temp(2));
else
    set(p,'linewidth',plot_temp(1));
    set(p,'markersize',plot_temp(2));
end

end

```

---

## Fit External

```
%{
This function is used to fit a sinusoidal data to its 18th harmonic using
optimization toolbox in matlab

it uses an external function fit_simp18

inputs
1.two 1 dimensional array containing X,Y data to be fitted
2.initial frequency used as initial guess for the fundamental frequency.

output
array containing the fitted data.

%}

function Y_new = fit_external(x_data,y_data,freq)
T = x_data;
Y = y_data; %Y is the data of the variable (microphone pressure) used in
fitting

% Initial solution: X0=[ 9 amplitudes , 9 angles in degrees, fundamental
frequency ]
X0=[500 400 300 50 50 50 50 50 25 0 20 30 0 20 30 0 20 30 freq]';

% Lower limits: lb=[ 9 amplitudes , 9 angles in degrees, minimum expected
fundamental frequency ]
lb = [0 0 0 0 0 0 0 0 0 -360 -360 -360 -360 -360 -360 -360 -360 -360
freq-10 ]';

% Upper limits: ub=[ 9 amplitudes , 9 angles in degrees, maximum expected
fundamental frequency ]
ub = [1000000 1000000 1000000 1000000 1000000 1000000 1000000 1000000
1000000 360 360 360 360 360 360 360 360 freq+10]';

% Set an options file for LSQNONLIN to use the medium-scale algorithm
options = optimset('algorithm','trust-region-reflective','TolX', 1e-
15,'TolFun',1e-15,'display','on');

% Calculate the new coefficients using LSQNONLIN.
[x,resnorm,residual,exitflag,output]=lsqnonlin(@fit_simp18,X0,lb,ub,options,T
,Y);

% Plot the original and experimental data.
fund = x(19);

Y_new =
x(1).*sin(2*pi*fund.*T+x(10)*pi/180)+x(2).*sin(4*pi*fund.*T+x(11)*pi/180)+x(3
).*sin(6*pi*fund.*T+x(12)*pi/180)+x(4).*sin(8*pi*fund.*T+x(13)*pi/180)+x(5).*
sin(10*pi*fund.*T+x(14)*pi/180)+x(6).*sin(12*pi*fund.*T+x(15)*pi/180)+x(7).*s
```

```
in(14*pi*fund.*T+x(16)*pi/180)+x(8).*sin(16*pi*fund.*T+x(17)*pi/180)+x(9).*sin(18*pi*fund.*T+x(18)*pi/180);
```

end

---

## **Fit Simple 18**

```
%{  
This function is called by lsqnonlin.  
x is a vector which contains the coefficients of the  
equation. X and Y are the option data sets that were  
passed to lsqnonlin.
```

```
%}
```

```
function diff = fit_simpl8(x,X,Y)
```

```
A=x(1);  
B=x(2);  
C=x(3);  
D=x(4);  
E=x(5);  
F=x(6);  
G=x(7);  
H=x(8);  
I=x(9);
```

```
fund = x(19);
```

```
Phi1=x(10);  
Phi2=x(11);  
Phi3=x(12);  
Phi4=x(13);  
Phi5=x(14);  
Phi6=x(15);  
Phi7=x(16);  
Phi8=x(17);  
Phi9=x(18);
```

```
diff =
```

```
A.*sin(2*pi*fund.*X+Phi1*pi/180)+B.*sin(4*pi*fund.*X+Phi2*pi/180)+C.*sin(6*pi  
*fund.*X+Phi3*pi/180)+D.*sin(8*pi*fund.*X+Phi4*pi/180)+E.*sin(10*pi*fund.*X+P  
hi5*pi/180)+F.*sin(12*pi*fund.*X+Phi6*pi/180)+G.*sin(14*pi*fund.*X+Phi7*pi/18  
0)+H.*sin(16*pi*fund.*X+Phi8*pi/180)+I.*sin(18*pi*fund.*X+Phi9*pi/180) - Y;
```

```
end
```

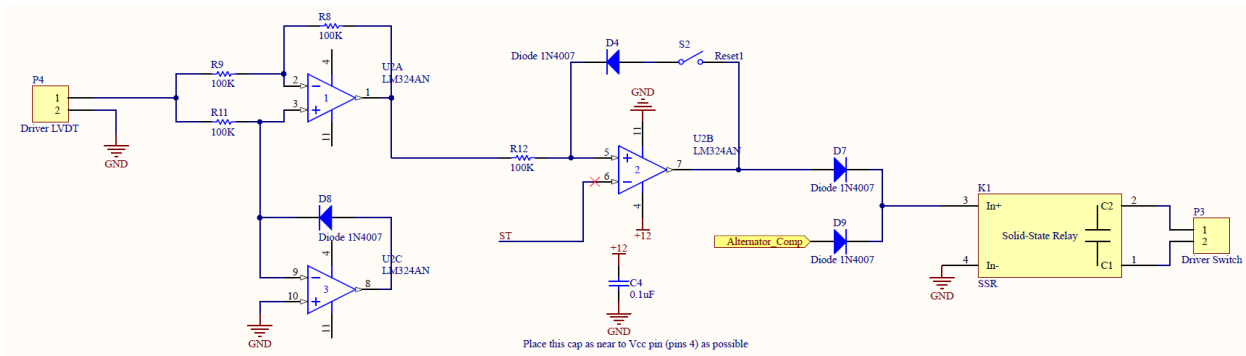
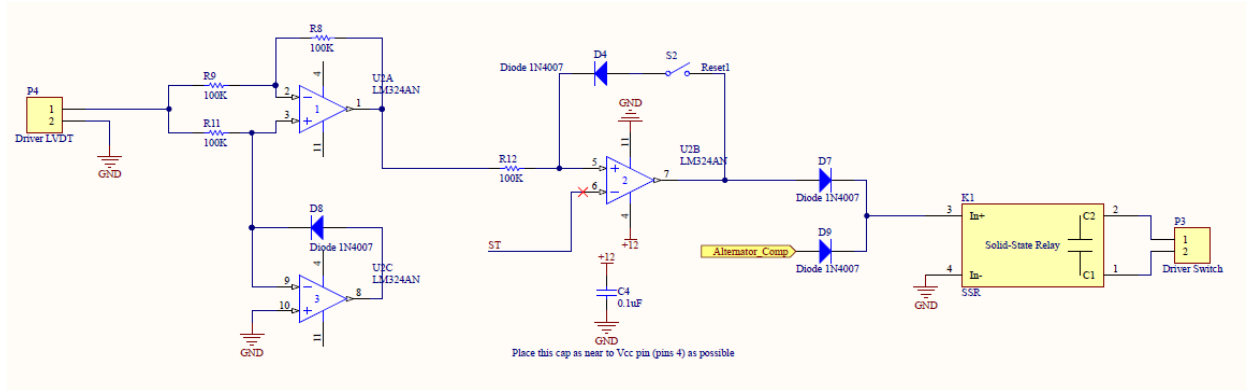
## Appendix F - Stroke Control Circuit

Item No.	Item designator	Component name	Description and purpose	Main specs
<b>Power supply circuit</b>				
2	P5	Terminal block	(Rosette) for input of 220 V AC input	Withstand the current and voltage passing through it
1	S3	On/Off switch	ON/Off for 220 V power supply	Power switch Single-Pole, Single-Throw Switch. Must withstand the current and voltage passing through it
27	F1	Input Fuse	Protection against excessive current	100 mA
26	R16	Transient voltage suppressor Varistor (Voltage-Sensitive Resistor)	If the applied voltage exceeds the rated voltage (240V), its resistance drops significantly causing excessive current withdrawal causing the fuse to blow and thus protects the circuit against over-voltage	Rated voltage 240 V. Part number 14N391K
3	T1	Transformer	Step-down transformer to decrease input AC voltage from 220 V to 12 V	220 V input/12 Volt output 1 A
23	D10, D12, D13 AND D14	Diodes (Qty =4)	Full-wave rectifier (convert AC to DC)	General purpose diode. Part number 1N4007
25	C5	Capacitor	Power supply filter (smoothing capacitor) to Remove ripples from rectifier output	1000 $\mu$ F



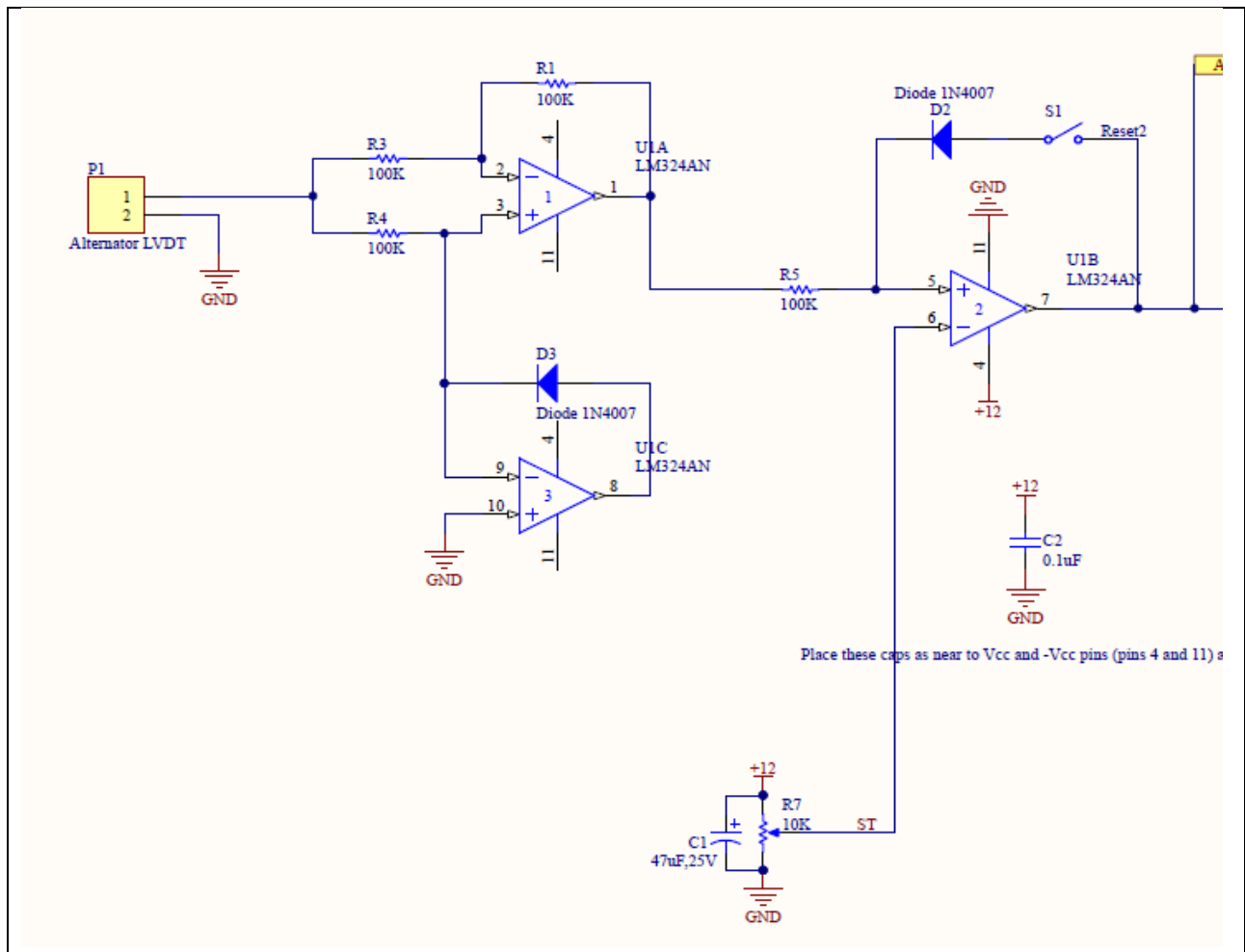
4	VR1	Voltage regulator	Regulates the output voltage to 12 V	12V output voltage (DC) and 1 A current limit. Part number LM7812.
8	C6	capacitor	Required for fast response of voltage regulator	0.1 $\mu$ F
5	D11	LED	Visual indicator for power ON	
7	R15	Resistance	Provides current limit for the LED D11	1k $\Omega$

**Now you have 12 V<sub>DC</sub> power input to OP Amps**

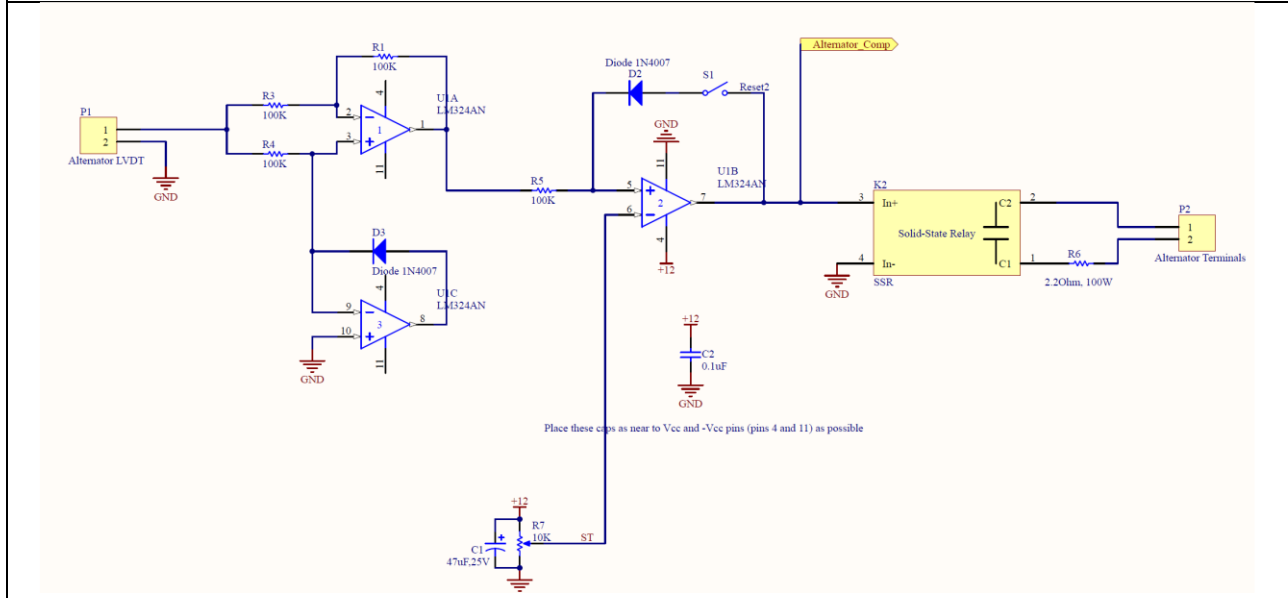


Precision rectifier circuit				
Item No.	Item designator	Component name	Description and purpose	Main specs
24	P1	Terminal block	Input of LA LVDT signal	Withstand the current and voltage passing through it
10 & 21	5&16	Precision rectifier Qty = 2 (one for AC & one for LA)	Rectification of LVDT signal	LM324 (uses two op-amps inside LM324AN). General purpose op-amp
22	R1, R3 and R4	Resistances (Qty =3)	Required for LM324 precision rectifier circuit	Equal resistance of the three resistances – Large resistance values are needed because they will not withdraw large current from the supply
28	D2&D4	Diodes (Qty = 2)	Diode, part of the precision rectifier circuit	General purpose diode 1N4007
29	D4 & D8	Diodes (Qty = 2)	Diode, part of the precision rectifier circuit	General purpose diode 1N4007
30	-	LED	Linear alternator over-stroke LED Typical INFRARED GaAs LED, 0.5 mm	Built into the normally open solid-state relay

Comparator and Latching circuit				
Item No.	Item designator	Component name	Description and purpose	Main specs
21	U1	Analog comparator LM324AN	Compares the measured LVDT voltage to the set point	
22	R5	Resistance 100 k	Part of the latching circuit	
28	D2	Diode	Part of the latching circuit	
11 & 18	S1(LA) & S2 (AD)	On/off switch	Latching reset	General purpose Single-Pole, Single-Throw Switch
19	R7	Potentiometer	Potentiometer for the set point of the over-stroke voltage	Multi-turn for high resolution setting of set voltage, 10 k $\Omega$
20	C1	Capacitor	Power supply noise filter (Between Vcc and ground of potentiometer)	47 $\mu$ F or higher
-	C2	0.1 $\mu$ F capacitor	Decoupling capacitor for the op-amp LM324AN of the alternator (U1)	0.1 $\mu$ F ceramic capacitor, Low equivalent series resistance (ESR)
-	C4	0.1 $\mu$ F capacitor	Decoupling capacitor for the op-amp LM324AN of the driver (U2)	0.1 $\mu$ F ceramic capacitor. Low equivalent series resistance (ESR)

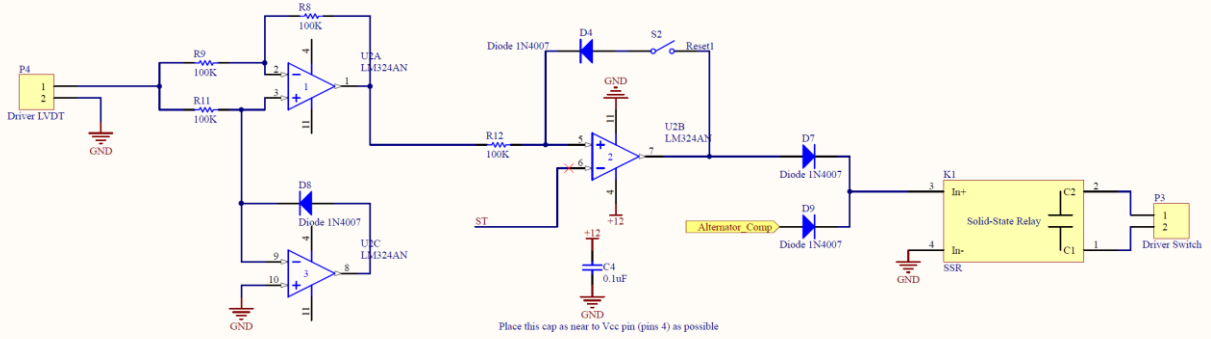


## Control action taken based on comparator output in the alternator



Item No.	Item designator	Component name	Description and purpose	Main specs
17	K2	Normally-open Solid-state relay	To introduce stall circuit in parallel to the alternator to avoid over-stroking	Normally-open Proper power rating
14	R6	2.2 Ω 100-W resistance	This is the stall circuit	Low resistance, large power resistance
16	P2	Terminal block	To connect to the alternator	

**Control action taken based on comparator output in the Driver**  
**Same as above except using normally-closed solid state relay rather than normally-open solid state relay plus use of OR gate**



Item No.	Item designator	Component name	Description and purpose	Main specs
12	D7 and D9	Diodes (Qty =2)	Together they make an OR gate	General purpose diode 1N4007
13	K1	Solid-State Relay	Normally closed to disconnect the driver power in case of overstroke.	125VAC @ 10A
9 & 22	Several	Resistors	Part of the precision rectifier and latching circuits.	¼ W
6	P4	Terminal block	Acoustic driver LVDT input Header, 2-Pin	220V @ 10A
15	P3	Terminal block	Driver disconnect terminals Header, 2-Pin	220V @ 10A